



Turun yliopisto  
University of Turku

# MECHANISMS OF FIMBRIAL ASSEMBLY VIA NON-CLASSICAL CHAPERONE-USHER PATHWAYS AND RECEPTOR RECOGNITION BY FIMBRIAL ADHESINS

---

Natalia Pakharukova

## University of Turku

---

Faculty of Mathematics and Natural Sciences  
Department of Biochemistry  
Biochemistry  
Doctoral Program in Molecular Life Sciences

## Supervised by

---

Docent Anton Zavialov, Ph.D.  
Department of Chemistry  
University of Turku

## Reviewed by

---

Prof. Adrian Goldman, Ph.D.  
Department of Bioscience  
University of Helsinki  
Helsinki, Finland

Prof. Stefan Knight, Ph.D.  
Uppsala Biomedical Centre  
Swedish University of Agricultural Sciences  
Uppsala, Sweden

## Opponent

---

Docent Julie Bouckaert, Ph.D.  
Structural and Functional Glycobiology Unit  
University of Science and Technology Lille 1  
Lille, France

The originality of this thesis has been checked in accordance with the University of Turku quality assurance system using the Turnitin OriginalityCheck service.

ISBN 978-951-29-6661-5 (PRINT)

ISBN 978-951-29-6662-2 (PDF)

ISSN 0082-7002 (Print)

ISSN 2343-3175 (Online)

Painosalama Oy - Turku, Finland 2016

*A journey of a thousand miles begins with a single step*  
*(Lao Tzu)*





## CONTENTS

<b>LIST OF ORIGINAL PUBLICATIONS .....</b>	<b>5</b>
<b>ABSTRACT .....</b>	<b>6</b>
<b>TIIVISTELMÄ .....</b>	<b>7</b>
<b>ABBREVIATIONS .....</b>	<b>8</b>
<b>ABBREVIATIONS OF THE AMINO ACID RESIDUES.....</b>	<b>10</b>
<b>1. INTRODUCTION.....</b>	<b>11</b>
<b>1.1 General introduction .....</b>	<b>11</b>
<b>1.2 The CU pathways .....</b>	<b>12</b>
1.2.1 Classical CU pathway .....	14
1.2.2 Alternative (alternate) CU pathway .....	22
1.2.3 Archaic CU pathway ( $\sigma$ -fimbriae).....	23
<b>1.3 Applications of adhesive organelles in medicine.....</b>	<b>25</b>
<b>2. AIMS OF THE STUDY .....</b>	<b>27</b>
<b>3. MATERIALS AND METHODS .....</b>	<b>28</b>
<b>3.1 Design of donor strand complemented monomers and expression construct     CsuC-CsuA/B (original publications I–V) .....</b>	<b>28</b>
<b>3.2 Protein expression (original publications I–V).....</b>	<b>28</b>
<b>3.3 Protein purification.....</b>	<b>28</b>
3.3.1. Purification of His6-tagged proteins (AggAdsc, MyfAdsc, CsuC-CsuA/B, and CsuA/Bdsc) (papers I, III–VI).....	28
3.3.2. Purification of His6-tag-free AggBdsc and PsaAdsc (papers II, III) .....	29
<b>3.4 Incorporation of selenomethionine (papers III–VI).....</b>	<b>30</b>
<b>3.5 Protein crystallization (papers I–IV, VI).....</b>	<b>30</b>
<b>3.6 X-ray diffraction data collection (papers I–IV, VI) .....</b>	<b>30</b>
<b>3.7. Protein structure determination (papers I–IV, VI).....</b>	<b>31</b>
<b>3.8 Site-directed mutagenesis (papers II, III, V) .....</b>	<b>33</b>
<b>3.9 Surface plasmon resonance (SPR) binding experiments (papers II, V).....</b>	<b>33</b>
<b>3.10 Stability analysis of CsuC-CsuA/B and CsuA/Bdsc (paper VI).....</b>	<b>33</b>
<b>3.11 Isolation of Myf and Psa fimbriae (paper III).....</b>	<b>33</b>
<b>3.12 Determination of receptor binding by Myf and Psa (paper III).....</b>	<b>34</b>
<b>3.13 Characterization of Myf receptor binding specificity (paper III).....</b>	<b>34</b>
<b>3.14 Characterization of MyfAdsc binding to lactose and galactose (paper III)     .....</b>	<b>34</b>
<b>4. RESULTS AND DISCUSSION.....</b>	<b>35</b>

<b>4.1 High-resolution structures of polyadhesin fimbrial subunits (papers I-III)</b>	<b>35</b>
<b>4.2 The structural basis for host cell receptor recognition in AAF/I, Myf, Psa fimbriae (papers I-III)</b>	<b>39</b>
<b>4.2.1 AAF/I specifically binds fibronectin using a positively charged surface (paper II)</b>	<b>39</b>
4.2.2 Myf binds to terminal $\beta$ -1-3- or $\beta$ -1-4-linked galactose of glycosphingolipids (paper III)	42
4.2.3 PsaA binds phosphatidylcholine using a tyrosine-rich surface (paper III)	44
<b>4.3 The biological significance of polyvalent attachment (papers II-III)</b>	<b>48</b>
<b>4.4. Structural insights into archaic pili biogenesis (papers IV-VI)</b>	<b>50</b>
4.4.1 DSC mechanism governs Csu pilus assembly (paper V)	50
4.4.2 The CsuC chaperone displays several unique features	51
4.4.3 The CsuA/B subunit complexed with its chaperone is only partially folded	53
4.4.4 Both domains of CsuC are involved in the anchoring of CsuA/B	54
4.4.5 The donor-strand register is shifted in the CsuC-CsuA/B complex	56
4.4.6 The fiber-inserted conformation of the CsuA/B subunit has a unique structure of $\beta$ -sheet ABE	57
4.4.7 Archaic CsuC chaperone provides incomplete structural information for the folding of CsuA/B	58
4.4.8 Assembly of the archaic fimbriae is driven by subunit folding energy	60
4.4.9 Non-classical CU systems might display a more flexible mode of DSE	62
4.4.10 Archaic and alternative systems – a distinct assembly pathway of CU organelles	64
<b>5. CONCLUDING REMARKS AND FUTURE PROSPECTS</b>	<b>65</b>
<b>6. ACKNOWLEDGEMENTS</b>	<b>67</b>
<b>REFERENCES</b>	<b>69</b>
<b>REPRINTS OF ORIGINAL PUBLICATIONS</b>	<b>79</b>

## LIST OF ORIGINAL PUBLICATIONS

The thesis is based on the following publications, referred in the text by Roman numerals I-VI.

- I. Pakharukova, N., Tuittila, M. and Zavialov A. (2013). Crystallization and sulfur SAD phasing of AggA, the major subunit of aggregative adherence fimbriae type I from the *Escherichia coli* strain that caused an outbreak of haemolytic-uraemic syndrome in Germany. Acta crystallographica. Section F, Structural Biology Communications 69, 1389-1392.
- II. Berry, A.\*, Yang, Y.\*, Pakharukova, N.\*, Garnett, J., Lee, W., Cota, E., Marchant, J., Roy, S., Tuittila, M., Liu, B., Inman, K., Ruiz-Perez, F., Mandomando, I., Nataro, J., Zavialov, A. and Matthews S. (2014). Structural insight into host recognition by aggregative adherence fimbriae of enteroaggregative *Escherichia coli*. Plos Pathogens 10, e1004404. \*- Equal contribution.
- III. Pakharukova, N.\*, Roy, S.\*, Tuittila, M.\*, Rahman, M., Paavilainen, S., Ingars, A.-K., Skaldin, M., Lamminmäki, U., Härd, T., Teneberg, S. and Zavialov A. (2016). Structural basis for Myf and Psa fimbriae-mediated tropism of pathogenic strains of *Yersinia* for host tissues. Molecular Microbiology doi: 10.1111/mmi.13481 [Epub ahead of print] \*- Equal contribution.
- IV. Pakharukova, N., Tuittila, M., Paavilainen, S. and Zavialov, A. (2015). Crystallization and preliminary X-ray diffraction analysis of the Csu pili CsuC-CsuA/B chaperone-major subunit pre-assembly complex from *Acinetobacter baumannii*. Acta crystallographica. Section F, Structural Biology Communications 71, 770-774.
- V. Pakharukova, N., Garnett, J., Tuittila, M., Paavilainen, S., Diallo, M., Xu, Y., Matthews, S. and Zavialov, A. (2015). Structural insight into archaic and alternative chaperone-usher pathways reveals a novel mechanism of pilus biogenesis. Plos Pathogens 11, e1005269.
- VI. Pakharukova, N., Tuittila, M., Paavilainen, S., Parilova O., Malmi, H. and Zavialov, A. (2016). Chaperones from non-classical chaperone-usher pathways preserve folding energy of pilins by providing them an incomplete structural information. Manuscript

The original articles I, IV were reprinted with the permission of © International Union of Crystallography, the original articles II, V were reprinted with the permission of © Public Library of Science, the original article III was reprinted with the permission of © Wiley-Blackwell.

## ABSTRACT

The attachment of a pathogen to target cells is a critical step in establishing an infection. Most Gram-negative pathogens display specialized adhesive pili, or fimbriae, assembled via the dedicated classical, alternative and archaic chaperone-usher (CU) pathways from protein subunits. CU pathways represent attractive inhibition targets, as the suppression of bacterial adhesion will allow the natural clearance of the pathogen without the development of antibiotic resistance. This thesis explores the mechanism and biological significance of the polyvalent attachment of fimbrial adhesins to host cell receptors and elucidates the assembly mechanism of fimbriae via the archaic CU pathway.

In this study, we focused on several medically important polyadhesins: AAF/I (*Escherichia coli* O4H104), Myf (*Yersinia enterocolitica*), and Psa (*Y. pestis* and *Y. pseudotuberculosis*). We present the atomic resolution crystal structures of the fiber forming subunits of these organelles and show that they are assembled into linear homo- (Myf and Psa) or heteropolymers (AAF/I) by donor strand complementation. Each protein subunit of these three fimbriae binds to host cell receptors, thereby establishing multipoint attachment. The AggA subunits of AAF/I bind to fibronectin via a unique positively charged surface at inter-subunit interfaces. The co-crystal structures of the subunits of Myf and Psa with galactose and choline, respectively, reveal the receptor binding sites and explain differences in the tissue tropism of pathogenic species of *Yersinia*. The high avidity of the attachment and the ability of polyadhesins to recognize several receptors represent a significant challenge for drug development and underlines the importance of multivalent inhibitors.

To elucidate the fimbriae biogenesis via the archaic CU pathway, we determined the crystal structures of the CsuC-CsuA/B chaperone-subunit preassembly complex and self-complemented CsuA/B pilin subunit from the Csu fimbriae of *Acinetobacter baumannii*. We show that the biogenesis of archaic systems is strikingly different from that of the classical CU pathway. The CsuC chaperone utilizes a unique subunit anchoring mechanism involving both domains of the protein. Furthermore, CsuC maintains the CsuA/B subunit in a partially disordered state, which allows for a more flexible mode of donor strand exchange. The accessible core of the chaperone-bound subunit might represent a potential inhibition target for archaic pili assembly in bacterial pathogens.

## TIIVISTELMÄ

Taudinaiheuttajien kiinnittyminen kohdesoluihin infektion alkaessa on kriittinen vaihe. Useimmilla gramnegatiivisilla bakteereilla on tarttumiseen erikoistuneita fimbrioita, adhesiineja, jotka muodostuvat proteiinialayksiköistä klassisen, vaihtohtoisen ja arkaaisen kaitsija-portieeri (chaperon-usher, CU) -eritysjärjestelmän kautta. CU-järjestelmät ovat houkuttelevia inhibition kohteita, koska bakteerien kiinnittymisen ehkäisy mahdollistaa taudinaiheuttajien luonnollisen poistamisen ilman, että kehittyä antibioottiresistenssiä. Tässä väitöskirjassa käsitellään polyadhesiinien kiinnittymismekanismia kohdereseptoreihin ja arkaaisen CU-järjestelmän mukaisia fimbrioiden muodostumisperiaatteita.

Tutkimuksemme kohteena olivat lääketieteellisesti tärkeät polyadhesiinit AAF/I (*Escherichia coli* O4H104), Myf (*Yersinia enterocolitica*) ja Psa (*Y. pestis* ja *Y. pseudotuberculosis*). Ratkaisimme näiden alayksiköiden kiderakenteet atomin tarkkuudella, ja osoitimme, että alayksiköt ryhmittyvät lineaarisiin homo- (Myf ja PSA) tai heteropolymeereihin (AAF/I) donorisäikeen komplementaatio -periaatteen mukaisesti. Jokainen proteiinialayksikkö pystyy kiinnittymään isäntäsolun reseptoreihin, joten polyadhesiinit varmistavat monipistekiinnityksen. AAF/I:t käyttävät AggA- alayksiköiden välillä sijaitsevia ainutlaatuisia positiivisesti varautuneita pintoja kiinnittyäkseen fibronektiiniin. Myf-fimbrioiden alayksikön kiderakenne galaktoosin ja Psa-fimbrioiden alayksikön kiderakenne koliinin kanssa paljastivat reseptorien sitoutumiskohdat ja selittivät näiden patogeenisten *Yersinioiden* solutropismin erot. Fimbrioiden voimakas sitoutumiskyky ja kyky tunnistaa useita reseptoreita on merkittävä haaste lääkekehitykselle, ja korostaa multivalenttien inhibiittorien käytön tärkeyttä.

Arkaaisten CU-fimbrioiden biogeneesiä valottaaksemme olemme ratkaisseet CsuC-CsuA/B-kaitsija-alayksikkö -kompleksin ja itsekomplementoidun CsuA/B-alayksikön kiderakenteet *Acinetobacter baumannii* Csu-fimbrioista. Osoitimme, että arkaaisten fimbrioiden biogeneesi eroaa olennaisesti klassisesta CU-eritysjärjestelmästä sekä molekyyliarakenteeltaan että toimintamekanismiltaan. CsuC-kaitsijaproteiini käyttää ainutlaatuista alayksikön ankkurointimekanismia, johon proteiinin molemmat domainit osallistuvat. Lisäksi CsuC pitää CsuA/B-alayksikön vain osittain laskostettuna, mikä saattaa mahdollistaa joustavamman donori-säikeen vaihdon. Kaitsijaan sidotun alayksikön suojaan ydin on mahdollinen inhibiitiokohde, mikä saattaa auttaa kehittämään uusia mikrobilääkkeitä, joilla pystytään estämään arkaaisten CU-fimbrioiden muodostamista.

**ABBREVIATIONS**

<b>AAF</b>	Aggregative adherence fimbriae
<b>ABTS</b>	2,2'-azino-bis(3-ethylbenzothiazoline-6-sulphonic acid)
<b>CD</b>	Circular dichroism
<b>CFA/I</b>	Colonization factor antigen I (CFA/I), coli surface antigens
<b>CTD1</b>	C-terminal domain 1 (usher protein)
<b>CS</b>	Coli surface antigen
<b>CTD2</b>	C-terminal domain 2 (usher protein)
<b>CU</b>	Chaperone-usher
<b>DSC</b>	Donor strand complementation
<b>DSE</b>	Donor strand exchange
<b>DTTA</b>	N <sup>1</sup> -(p-isothiocyanatobenzyl)-diethylenetriamine-N <sup>1</sup> ,N <sup>2</sup> ,N <sup>3</sup> ,N <sup>3</sup> -tetraacetic acid
<b>EAEC</b>	Enterotoxigenic <i>Escherichia coli</i>
<b>ECDC/EMA</b>	European Center for Disease prevention and control/European Medicines Agency
<b>EDTA</b>	Ethylenediaminetetraacetic acid
<b>EHEC</b>	Enterohemorrhagic <i>Escherichia coli</i>
<b>ESRF</b>	European Synchrotron Radiation Facility
<b>ETEC</b>	Enterotoxigenic <i>Escherichia coli</i>
<b>FGL</b>	F1-G1 loop long (chaperone)
<b>FGS</b>	F1-G1 loop short (chaperone)
<b>Gd</b>	Donor strand of the pilin subunit
<b>HEPES</b>	4-(2-hydroxyethyl)-1-piperazineethanesulfonic acid
<b>Ig</b>	Immunoglobulin
<b>MSCRAMMs</b>	Microbial Surface Components Recognizing Adhesive Matrix Molecules

---

<b>NTD</b>	N-terminal domain (usher protein)
<b>PEG</b>	Polyethylene glycol
<b>SDS-PAGE</b>	Sodium dodecyl sulfate polyacrylamide gel electrophoresis
<b>Se-SAD</b>	Selenium single wavelength anomalous diffraction
<b>SPR</b>	Surface plasmon resonance
<b>S-SAD</b>	Sulfur single wavelength anomalous diffraction
<b>Stx2</b>	Shiga-toxin 2
<b>UPEC</b>	Uropathogenic <i>Escherichia coli</i>
<b>WHO</b>	World Health Organization

**ABBREVIATIONS OF THE AMINO ACID RESIDUES**

<b>A</b>	Ala	Alanine
<b>C</b>	Cys	Cysteine
<b>D</b>	Asp	Aspartic acid
<b>E</b>	Glu	Glutamic acid
<b>F</b>	Phe	Phenylalanine
<b>G</b>	Gly	Glycine
<b>H</b>	His	Histidine
<b>I</b>	Ile	Isoleucine
<b>K</b>	Lys	Lysine
<b>L</b>	Leu	Leucine
<b>M</b>	Met	Methionine
<b>-</b>	Mse	Selenomethionine
<b>N</b>	Asn	Asparagine
<b>P</b>	Pro	Proline
<b>Q</b>	Gln	Glutamine
<b>R</b>	Arg	Arginine
<b>S</b>	Ser	Serine
<b>T</b>	Thr	Threonine
<b>V</b>	Val	Valine
<b>W</b>	Trp	Tryptophan
<b>Y</b>	Tyr	Tyrosine



## 1. INTRODUCTION

*“The serious threat is happening right now in every region of the world and has the potential to affect anyone, of any age, in any country. Antibiotic resistance...is now a major danger to public health”*

- World Health Organization  
(WHO), 2014

### 1.1 General introduction

Bacteria, the pioneers of the Earth, have had a great impact on our planet. Nowadays this domain includes a tremendous number of species that have evolved to populate various ecosystems. Apart from inhabiting soil, atmosphere, water and living organisms, bacteria also dwell in hot springs, the Mariana Trench (Kato *et al.*, 1998) and even radioactive waste (Fredrickson *et al.*, 2004). Bacteria include photosynthetic organisms involved in the primary production of organic carbon by converting light energy into the energy of chemical bonds. During evolution, the activity of cyanobacteria led to the accumulation of oxygen enabling the emergence of aerobic forms of life. Bacteria play a major role in the biodegradation of complex organic materials thereby “recycling” the main elements that constitute all living organisms (Todar, 2012). The ability of some bacteria to convert atmospheric nitrogen into the nitrogen available for plants has a primary importance for agriculture. In industry, bacteria are employed in waste disposal, as well as the production of biofuels and various foods such as fermented dairy products and pickles.

Bacteria also have a major impact on our health. The bacterial cells of human flora significantly outnumber human cells in the whole body (Ouweland *et al.*, 2003). The gut microbiota participates in digestion, produces vitamins (B12 and K), and plays an important role in the functioning of the immune system (Villanueva-Millan *et al.*, 2015; Sears, 2005). Around 1% of bacteria cause various diseases in plants, humans and animals (Black, 1999). Despite this insignificant number, some pathogenic species have seriously endangered the well-being and even the existence of human civilization throughout history. The “Black Death”, the most devastating plague pandemic to date, killed half of Europe’s total population (Alchon, 2003). By the beginning of the 20<sup>th</sup> century, bacterial diseases accounted for one third of deaths around the world (Todar, 2012). The development of sanitation and hygiene, the discovery of antibiotics and

vaccines, and the technological progress in the diagnosis of infections have greatly improved disease control and prevention. However, pathogenic bacteria still represent a serious threat to global health (WHO, 2014). The emergence and the fast propagation of antibiotic resistance show that the war against bacterial diseases is still ongoing. Gram-negative bacteria acquire multidrug resistance at a frightening pace (Coque *et al.*, 2008; Unal *et al.*, 2005). In Europe alone, antibiotic-resistant infections claim the lives of 16,000 patients annually and account for an economic burden of 1.5 billion euro (ECDC/EMEA, 2009). In the absence of novel antimicrobial drugs, mortality from Gram-negative bacterial pathogens will inevitably increase over the next few years. Recent outbreaks of multi-resistant *Acinetobacter baumannii* and *Pseudomonas aeruginosa* infections in hospital care units worldwide illustrate the seriousness of the problem (McGrath *et al.*, 2011a, 2011b; Gomes *et al.*, 2012; Guo-Xin *et al.*, 2014). Growing antibiotic resistance and the lack of novel antimicrobial agents is “now threatening to take us back to the pre-antibiotic era” (ECDC/EMEA, 2009). To prevent devastating pandemics in the future, the discovery of new ways of treatment has to become a primary concern for humanity. This ambitious goal requires comprehensive knowledge on the major virulence factors of bacterial pathogens.

A bacterial infection starts with the colonization of a host. The process is dependent on the ability of bacteria to attach to target cells by recognizing their surface receptors. The attachment is mediated by filamentous surface organelles formed by the covalent (Gram-positive bacteria) or non-covalent (Gram-negative bacteria) polymerization of protein subunits (Proft & Baker, 2009). These organelles, termed bacterial adhesins (pili, or fimbriae), play an essential role in pathogenesis. In addition to the simple anchoring of bacteria to host tissues, adhesins promote the delivery of toxins and alter host cell signaling (Stones & Krachler, 2015). Adhesive structures are also implicated in the formation of biofilms, promoting bacterial survival and antibiotic resistance (Balcázar *et al.*, 2015). The assembly and secretion of bacterial adhesins is implemented through a variety of highly specialized and sophisticated secretion machineries (Costa *et al.*, 2015). In Gram-negative bacteria, the majority of adhesive fimbriae are assembled via the chaperone-usher (CU) secretion pathway.

## 1.2 The CU pathways

CU pathways mediate the biogenesis and secretion of versatile fimbrial organelles found in both pathogenic and non-pathogenic Gram-negative bacteria (Zav'yalov V. *et al.*, 2010). Pathogenic species expressing CU fimbriae cause a wide range of diseases, including life-threatening bubonic and pneumonic plague (*Yersinia pestis*), enteric typhoid fever (*Salmonella typhi*) and wound infections (*Acinetobacter baumannii*). CU fimbrial organelles were shown to play an important role in bacterial virulence. Thus, they are directly involved in host cell receptor recognition (Dodson *et al.*, 2001),

biofilm formation (Tomaras *et al.*, 2003; Wright *et al.*, 2007), and spore coat formation (Leng *et al.*, 2011).

A CU pathway includes one or several structural proteins (pilin subunits), a periplasmic chaperone and an outer membrane usher (Hung *et al.*, 1998). Upon synthesis, all elements of the CU pathway are transported into the periplasmic space via the Sec secretory pathway involving the cleavage of their signal peptides (Pugsley, 1993). Chaperones capture nascent pilin subunits in the periplasm and transport them to the usher protein. The usher governs the ordered assembly of pilin subunits into a linear polymer (Zavialov *et al.*, 2003) as well as its secretion across the outer membrane into the extracellular space (Dodson *et al.*, 1993; Saulino *et al.*, 1998; 2000, Nishiyama *et al.*, 2008; Phan *et al.*, 2011) (Figure 1):

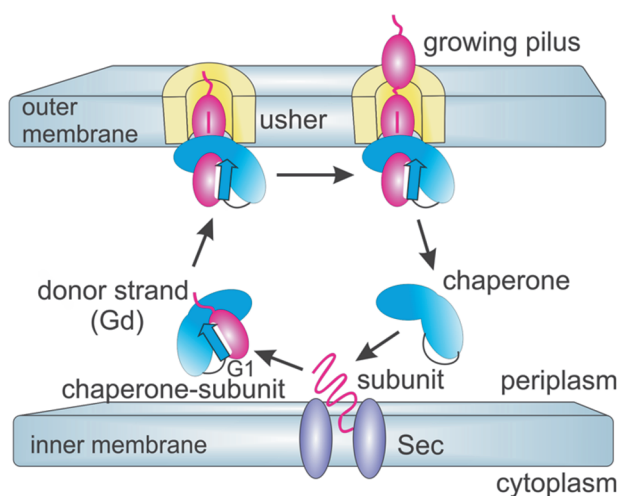


**Figure 1.** The scheme of the chaperone-usher (CU) pathway assembling fimbrial organelles on the bacterial surface

CU fimbriae are strikingly diverse. One group of CU organelles is represented by thick rigid or thin flexible pili of a complex subunit composition, whereas the other group shows a non-pilar, amorphous or capsule-like morphology (Zav'yalov *et al.*, 2010). Furthermore, CU fimbriae utilize different modes to bind the target receptor. Thus, the majority of pili possess only one highly specific adhesive site whilst amorphous CU organelles are capable of establishing multiple interactions with host cell receptors (Zavialov *et al.*, 2007). Considering the morphological and functional diversity of CU adhesins, the additional subdivision of the CU pathway into the phylogenically related groups is deemed necessary. Nuccio & Baumler (2007) proposed a categorization of CU fimbriae on the basis of their usher sequences, as it is the most conserved protein within the class. The phylogenetic analysis of 189 usher proteins revealed six distinct fimbrial clades ( $\alpha$ ,  $\beta$ ,  $\gamma$ ,  $\pi$ ,  $\kappa$ , and  $\sigma$ ), each sharing a common ancestor (Figure 2).

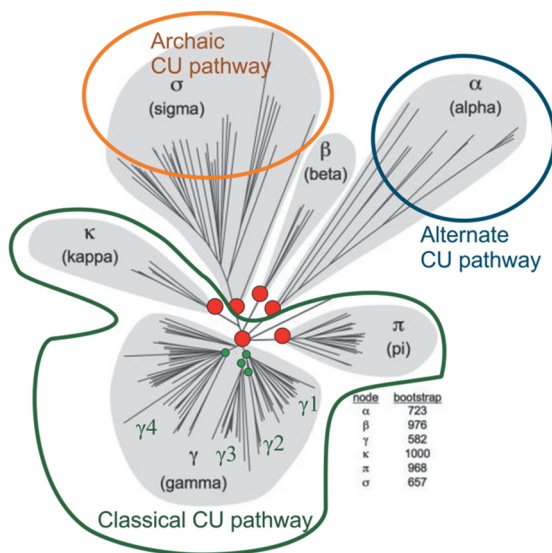


**Figure 2.** The phylogenetic tree of the fimbrial usher protein family generated by analyzing the amino acid sequences of 189 ushers (the redrawing is based on Nuccio & Baumler, 2007). The nodes of clades are shown as red circles, and the nodes of the  $\gamma$ -fimbrial clade are indicated as green circles.

The entire body of knowledge regarding the biogenesis of CU fimbriae is almost exclusively restricted to clades  $\gamma$ ,  $\pi$ , and  $\kappa$ , which, together with clade  $\beta$ , were designated “the classical CU pathway” (Nuccio & Baumler, 2007). The limited sequence homology of the two remaining clades of  $\alpha$ - and  $\sigma$ -fimbriae with regard to each other or the members of the classical CU pathway suggest the existence of so-called “non-classical” CU machineries, which are named alternative (alternate) and archaic systems, respectively (Nuccio & Baumler, 2007). According to our new results (unpublished data), clades  $\sigma$ ,  $\alpha$  and  $\beta$  belong to non-classical systems, whereas  $\gamma$ ,  $\pi$ , and  $\kappa$  are classical.

### 1.2.1 Classical CU pathway

According to the classification proposed by Nuccio & Baumler (2007), the classical CU pathway includes  $\beta$ -,  $\gamma$ - (subdivided into  $\gamma_1$ - $\gamma_4$ ),  $\pi$ -, and  $\kappa$ -fimbriae found in *Gammaproteobacteria* and *Betaproteobacteria*. Numerous pathogenic species assembling classical CU fimbriae include *Salmonella enterica*, *Yersinia pestis*, *Bordetella pertussis*, *Pseudomonas aeruginosa*, as well as uropathogenic, enterotoxigenic, and enteroaggregative *Escherichia coli* (EAEC).

Based on the structural features of chaperones and the composition of subunits in the fiber, classical fimbriae have been divided into two groups termed FGS-assembled and FGL-assembled fimbriae (Zav’yalov *et al.*, 1995; Hung *et al.*, 1996). Periplasmic chaperones with a short F1-G1 loop (FGS-subfamily) form a polyphyletic group comprising clades  $\beta$ ,  $\pi$ ,  $\kappa$ , and  $\gamma_1$ ,  $\gamma_2$ ,  $\gamma_4$ , and assemble highly diverse fimbrial structures (Nuccio & Baumler, 2007). Perhaps, the best-characterized FGS-assembled fimbriae

are the type 1 fimbriae and P-pili of uropathogenic *E. coli* (UPEC) (Figure 3, a) belonging to the  $\gamma_1$  and  $\pi$  clades, respectively. Both organelles have a complex subunit composition with a two-domain tip adhesin subunit (Figure 3, a) (Kuehn *et al.*, 1992; Buts *et al.*, 2003). Its C-terminal domain, which is structurally similar to the shaft-forming subunits, accepts a donor strand from the most distal polymerizing subunit, whereas the N-terminal domain exhibits the receptor-binding site (Kuehn *et al.*, 1992; Dodson *et al.*, 2001; Buts *et al.*, 2003; Hung *et al.*, 2002). Fimbriae possessing only one adhesive domain on the tip of the organelle are named mono adhesins (Zavialov *et al.*, 2007). In addition to mono adhesins, the FGS-chaperone subfamily also governs the biogenesis of morphologically and functionally different polyadhesins (Zavialov *et al.*, 2007), establishing multiple interactions with host cell receptors (Van den Broeck *et al.*, 2000; Chessa *et al.*, 2008) (Figure 3, b).

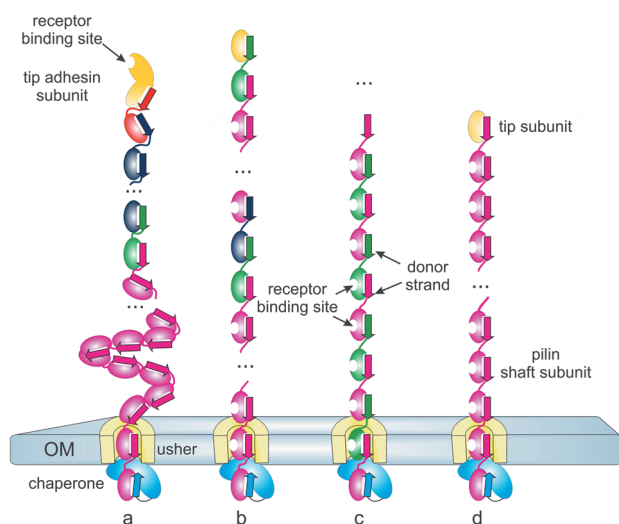


**Figure 3.** A schematic representation of FGS- and FGL-chaperone-assembled fimbriae:

- a - FGS-chaperone-assembled mono adhesive fimbriae (P-pili) (Kuehn *et al.*, 1992; Roberts *et al.*, 1994; Sauer *et al.*, 2000; 2004);
- b - FGS-chaperone-assembled heteropolyadhesin (K88, (F4) pili) (Van den Broeck *et al.*, 2000);
- c - FGL-chaperone-assembled heteropolyadhesin (CS6 colonization factor) (Roy *et al.*, 2012);
- d - FGL-chaperone-assembled homopolyadhesin (AfaE) (Anderson *et al.*, 2004).

In contrast to the FGS-chaperone subfamily, FGL-chaperones (long F1-G1 loop) form a monophyletic group of CU fimbriae belonging to the  $\gamma_3$ -clade. This class exclusively assembles polyadhesins composed of one or two distinct types of subunits, each possessing independent adhesive sites to host cell receptors (Zavialov *et al.*, 2007; Roy *et al.*, 2012) (Figure 3, c, d). This class of fimbriae includes Sef and Saf (*Salmonella enterica* and *S. paratyphi*, respectively), F1 and Psa (pH6) antigens (*Yersinia pestis*),

Myf fimbriae (*Y. enterocolitica*), aggregative adherence fimbriae (AAF), Dr (Afa) adhesins, as well as CS3 and CS6 antigens (*E. coli*).

As the classical CU systems have been studied for several decades, the general principle of their assembly is well documented and generally understood. Fimbrial subunits have an incomplete immunoglobulin (Ig) fold lacking the seventh  $\beta$ -strand G (Choudhury *et al.*, 1999; Sauer *et al.*, 1999; Sauer *et al.*, 2002; Zavialov *et al.*, 2003). The absence of one strand creates a deep hydrophobic cavity inside the protein core, making it vulnerable to aggregation and subsequent proteolysis in the periplasm (Jones *et al.*, 2002). To prevent degradation and facilitate proper folding, the nascent subunit is captured by the chaperone. The periplasmic chaperone adopts a fold with two Ig-like domains joined together perpendicularly (Figure 4) (Holmgren & Branden, 1989; Choudhury *et al.*, 1999; Knight *et al.*, 2002; Zavialov *et al.*, 2003). The subunit is anchored to the chaperone by electrostatic interactions formed between two conserved basic residues of the N-terminal domain of the chaperone and the C-terminus of the subunit (Kuehn *et al.*, 1993; Zavialov *et al.*, 2003). The chaperone stabilizes the subunit by inserting its G1 strand into the hydrophobic groove of the subunit in a parallel orientation (Choudhury *et al.*, 1999; Sauer *et al.*, 1999) (Figures 4, 5). This unique process of non-covalent interactions between chaperone and subunit is known as donor strand complementation (DSC) (Choudhury *et al.*, 1999). The G1 strand of the chaperone inserts three (FGS chaperones) or five (FGL chaperones) donor residues occupying corresponding acceptor pockets (named P1–P5) of the subunit hydrophobic groove (Figures 4, 5) (Sauer *et al.*, 2002; Zavialov *et al.*, 2003). Pocket P5 plays a key role in pilus polymerization governed by the process of donor strand exchange (DSE) (Choudhury *et al.*, 1999; Zavialov *et al.*, 2003; Remaut *et al.*, 2006). The structural motif at the N-terminus of the incoming pilin subunit (termed donor strand (Gd)) replaces the donor strand of the chaperone and creates the more energetically favorable antiparallel Ig-fold (Zavialov *et al.*, 2005) (Figure 5). Subunit polymerization starts when the incoming pilin subunit inserts its P5 residue in the P5 pocket (initiation site) (Remaut *et al.*, 2006; Yu *et al.*, 2012a) (Figure 5). The hydrophobic residues of the chaperone are then gradually replaced by the Gd strand of the subunit in “zip-in-zip-out” mode (Zavialov *et al.*, 2003; Remaut *et al.*, 2006; Rose *et al.*, 2008).

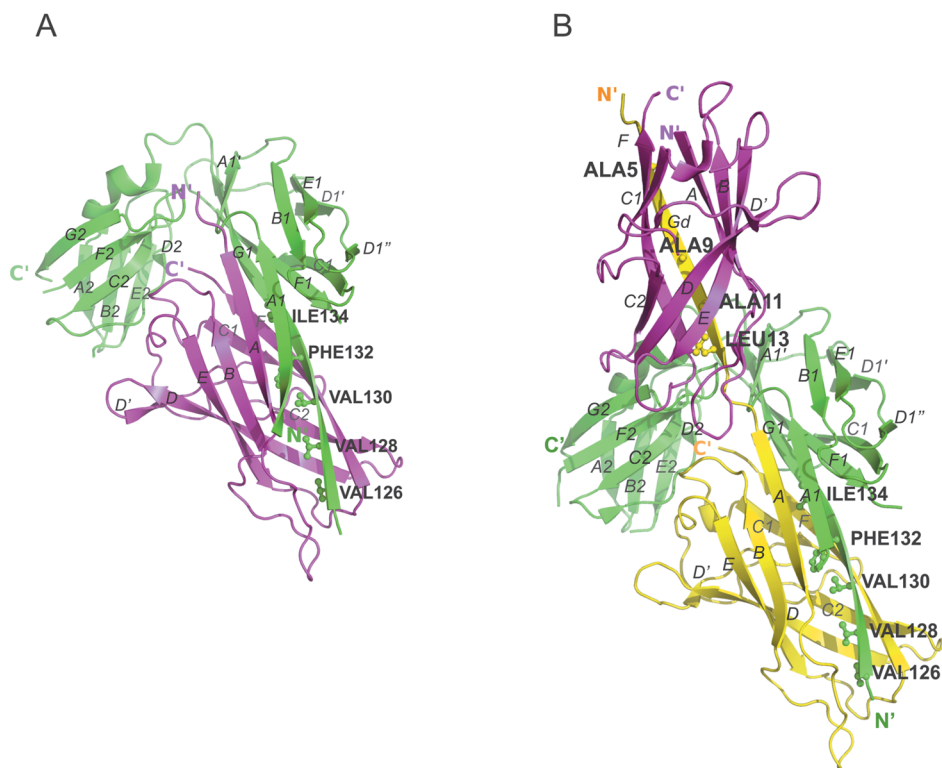


**Figure 4.** The high-resolution structure of the Caf1M-Caf1 preassembly complex (A) and F1-antigen mini-fiber (Caf1M-Caf1'-Caf1'') (B), cartoon representation (PDB codes 1P5V and 1Z9S). Caf1M, Caf1', Caf1'' are colored in green, magenta and yellow, respectively. The  $\beta$ -strands as well as N- and C-termini are indicated. Donor residues are shown as ball-and-sticks and labeled.

Interestingly, subunit assembly is independent of cellular energy (Jacob-Dubuisson *et al.*, 1994). The adoption of the canonical antiparallel Ig-fold significantly increases the stability of the subunits in the fiber in comparison with the subunit-chaperone complex (Zavialov *et al.*, 2005). The chaperone “traps” the subunit in a high-energy conformation state and prevents the folding from being completed. Thereby the chaperone preserves a part of this folding energy, which is used to drive fiber formation (Zavialov *et al.*, 2003). DSE leads to the collapse of the subunit’s hydrophobic core and its optimal “closed” conformation (Zavialov *et al.*, 2005; Vitagliano *et al.*, 2008).

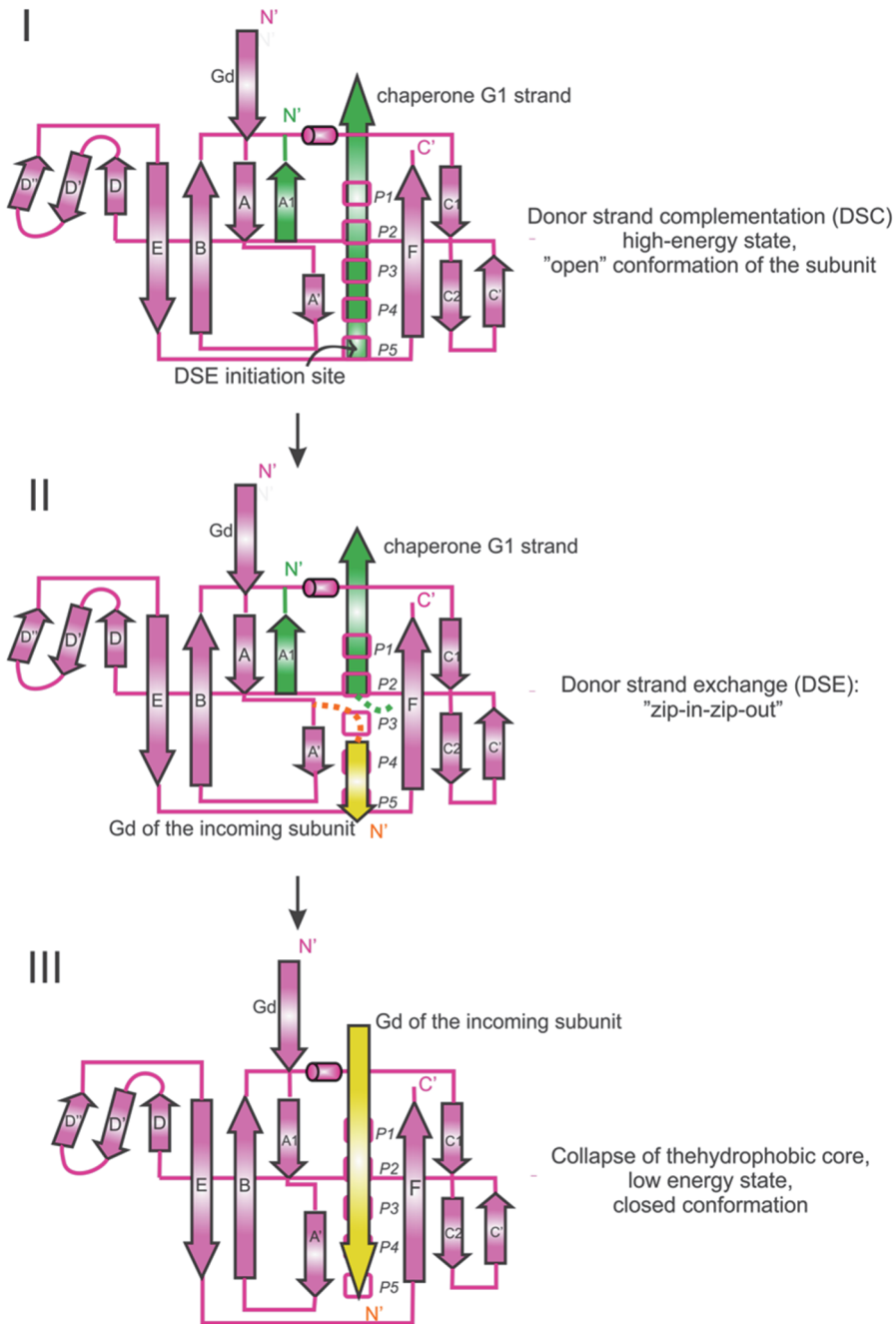


**Figure 5.** Donor strand complementation (DSC) and donor strand exchange (DSE) mechanisms in the pilus assembly; the topology diagrams are based on the structures published by Zavialov *et al.* (2003; 2005) (PDB codes 1P5V and 1Z9S).



The process of subunit polymerization is governed by an usher assembly platform. The usher comprises a membrane-spanning domain, a periplasmic N-terminal domain (NTD), a plug domain, and two C-terminal domains (CTD1 and CTD2) (Thanassi *et al.*, 2002; Nishiyama *et al.*, 2005; Capitani *et al.*, 2006; Yu *et al.*, 2009; Dubnovitsky *et al.*, 2010; Phan *et al.*, 2011; Yu *et al.*, 2012b) (Figure 6). Structural and biochemical studies on various CU systems have helped to understand the role of the usher in the assembly process of classical CU fimbriae.

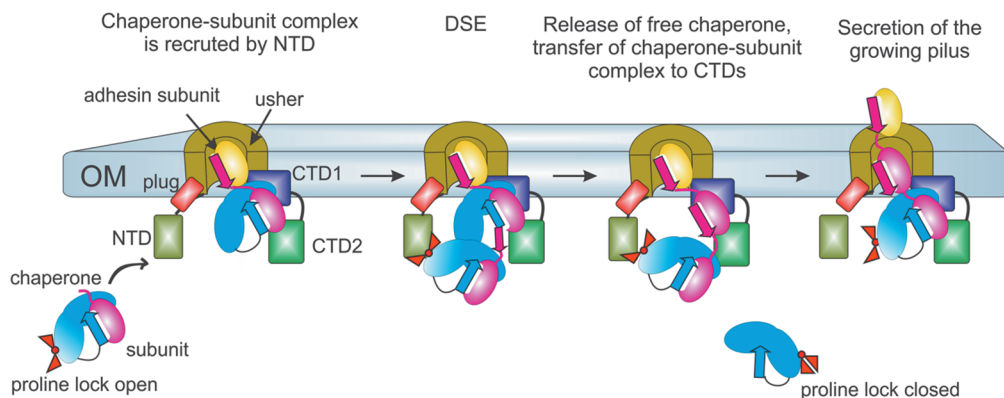


**Figure 6.** The proposed model of pilus assembly via the CU pathway (OM – outer membrane, DSE – donor strand exchange, NTD – usher’s N-terminal domain, CTD1 and CTD2 – usher’s C-terminal domains 1 and 2).

Both NTD and CTDs can recruit two chaperone-subunit complexes simultaneously (Ng *et al.*, 2004). CTDs accommodate a chaperone-subunit complex at the proximal end of the growing pilus (Phan *et al.*, 2011), whereas the NTD domain recruits new chaperone-subunit complexes (Nishiyama *et al.*, 2005; Yu *et al.*, 2012b). The chaperone-usher interactions are allosterically regulated (Yu *et al.*, 2012b). A conserved “proline lock” of the free chaperone prevents its binding to the usher (Figure 6). The formation of the chaperone-subunit complex rotates the proline lock away and opens the usher-binding surface of the chaperone. The close positioning of the subunits on the NTD and CTDs of the usher initiates the process of DSE (Zavialov *et al.*, 2003; Phan *et al.*, 2011). Upon the subunit’s polymerization, the subunit-free chaperone leaves the CTD binding pocket. The next step involves the transfer of the chaperone-subunit complex from the NTD to the CTD and the secretion of the distal subunit through the usher pore towards the cell surface (Figure 6) (Kuehn *et al.*, 1993; Thanassi *et al.*, 2002, Nishiyama *et al.*, 2005; 2008; Li *et al.*, 2004; Remaut *et al.*, 2008).

### 1.2.1.1 Aggregative adherence fimbriae (AAF) in the pathogenesis of Enteroaggregative *Escherichia coli* (EAEC)

Enteroaggregative *Escherichia coli* (EAEC) infections are commonly associated with diarrhea in infants, travellers and immunocompromised patients (Harrington *et al.*, 2006). The characteristic feature of all EAEC strains is their attachment to the intestinal mucosa in a stack-brick adherence manner (Nataro *et al.*, 1987; 1995). The attachment is mediated by aggregative adherence fimbriae (AAF) belonging to the FGL group of CU adhesins. Five variants of AAF (I–V) are currently known. The AAF are long flexible fibers found in bundles (AAF/I, AAF/II) or existing as individual filaments (AAF/III) (Nataro *et al.*, 1993; Czczulin *et al.*, 1997). Similarly to other representatives of the Afa/Dr group, each fiber is a polymer of major subunits (A) capped with a minor subunit (B). In contrast to the relatively conserved minor subunits, the major subunits of the different AAF variants are highly variable. The low sequence similarity of the major subunits and differences in erythrocyte agglutination (Boisen *et al.*, 2008) indicate that different AAF variants might recognize different receptors. It has been previously shown that AAF/II binds to laminin, fibronectin and type IV collagen, but the mechanism of the adhesion is not currently known (Farfan *et al.*, 2008). The receptor-binding specificity of other AAF variants is yet to be determined. Apart from their purely adhesive function, AAF were shown to trigger an inflammatory response by increasing cytokine production (Harrington *et al.*, 2005), and to promote biofilm formation on abiotic surfaces (Sheikh *et al.*, 2001).

All AAF variants are encoded by a pAA virulence plasmid, and their expression is regulated by the *aggR* gene, which is also located on the pAA (Vial *et al.*, 1988). Different strains of EAEC usually express only one variant of AAF (Harrington *et al.*, 2006). In addition to AAF, EAEC produce other virulence factors, including ShET1 (*Shigella* enterotoxin 1) (Navarro-Garcia *et al.*, 1998), Pet (plasmid-encoded toxin) (Eslava *et al.*, 1998), EAST1 (EAEC heat-stable enterotoxin 1) (Savarino *et al.*, 1993) and autotransporters (Navarro-Garcia *et al.*, 2011). Interestingly, the set of virulence factors is unique for each isolate (Navarro-Garcia *et al.*, 2014). The recently emerged EAEC O104:H4 strain responsible for a severe outbreak of hemorrhagic diarrhea in 2011 additionally produces Shiga-toxin 2 (Stx2) (Nataro *et al.*, 2011), commonly expressed by enterohemorrhagic *E. coli* (EHEC). Interestingly, the Stx2-producing EAEC O104:H4 strain was far more virulent than EHEC. One of the reasons might be the presence of EAEC-specific AAF (AAF/I variant), enabling the tight adhesion of bacteria to the intestinal mucosa (Navarro-Garcia *et al.*, 2014). Interactions of AAF/I with host cells lead to the disruption of the epithelial barrier and consequently to the faster absorption of Stx2 (Boisen *et al.*, 2015). Thereby, the “cocktail” of virulence factors acquired from both EAEC and EHEC explains the severe outcome of the EAEC O104:H4 infection, which accounted for 54 deaths and 845 cases of hemolytic uremic syndrome (Frank *et al.*, 2011; Navarro-Garcia *et al.*, 2014).

The emergence of the Stx-producing EAEC O104:H4 strain raises the concern that other virulent clones of EAEC might appear in the future. To be able to address this challenge, further research into EAEC pathogenesis is required. Structural and biochemical studies of different AAF variants will provide important insights into the adhesion mechanisms governing the initial stage of the infection.

### 1.2.1.2 Myf and Psa fimbriae in the pathogenesis of *Yersinia*

The genus of *Yersinia* contains three pathogenic species: *Y. pestis*, *Y. pseudotuberculosis* and *Y. enterocolitica*. Despite their phylogenetic propinquity (97% genome identity), these pathogens utilize various routes of transmission and cause strikingly different diseases (Galindo *et al.*, 2011). Plague caused by *Y. pestis* is spread via a bite from an infected flea (Anisimov *et al.*, 2004) or via air droplets from human to human (Perry & Fetherston, 1997). Airborne transmission leads to the most severe and highly fatal pneumonic plague (Perry & Fetherston, 1997). Yersiniosis, mostly caused by *Y. enterocolitica* and less commonly by *Y. pseudotuberculosis*, is spread exclusively via the fecal-oral route (Galindo *et al.*, 2011). Intriguingly, *Y. pseudotuberculosis* can additionally cause a lethal lung infection, similar to pneumonic plague in guinea pigs and some mice (Wagner *et al.*, 1976; Paczosa *et al.* 2014; Worsham *et al.*, 2012).

All three pathogenic *Yersinia* species elaborate adhesive organelles via the CU pathway (Mikula *et al.*, 2012). Closely related *Y. pseudotuberculosis* and *Y. pestis* assemble Psa fimbriae, whereas *Y. enterocolitica* forms the mycoid *Yersinia* factor, or Myf fimbriae. Both Psa and Myf fimbriae are expressed *in vivo* at 37°C and low pH (< 6) (Lindler & Tall, 1993; Iriarte *et al.*, 1993; 1995). The presence of Psa fimbriae was shown to be important for the virulence of *Y. pestis*. In particular, Psa contributes to the translocation of cytotoxic Yops to the host cells via the dedicated type III secretion system (Felek *et al.*, 2010) and inhibits phagocytosis by macrophages (Huang & Lindler, 2004). Purified Psa also binds to  $\beta$ 1-linked galactosyl residues in glycosphingolipids (Payne *et al.*, 1998). Additionally, Psa fimbriae mediate the colonization of lungs by interacting with phosphatidylcholine, the major component of pulmonary surfactant (Liu *et al.*, 2006; Galván *et al.*, 2007). The structural basis for the Psa-mediated receptor recognition was recently determined (Bao *et al.*, 2013).

In contrast to Psa, the implication of Myf fimbriae in the pathogenesis of yersiniosis remains unclear. The presence of Myf only in the pathogenic serotypes of *Y. enterocolitica* suggests its potential importance for virulence (Iriarte *et al.*, 1993). Furthermore, the high degree of sequence identity (44%) between the pilin subunits of Myf and Psa indicates that the adhesins play a similar role in the infection (Lindler *et al.*, 1990; Lindler & Tall, 1993).

### 1.2.2 Alternative (alternate) CU pathway

The alternative CU pathway assembles a relatively small (15 representatives from *Gammaproteobacteria* and 1 representative from *Betaproteobacteria*) but surprisingly divergent group of fimbriae. Members of this family have been found in pathogenic species including enterotoxigenic *Escherichia coli* (ETEC), *Burkholderia cepacia*, *Yersinia pestis*, as well as *Salmonella enterica* Typhi and Paratyphi (Nuccio & Baumber, 2007). Furthermore, the alternative fimbriae were shown to contribute directly to bacterial virulence. Thus, colonization factor antigen I (CFA/I), coli surface antigens (CS1, CS2, CS4, and CS5 of ETEC mediate the colonization of the human small intestine (Gaastra & Svennerholm, 1996; Viboud *et al.*, 1996).

Earlier studies revealed that the assembly of fimbriae via the alternative CU pathway requires four essential proteins: a periplasmic chaperone, an usher, a polymerizing shaft subunit, and a tip subunit serving as an adhesin (Sakellaris *et al.*, 1996; Sekellaris & Scott, 1998; Voegelé *et al.*, 1997; Poole *et al.*, 2007). High-resolution structures of the CfaEdsc tip adhesin subunit (Li *et al.*, 2007), CfaB major subunit (Li *et al.*, 2009), and CfaA chaperone (Bao *et al.*, 2014) from CFA/I enabled the elucidation of the overall architecture of alternative fimbriae.

Despite the low sequence similarity between alternative and classical CU machineries, the architecture of CFA/I resembles that of type 1 fimbriae. This phenomenon might be explained by the convergent evolutionary specialization of these fimbriae to the same host microenvironment (Poole *et al.*, 2007; Li *et al.*, 2007; 2009).

Both the CfaB major subunit and the CfaEdsc tip adhesin subunit from CFA/I structurally resemble the Ig-like domain structure of the corresponding subunits FimA and FimH from type 1 fimbriae (Li *et al.*, 2007; 2009). CfaB displays one Ig-folded domain (Li *et al.*, 2009), whereas CfaEdsc comprises two Ig-like domains connected with a short linker (Li *et al.*, 2007). The N-terminal domain of CfaE mediates the specific attachment of the fimbriae to host cell receptors, whilst the C-terminal domain connects the subunit to the tip of the fiber (Poole *et al.*, 2007). In contrast to the relatively flexible FimH subunit from the classical CU pathway, the CfaE domains form a rigid structure with limited motility (Li *et al.*, 2007). Conserved basic residues (Arg67 and Arg181) located at the upper surface of the CfaE N-terminal domain form the binding site, presumably for negatively charged sialylated receptors (Li *et al.*, 2007).

Structural data demonstrate that alternative fimbriae utilize similar mechanisms of DSC and DSE to drive the assembly of subunits (Poole *et al.*, 2007; Li *et al.*, 2007). However, low sequence identity between the assembly proteins of classical and alternative CU pathways suggests significant differences in chaperone-subunit and

subunit-subunit interactions (Nuccio & Baumber, 2007; Soto & Hultgren, 1999). Indeed, the recently determined structure of the CfaA chaperone displays unique features, distinguishing it from both FGL and FGS chaperones (Bao *et al.*, 2014). On the one hand, CfaA possesses a long F1-G1 loop specific to FGL chaperones. On the other hand, similarly to FGS chaperones, CfaA lacks a disulfide bridge that is supposed to stabilize the F1-G1 loop (Bao *et al.*, 2014). In contrast to both FGS and FGL chaperones, CfaA exhibits D1' and C2-D2' insertions that might be important for subunit capturing. A different set of residues at the inter-domain cleft of the chaperone might also indicate a unique subunit anchoring mechanism (Bao *et al.*, 2014).

Despite the significant progress that has been made towards the understanding of alternative fimbriae architecture, further structural and functional studies are required to elucidate their biogenesis. High-resolution structures of chaperone-subunit binary complexes will provide necessary information for unraveling the precise mechanism of pilus assembly via the alternative CU pathway.

### 1.2.3 Archaic CU pathway ( $\sigma$ -fimbriae)

The archaic CU pathway comprises the most ubiquitous group of fimbriae. Numerous representatives of  $\sigma$ -fimbriae were identified in *Alpha*-, *Beta*-, *Gamma*-, and *Deltaproteobacteria* as well as in the phyla *Deinococcus-Thermus* and *Cyanobacteria* (Nuccio & Baumber, 2007). Bacteria assembling archaic fimbriae include non-pathogenic soil, marine and aquatic microbes as well as various plant and human pathogens. Pathogenic species cause serious diseases, such as plague (*Yersinia pestis*), pneumonia (*Acinetobacter baumannii*, *Burkholderia cepacia*), septicemia (*A. baumannii*, *Vibrio vulnificus*), and cystic fibrosis (*Pseudomonas aeruginosa*), and they primarily affect immunocompromised individuals. Interestingly, archaic CU fimbriae are found in many multidrug-resistant pathogens (Nuccio & Baumber, 2007). Thus, *A. baumannii* and *P. aeruginosa*, the two pathogens of the ESKAPE group acquiring antibiotic resistance most rapidly (Tommasi *et al.*, 2015), express homologous archaic fimbriae (Nuccio & Baumber, 2007; Tomaras *et al.*, 2003; Giraud & de Bentzmann, 2012). Plant pathogens, including species of *Xanthomonas*, *Erwinia* and *Acidovorax*, infect a large group of economically important plants, such as citrus and apple trees, rice, cotton, and potato (Nuccio & Baumber, 2007). The caused crop diseases often have devastating consequences for agriculture and might lead to a complete loss of the harvest.

Despite the wide phylogenetic distribution of archaic fimbriae and their significance for both medicine and agriculture, neither the structural organization nor the precise assembly mechanisms of these organelles are currently known. Recent biochemical studies of the Mcu system of *Myxococcus xanthus* demonstrate that Mcu assembly is governed by a DSE mechanism similar to that of the classical systems (Zhu *et al.*,

2013; Wu *et al.*, 2014). However, subunit anchoring in archaic systems is likely to occur through a different mechanism (Zhu *et al.*, 2013). In classical fimbriae, two basic residues of the chaperone interact with the C-terminal carboxyl groups of the subunit (Kuehn *et al.*, 1993; Zavialov *et al.*, 2003). However, the corresponding residues of the archaic Mcu chaperone were dispensable for chaperone function (Zhu *et al.*, 2013). To elucidate the precise molecular mechanism of archaic pili biogenesis, high-resolution structural studies are required.

### 1.2.3.1 *Acinetobacter baumannii* infections and Csu fimbriae

Multidrug-resistant *Acinetobacter baumannii* thriving in the hospital environment has quickly become one of the most difficult Gram-negative bacteria to control and treat (Maragakis & Perl, 2008). This opportunistic pathogen targets immunocompromised individuals and causes a wide range of infections, including pneumonia, meningitis, septicemia and urinary tract infections. The resistance of *A. baumannii* to almost all available antibiotics poses a serious threat to patients. As the pathogen usually affects individuals with severe underlying illnesses, its impact on the mortality rate is hard to evaluate. However, *A. baumannii* infections certainly correlate with increased morbidity and the length of the hospital stay (Maragakis & Perl, 2008).

The extraordinary ability of *A. baumannii* to survive on abiotic surfaces contributes to the severity of its outbreaks in health care units around the globe (Bergogne-Bérézin & Towner, 1996). The pathogen was shown to colonize various objects, including glass and plastic medical equipment and tools, hospital furniture, curtains, and bed linen (Wilks *et al.*, 2006). The outstanding survival properties and remarkable antibiotic resistance of *A. baumannii* are likely to be associated with the formation of dense biofilms on biotic and abiotic surfaces (Tomaras *et al.*, 2003). Tomaras *et al.* (2003; 2008) demonstrated that the biofilm formation in *A. baumannii* is mediated by archaic Csu pili composed of CsuA/B, CsuA, CsuB, and CsuE subunits assembled by the chaperone CsuC and the usher CsuD. The authors confirmed the importance of  $\sigma$ -fimbriae for bacterial virulence, as the disruption of *csuC* and *csuE* gene expression abrogated pilus assembly and biofilm formation (Tomaras *et al.*, 2003). Intriguingly, another multi-resistant pathogen, *Pseudomonas aeruginosa*, forms Csu-homologous CupE pili that play a significant role in the development of biofilms enabling the pathogen to evade host immune defense and preventing the penetration of antibacterial drugs (Giraud *et al.*, 2011; Giraud & de Bentzmann, 2012).

The exceptional antibiotic resistance of both *A. baumannii* and *P. aeruginosa* underlines the necessity for novel therapeutic approaches to counter these infections. Targeting the assembly of biofilm-mediating pili represents a promising alternative to traditional antibiotics.

### 1.3 Applications of adhesive organelles in medicine

The fimbrial adhesins of pathogenic Gram-negative bacteria play a key role in establishing infections by mediating the attachment to target tissues, biofilm formation, and evasion of host immune defense (Zav'yalov *et al.*, 2010; Lo *et al.*, 2013). CU fimbriae are considered to be indispensable tools for bacterial pathogenesis, as strains deprived of these organelles display drastically reduced virulence (Cegelski *et al.*, 2008). Thus, bacterial adhesins are promising targets for the next generation of antibacterial drugs (Zav'yalov *et al.*, 2010; Geibel & Waksman, 2014). The concept of disarming bacteria by attacking their virulence factors has a significant advantage over traditional antimicrobial therapy. The inhibition of bacterial adhesion without placing an immediate life threat on the pathogen will allow for natural clearance of the infection and prevent the development of drug resistance (Zav'yalov *et al.*, 2010). Additionally, the specific targeting of virulence factors will minimize the risk of dysbiosis often associated with broad-spectrum antibiotics (Lo *et al.*, 2013).

Two general strategies of bacterial virulence attenuation are currently explored (Cusumano & Hultgren, 2009). The first approach involves the specific inhibition of bacterial adhesion to host cells by introducing agents mimicking host-cell receptors. This strategy of competitive binding was shown to be successful for the treatment of urinary tract infections (Cusumano *et al.*, 2011; Jiang *et al.*, 2012). Mannosides exhibiting the natural FimH binding determinant D-mannose prevented biofilm formation and the adhesion of UPEC to epithelial cells (Bouckaert *et al.*, 2005). However, this approach is only relevant for monovalent adhesins displaying one high affinity site to a particular receptor. Deceiving the bacteria with receptor analogues might be problematic in the case of polyadhesins possessing multiple binding sites along the fimbriae (Lo *et al.*, 2013).

Another approach to targeting bacterial virulence involves the interruption of fimbriae biogenesis at different stages. Structural data demonstrate that the binding of the chaperone-subunit complex to the usher assembly platform is critical for the formation of fimbriae (Phan *et al.*, 2011). This observation led to the development of pilicides, derivatives of dihydrothiazolo ring-fused 2-pyridones (Svensson *et al.*, 2001; Pinkner *et al.*, 2006). Pilicides were shown to prevent interactions of the N-terminal domain of the usher with the chaperone-subunit complex and to effectively inhibit the biogenesis of P pili, type 1 and Dr fimbriae of UPEC (Chorell *et al.*, 2010; Greene *et al.*, 2014; Piatek *et al.*, 2013). However, additional studies are required to evaluate the effect of pilicide-treated bacteria *in vivo* (Lo *et al.*, 2013). New structural data on fimbriae biogenesis might provide novel inhibition targets fueling the development of other virulence-attenuating compounds.

Apart from pure drug design applications, CU fimbriae, particularly highly immunogenic polyadhesins, can also be used for the accurate diagnosis of infections as well as vaccine development (Zav'yalov *et al.*, 2010). For example, a vaccine based on the F1 and V antigens of *Y. pestis* provides a high degree of protection against pneumonic plague (Powell *et al.*, 2005; Williamson *et al.*, 2005). In addition, passive immunization with monoclonal antibodies against F1-antigen can serve as an effective post-exposure treatment for the *Y. pestis* infection (Anderson *et al.*, 1997; Hill *et al.*, 2006). Monoclonal antibodies to SefD or SafD fimbrial subunits can be used to distinguish main *Salmonella* infections (Zav'yalov *et al.*, 2010).

The recent discovery of non-classical CU pathways opened new horizons for the further exploration of fimbrial organelles. Non-classical fimbriae are present in various classes of bacteria, including a vast number of human and plant pathogens. Thorough research into archaic and alternative fimbriae biogenesis will provide new insights into the mechanisms of bacterial virulence and facilitate further drug development efforts.



## 2. AIMS OF THE STUDY

The aim of this thesis is to explore the mechanism and biological significance of the polyvalent attachment of fimbrial adhesins to host cell receptors and elucidate the assembly mechanism of fimbriae via the archaic chaperone-usher (CU) pathway. This study is of fundamental and practical significance. Unraveling the molecular grounds for polyadhesin-mediated attachment and archaic fimbriae biogenesis will provide important insights into how to fight bacterial infections by suppressing either pilus assembly or host-pathogen interactions. Novel structural data can be directly employed in the development of novel anti-adhesion drugs against Gram-negative bacteria, including multi-resistant *Acinetobacter baumannii*.

The specific objectives of the study are:

1. to determine the high-resolution structures of fimbrial subunits from aggregative adherence fimbriae type I (AAF/I), Psa and Myf polyadhesins;
2. to elucidate the structural basis for host receptor recognition mediated by the above-mentioned fimbriae;
3. to determine the high-resolution structures of the donor strand complemented major subunit CsuA/B and the chaperone-major subunit CsuC-CsuA/B pre-assembly complexes from the archaic Csu CU system;
4. to analyze the mechanism of donor strand exchange in the CsuC-CsuA/B preassembly complex.

### 3. MATERIALS AND METHODS

#### 3.1 Design of donor strand complemented monomers and expression construct CsuC-CsuA/B (original publications I–V)

Donor strand-complemented (DSC) pilin subunits (AggAdsc, AggBdsc, PsaAdsc, MyfAdsc, and CsuA/Bdsc) were engineered by placing residues corresponding to the N-terminal donor strand at the C-terminus extended with a DNKQ linker (AggAdsc, AggBdsc, PsaAdsc, and MyfAdsc) or GG-linker (CsuA/Bdsc). A His6-tag was added after the signal peptide cleavage site to all constructs, except AggBdsc and PsaAdsc. All protein sequences were ordered from GenScript and placed under the T7-promoter of the pET101D expression vector (Invitrogen). To produce the recombinant CsuC-CsuA/B complex, co-expression plasmid pET101-CsuC-6HCsuA/B was created. Residues 4–12 in the mature sequence of CsuA/B were replaced with a His6-tag.

#### 3.2 Protein expression (original publications I–V)

The expression plasmids were transformed into *Escherichia coli* strain BL21-AI (Invitrogen). *E. coli* transformants were cultivated in Luria-Bertani medium containing ampicillin ( $100 \mu\text{g ml}^{-1}$ ) at 310 K. To initiate the expression of a target protein, cells grown to an optical density of 0.8–1 at 600 nm were induced with 1 mM isopropyl  $\beta$ -D-1-thiogalactopyranoside and 0.2 % of arabinose. After induction, the culture was further grown for 2.5 hours. Induced bacterial cells were subjected to osmotic shock. CsuC-CsuA/B, CsuA/Bdsc, MyfAdsc, PsaAdsc, and AggBdsc were extracted with 5 mM magnesium sulfate (periplasmic fraction), whereas AggAdsc was found in the sucrose fraction (20 % sucrose, 5 mM EDTA, 50 mM Tris-HCl pH 8.0).

#### 3.3 Protein purification

##### 3.3.1. Purification of His6-tagged proteins (AggAdsc, MyfAdsc, CsuC-CsuA/B, and CsuA/Bdsc) (papers I, III–VI)

The purification of His6-tagged proteins started with the Ni-chelate chromatography of dialyzed protein extracts. The composition of buffers used for various purification

steps is listed in Table 1. A 5–500 mM gradient of imidazole was used to elute the proteins. Further purification was performed using cation-exchange chromatography (AggA, CsuC-CsuA/B, and CsuA/Bdsc) or anion-exchange chromatography (MyfAdsc) (Table 1). The proteins were eluted with a 0–300 mM (AggA, CsuC-CsuA/B, and CsuA/Bdsc) or 0–600 mM (MyfAdsc) gradient of sodium chloride at 277 K. Prior to crystallization, AggAdsc, MyfAdsc and CsuA/Bdsc were additionally loaded on a Superdex 75 gel-filtration column (GE Healthcare) at 277 K. For the crystallization of CsuA/Bdsc, reductive methylation of lysine residues was performed prior to gel-filtration.

**Table 1.** Composition of buffers used for protein purification

Protein	Ni-chelate chromatography	Cation-exchange chromatography	Anion-exchange chromatography	Gel-filtration
AggAdsc	20 mM sodium phosphate, pH 7.4, 0.5 M sodium chloride, 5 mM imidazole	50 mM HEPES, pH 7.5	-	50 mM HEPES, pH 7.5, 150 mM sodium chloride
AggBdsc	-	20 mM HEPES, pH 7.2	20 mM Tris-HCl, pH 8.5	50 mM HEPES, pH 7.5, 150 mM sodium chloride
MyfAdsc	50 mM sodium phosphate, pH 8.0, 300 mM sodium chloride, 10 mM imidazole	-	20 mM Tris-HCl, pH 8.0	20 mM HEPES, pH 7.4, 150 mM sodium chloride
PsaAdsc	-	20 mM sodium acetate, pH 4.1	20 mM Tris-HCl, pH 7.8	20 mM HEPES, pH 7.4, 150 mM sodium chloride
CsuC-CsuA/B	20 mM sodium phosphate, pH 7.4, 0.5 M sodium chloride, 5 mM imidazole	50 mM HEPES, pH 7.2	-	-
CsuA/Bdsc	20 mM sodium phosphate, pH 7.4, 0.5 M sodium chloride, 5 mM imidazole	20 mM HEPES, pH 7.4	-	20 mM HEPES, pH 7.4, 150 mM sodium chloride

### 3.3.2. Purification of His6-tag-free AggBdsc and PsaAdsc (papers II, III)

His-tag-free proteins were purified using ion exchange chromatography (Table 1). The dialyzed periplasmic extract containing AggBdsc was first filtrated through a 20 ml Source 30Q column (GE healthcare). The PsaAdsc-containing periplasmic extract was loaded on a Source 30S column (GE Healthcare), and the protein was eluted with a 0–

300 mM gradient of sodium chloride. Further purification steps included cation exchange (AggBdsc) or anion exchange chromatography (PsaAdsc) with a 0–300 mM gradient of sodium chloride, followed by size-exclusion chromatography. The composition of buffers is indicated in Table 1.

### 3.4 Incorporation of selenomethionine (papers III–VI)

Selenomethionine was incorporated into MyfAdsc, CsuC-CsuA/B, and CsuA/Bdsc. *E. coli* BL21-DE3 transformants were grown in Luria-Bertani medium supplemented with ampicillin (100 mg ml<sup>-1</sup>) overnight at 310 K. The next morning, the cells were harvested by centrifugation (4000 g, 5 min) and suspended in M9 minimal medium (Doubl  , 2007) containing ampicillin (100 mg ml<sup>-1</sup>) at 310 K. Thirty minutes prior to induction, selenomethionine (50 mg l<sup>-1</sup>), lysine (100 mg l<sup>-1</sup>), valine (50 mg l<sup>-1</sup>), phenylalanine (100 mg l<sup>-1</sup>), threonine (100 mg l<sup>-1</sup>), isoleucine (50 mg l<sup>-1</sup>), and leucine (50 mg l<sup>-1</sup>) were added to the growing cells. The induction of protein expression and protein extraction were performed as described in 3.2.

### 3.5 Protein crystallization (papers I–IV, VI)

Prior to crystallization, the purity of all protein samples was verified using SDS-PAGE. Proteins were concentrated prior to crystallization experiments in a Vivaspin device with a molecular weight cut-off of 5 kDa (AggA, AggB, PsaA, MyfA, and CsuA/B) or 30 kDa (CsuC-CsuA/B). Initial crystallization conditions were obtained by the “sitting-drop” vapor-diffusion method using commercial screening kits: Index-HR2-144, Crystal Screen HT-HR2-130 and I+II (Hampton Research, USA), JCSG+ Suite (Qiagen), and PACT premier (Molecular dimensions). Optimization of the crystallization conditions was carried out manually by the “hanging drop” vapor-diffusion method. The optimized crystallization conditions for each protein are given in Table 2.

### 3.6 X-ray diffraction data collection (papers I–IV, VI)

Crystals were soaked for 30–60 s in cryoprotection solution (reservoir solution complemented with 30% PEG 400) and then frozen in liquid nitrogen. Diffraction data were collected at 100 K on beamlines BM14 (AggA), BM14U (native CsuC-CsuA/B), ID23-1 (AggB, CsuC-CsuA/B with incorporated selenomethionine (Mse), and native

CsuA/Bdsc) ID29 (native MyfAdsc, Mse-incorporated MyfAdsc, PsaAdsc in complex with choline, and Mse-incorporated CsuA/Bdsc), and ID23-2 (MyfAdsc in complex with galactose) at the European Synchrotron Radiation Facility (ESRF), Grenoble, France.

**Table 2. Crystallization conditions**

Protein	Method	Temperature (K)	Protein concentration (mg ml <sup>-1</sup> )	Protein solution	Reservoir solution	Volume, drop ratio	Reservoir volume (μl)
AggAdsc	SDVD	289	83	25 mM HEPES, 150 mM sodium chloride pH 7.5	0.2 M sodium acetate, 0.1 M sodium cacodylate pH 6.5, 30% (w/v) PEG 8000	2 μl, 1:1	80
AggBdsc	SDVD	289	33	25 mM HEPES, 150 mM sodium chloride pH 7.5	0.2 M Lithium sulfate monohydrate, 0.1 M Tris-HCl pH 8.5, 30% w/v PEG 4000	2 μl, 1:1	80
MyfAdsc	HDVD	278	30	10 mM HEPES, 150 mM sodium chloride pH 7.4	35% dioxane (v/v)	4 μl, 1:1	1000
PsaAdsc	HDVD	278	40	10 mM HEPES, 150 mM sodium chloride pH 7.4	0.1 M imidazole, pH 7.8, 0.2 M zinc acetate	4 μl, 1:1	1000
CsuC-CsuA/B	HDVD	289	23	25 mM HEPES, pH 7.2	0.1 M malic acid pH 7.0, 15% PEG 3350	4 μl, 1:1	1000
CsuA/Bdsc	HDVD	289	24	10 mM HEPES, 75 mM sodium chloride pH 7.4	28%–30% PEG 8000, 0.2M ammonium sulfate	4 μl, 1:1	1000

SDVD – “sitting drop” vapor diffusion method; “HDVD” – “hanging drop” vapor diffusion method

### 3.7. Protein structure determination (papers I–IV, VI)

X-ray diffraction data were processed using XDS (Kabsch, 2010) (AggA; AggB), the Grenoble automatic data processing system (GrenADeS) at ESRF (Monaco *et al.*, 2013) (CsuC-CsuA/B, CsuA/Bdsc), MOSFLM (Battye *et al.*, 2011), and SCALA program suite (CCP4, 1994) (MyfAdsc and PsaAdsc). Initial phases were determined

using a variety of methods: sulfur single wavelength anomalous dispersion (S-SAD) phasing (AggA), selenium single wavelength anomalous dispersion (Se-SAD) phasing (MyfAdsc, CsuC-CsuA/B, and CsuA/Bdsc), and molecular replacement (AggBdsc and PsaAdsc). The initial models were constructed and refined using the PHENIX (Adams *et al.*, 2002) and CCP4 (CCP4, 1994) software packages. Refinement statistics for the final models are presented in the Table 3. Manual corrections of the structures were done using COOT (Emsley *et al.*, 2010). Ligands were placed into the electron density by the LigandFit module of the PHENIX software package.

**Table 3. Refinement statistics**

Protein	AggAdsc	AggBdsc	MyfAdsc	MyfAdsc-galactose	PsaAdsc-choline	CsuC-CsuA/B	CsuA/Bdsc
Resolution (Å)	47.66-1.55	58.63-2.40	41.98-1.46	28.07-1.65	49.98-2.36	49.635-2.4	46.243-1.680
Rwork (%)	15.6	22.8	16.8	19.0	22.0	22.3	18.45
Rfree (%)	23.2	27.2	19.3	21.1	26.9	27.0	22.94
Number of protein residues / assymetric unit	310	1136	288	288	417	391	173
Ligands/ ions	-	-	-	1 galactose	3 choline	-	1 sulfate
Bond lengths (Å)	0.008	0.009	0.008	0.009	0.017	0.009	0.011
Bond angles (°)	1.344	1.352	1.158	1.137	1.839	1.249	1.388
Residues in outlier regions (%)	0	0.30	0.41	0.83	1.27	1.70	0
Residues in favoured regions (%)	98	93.0	95.87	96.69	92.11	93.90	1.96
Residues in allowed regions (%)	100	99.70	99.59	99.17	98.73	98.30	98.04

### 3.8 Site-directed mutagenesis (papers II, III, V)

Site-directed mutagenesis was performed by reverse polymerase-chain reaction according to the Quik-Change protocol with the PfuTurbo high-fidelity polymerase (Stratagene).

### 3.9 Surface plasmon resonance (SPR) binding experiments (papers II, V)

To characterize AggA binding to fibronectin, fibronectin (approximately 1800 RU) was loaded on a CM5 Sensor chip by amine coupling. To obtain the association and the dissociation curves, various concentrations of AggA were injected. To perform the kinetic analysis of the CsuC-CsuA/B binding, CsuC-CsuA/B-His6-tag was immobilized on an NTA-sensor chip. After CsuC was gradually washed off from the complex, samples of free CsuC at different concentrations were injected into the flow cell. The chips were regenerated after each cycle of the experiment. For all experiments, a Biacore X100 (GE Healthcare) was used.

### 3.10 Stability analysis of CsuC-CsuA/B and CsuA/Bdsc (paper VI)

Thermodynamic studies on CsuC-CsuA/B and CsuA/Bdsc were performed by differential scanning calorimetry using a Micro-Cal VP-ITC microcalorimeter with a cell volume of 0.5 ml at a heating rate 0.5–1°C/min.

### 3.11 Isolation of Myf and Psa fimbriae (paper III)

Psa fimbriae were expressed in *E. coli* BL21-AI transformants according to **3.2**. Myf fimbriae were purified from *Yersinia enterocolitica* strain 8081c (collection of Prof. Skurnik, University of Helsinki). Fimbriae were isolated by ammonium sulfate precipitation. Myf fimbriae were subsequently labeled with Eu<sup>3+</sup>-DTTA chelate using the DELFIA<sup>®</sup> Eu-Labeling kit (PerkinElmer) or <sup>125</sup>I using Na<sup>125</sup>I (100 µCi ml<sup>-1</sup>; Amersham Pharmacia Biotech).

### **3.12 Determination of receptor binding by Myf and Psa (paper III)**

Bacterial cells expressing the Psa fimbriae were added to microtiter plates coated with phosphatidylcholine. After a few cycles of washing, the adhered cells were fixed with 10% formaldehyde and stained with 1% crystal violet. After stain extraction with 0.2% Triton X-100, the absorbance at 570 nm was measured.

The isolated Psa or the  $\text{Eu}^{3+}$ -DTTA chelate labeled Myf fimbriae at different concentrations were added to microtiter plates coated with lactosylceramide (Myf) or phosphatidylcholine (Myf, Psa) blocked with 0.5% bovine serum albumin in phosphate-buffered saline. Wells with the added Psa fimbriae were additionally incubated with rabbit anti-Psa serum, goat anti-rabbit horseradish peroxidase, and ABTS substrate. The bound Psa fimbriae were detected by measuring the well's absorbance at 405 nm. The bound Myf fimbriae were detected by measuring  $\text{Eu}^{3+}$ -DTTA fluorescence at 615 nm following the well's excitation at 340 nm.

### **3.13 Characterization of Myf receptor binding specificity (paper III)**

The receptor binding specificity of the Myf fimbriae was analyzed by thin layer chromatography and chromatogram binding assay. Thin layer chromatograms of various glycosphingolipids were incubated with  $^{125}\text{I}$ -labeled Myf and then autoradiographed for 12 hours.

### **3.14 Characterization of MyfAdsc binding to lactose and galactose (paper III)**

The binding of MyfAdsc to galactose was analyzed by measuring its intrinsic protein fluorescence with and without the ligand. As the ligand directly interacts with Trp94 in MyfAdsc, it will decrease protein fluorescence. The binding of MyfAdsc to lactose was characterized by isothermal titration calorimetry.



## 4. RESULTS AND DISCUSSION

### 4.1 High-resolution structures of polyadhesin fimbrial subunits (papers I-III)

To elucidate the molecular basis for fimbriae-mediated receptor recognition, we performed high-resolution structural studies on fimbrial subunits. Three important members of the FGL (F1-G1 loop long) family of chaperone-usher (CU) fimbrial polyadhesins are in the focus of the thesis: AAF/I (from the outbreak strain of enteroaggregative *Escherichia coli* (EAEC) O4H104), Psa (from *Yersinia pestis* and *Y. pseudotuberculosis*), and Myf (from *Y. enterocolitica*). It has been previously shown that both AAF and Psa fimbriae are directly involved in pathogenesis (Czeczulin *et al.*, 1997; Yang *et al.*, 1996; Lindler *et al.*, 1990; Liu *et al.*, 2006), whereas the role of Myf for the virulence of *Y. enterocolitica* has not yet been clarified.

Considering the homology of the CU machineries, we hypothesized that the assembly of AAF/I, Myf and Psa fimbriae is governed by the donor strand complementation (DSC) mechanism (Sauer *et al.* 2002), similarly to other previously studied adhesins (Zavialov *et al.*, 2003; Anderson *et al.*, 2004; Remaut *et al.*, 2006; Roy *et al.*, 2012). A closer inspection of the protein sequences at the N-terminus revealed a characteristic pattern of alternating hydrophobic-hydrophilic residues that could act as a donor strand (Gd) linking the subunits in the fiber. Both Myf and Psa fimbriae are homopolymers, as *myf* and *ph6* gene clusters encode only one pilin subunit named MyfA and PsaA, respectively. In contrast, the *agg* gene cluster expresses two types of subunits: AggA (major subunit) and AggB (minor subunit). As the AggB subunit lacks the N-terminal sequence corresponding to the Gd strand, we assumed that the minor subunit is located on the tip of the pili whilst AggA, which is capable of polymerization, forms the shaft of the fiber.

To enable high-resolution structural studies on fimbrial subunits, their stable monomers have to be produced. This can be easily achieved by relocating the N-terminal Gd strand of the subunit to its C-terminus, thereby enabling the formation of a stable DSC monomer with a complete immunoglobulin (Ig) fold (Figure 7). Following this procedure, we engineered DSC subunits. The DSC monomers of AggA, PsaA and MyfA had their own Gd strand, whereas AggB was complemented with the donor sequence of AggA. The pilin subunits were expressed in *E. coli*, purified and crystallized, and thereafter their high-resolution structures were determined.

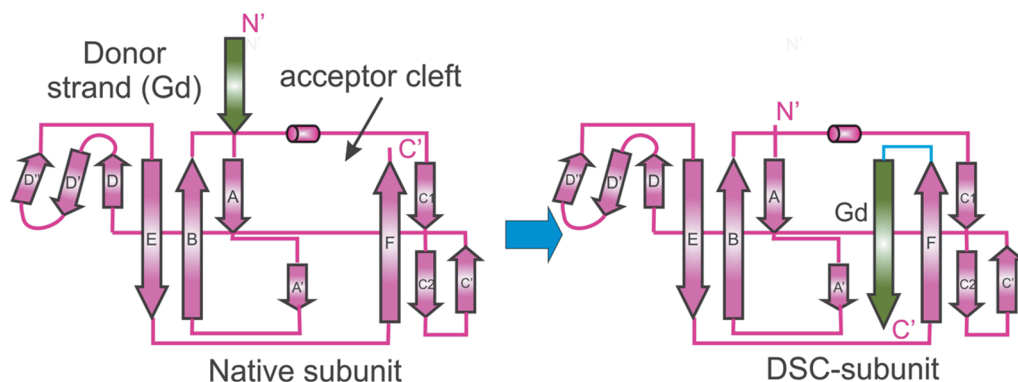


**Figure 7.** Design of DSC monomers. The topology diagram is based on the structure of Caf1 (PDB code 1Z9S).

As expected, the DSC monomers of all studied pilin subunits had a canonical Ig-fold composed of two  $\beta$ -sheets. Strands A, B, and E form  $\beta$ -sheet 1, strands C, F, and Gd form  $\beta$ -sheet 2, and strand D switches between the sheets (Figure 8). In all structures, the Gd strand is hydrogen-bonded only to strand F, which is a characteristic feature of the FGL CU family.

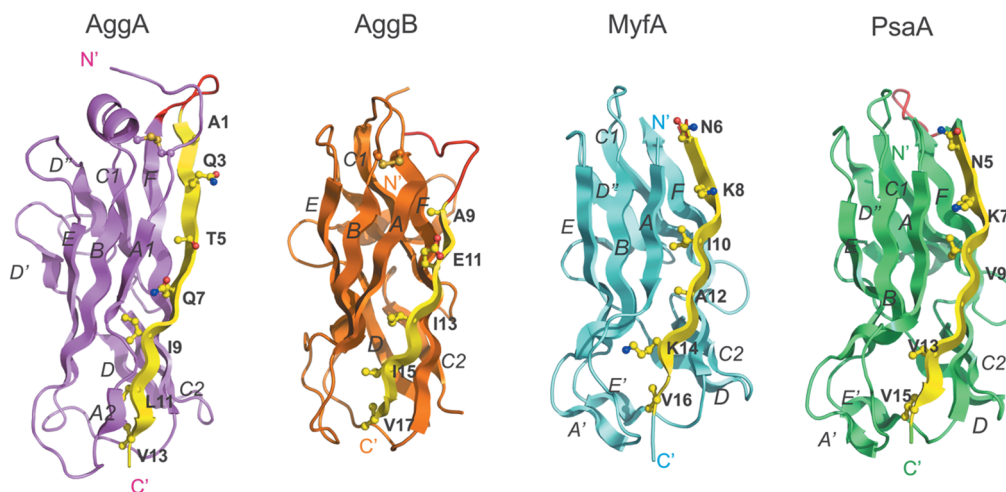


**Figure 8.** The high-resolution structures of the DSC-subunits of AggA, AggB, MyfA and PsaA, cartoon representation. The  $\beta$ -strands as well as N- and C-termini are labeled; the Gd strands are shown in yellow. The donor residues are shown as ball-and-sticks and labeled.

Despite the similarity of the overall fold, there are several remarkable differences between the studied pilin subunits, such as the number of donor residues/acceptor pockets in each subunit and the presence/absence of a conserved disulfide bond. Thus, the Gd strand of AggAdsc inserts seven classical donor residues into the acceptor cleft, whereas the Gd strands of MyfA and PsaA possess six of them, and the AggB tip subunit accommodates only five residues donated by the major subunit (Figure 8). Unlike MyfA and PsaA, both the major and minor subunits of AAF/I fimbriae have a pair of cysteine residues, forming a disulfide bond in the core structure of the molecule. However, in AggA this bond connects the beginning of the subunit fold with a short  $\alpha$ -helix between the strands B and C1, whilst in AggB the disulfide bond is formed between the BC1-loop and the F-strand of the molecule, thus protecting its acceptor cleft (Figure 9). Interestingly, the mentioned  $\alpha$ -helix of AggA is absent in all other studied subunits. The presence of an additional donor residue and the  $\alpha$ -helix gives AggA a more elongated shape compared to the other subunits.

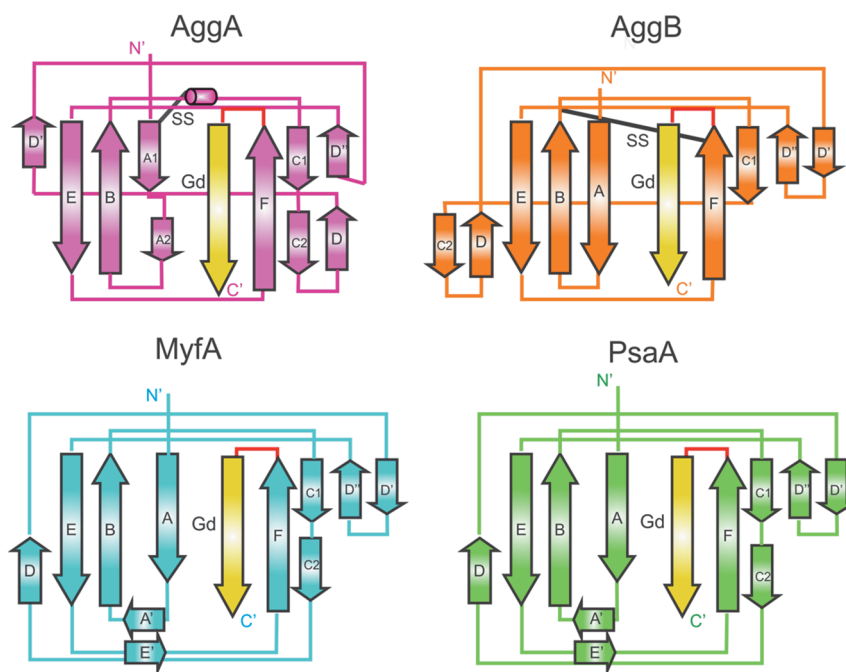


**Figure 9.** The topology diagrams of AggAdsc, AggBdsc, MyfAdsc, and PsaAdsc. The  $\beta$ -strands as well as N- and C-termini are labeled; the Gd strands are shown in yellow.

As expected, the highly homologous MyfA and PsaA have similar structures. In contrast to AggA and AggB, MyfA and PsaA possess the short strands A' and E'

(Figure 9). The only significant differences between PsaA and MyfA were observed in the structure of strand D and the orientation of the loops between strands A and B as well as D' and D''. In addition, the D'-D'' loop of MyfA is two residues shorter (paper III, Figure 1, Figure 3C). In the following chapters, I will demonstrate that these structural variations play a key role in the recognition of host cell receptors by these adhesins.

The calculation of the electrostatic potential of all studied pilin subunits revealed another important difference between them. Similarly to other known structures of pilin monomers, MyfA and PsaA are negatively charged (Figure 10). By contrast, AggA and AggB carry a highly positive charge, which is more pronounced in AggA. Indeed, AggA possesses a significant number of surface-exposed basic residues. Can this feature of AggA be essential for receptor recognition?

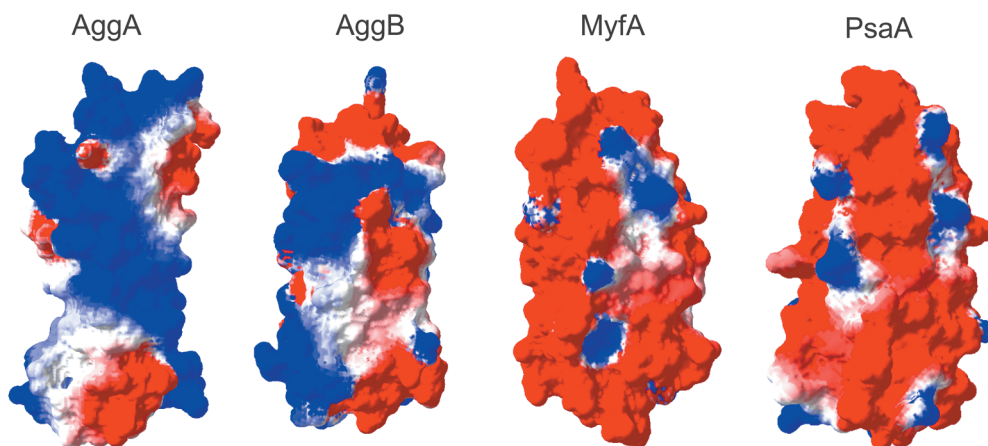


**Figure 10.** A surface representation of AggA, AggB, MyfA, and PsaA colored by electrostatic potential (Poisson-Boltzmann equation, DeepView – Swiss PDB Viewer (Guex & Peitsch, 1997)). Regions of positive surface potential are shown in blue and negative potential in red (scale is from -1.0 to 1.0 kT/e). The orientation of the structures is the same as in Figure 8.

Despite the above-mentioned differences, the structural organization of the studied polyadhesin subunits is similar to other fimbrial subunits of the FGL CU family (Zavialov *et al.*, 2003; Roy *et al.*, 2012). Therefore, the binding specificity of the polyadhesins is likely to be determined by the nature of residues exposed to the surface of the molecule.

## 4.2 The structural basis for host cell receptor recognition in AAF/I, Myf, Psa fimbriae (papers I–III)

### 4.2.1 AAF/I specifically binds fibronectin using a positively charged surface (paper II)

Based on the structures of the DSC monomers and the previously determined crystal structure of the mini-fiber of F1-antigen (Zavialov *et al.*, 2003), we proposed the atomic model of AAF/I fimbriae (paper II, Figure 4). The AAF/I shaft structure was constructed based on the structure of major subunits (AggA) with a terminal module of the minor subunit AggB. The circular permutation of the DSC-subunits was reverted by connecting the C-terminus of the Gd strands to the N-termini of the neighboring subunits by their native linker sequence TND. The artificial linker sequences bridging the C-termini of the DSC-subunits with the N-termini of the Gd strands were removed. The model of the AAF/I fiber revealed that most of the basic residues cluster at the junction between the neighboring subunits, forming a prominent basic surface with a shallow groove in the middle (paper II, Figure 6). The positively charged patch is formed by lysine side chains protruding towards the inter-subunit cleft (Figure 11).

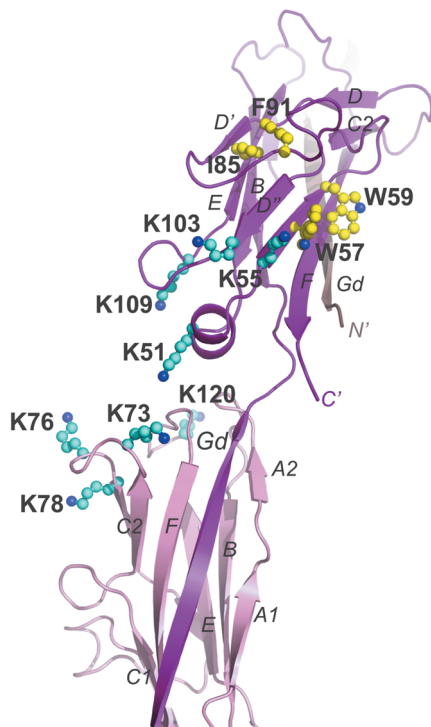


**Figure 11.** Positively charged patch at the inter-subunit cleft of AAF/I, cartoon representation. The  $\beta$ -strands are labeled. Residues of interest are shown as ball-and-sticks and labeled.

The comparison of AggA with the structures of other AAF monomers showed the consistency of the positively charged surface patch at the poles of the subunits (paper II, Figure 6), even though the patch-forming residues are not highly conserved and are located at different sequence positions (paper II, Figure S1). The presence of the basic surface at the subunit interfaces might have various implications in bacterial pathogenesis. Firstly, the repulsion of subunits in a fiber may enable the fimbrial shaft to protrude from the cell surface as far as possible. In addition, the basic inter-subunit groove might be directly involved in host receptor recognition.

It was previously demonstrated that AAF/II fimbriae mediate the attachment of EAEC strain 042 to the extracellular matrix protein fibronectin, which is a common receptor for various bacterial adhesins (Farfan *et al.*, 2008). Hence, we decided to investigate the possible adhesion of AAF/I subunits to this glycoprotein using surface plasmon resonance (SPR). The experiments revealed the specific binding of both the major and minor subunits of AAF/I fimbriae to fibronectin (paper II, Figure S8). However, the affinity of AggA to the receptor was significantly higher ( $K=16\pm 2 \mu\text{M}$ ) than that of AggB ( $K=100 \mu\text{M}$ ), suggesting a leading role of the shaft subunit in receptor recognition. Interestingly, the affinity of AggA to fibronectin changed depending on the ionic strength of the buffer, which suggests that the binding is mediated by ionic interactions (paper II, Figure S8).

To verify our hypothesis about the potential role of the basic surface at the subunits junction in receptor recognition, we substituted the corresponding residues with alanine and analyzed the effect of mutations on fibronectin binding by SPR (paper II, Table 1). The affinity of AggA to fibronectin decreased dramatically in all double mutants, whilst a triple mutation (Lys73, Lys76, and Lys78) completely abrogated the binding. To ascertain that the introduced triple mutation neither prevented the correct folding of the resulting monomer nor affected its stability, the circular dichroism (CD) spectra of both wild-type and mutant subunits were analyzed. Identical CD profiles and similar thermal denaturation curves of the studied proteins confirmed the structural integrity and stability of the mutant (paper II, Figure S10). Thus, the inability of a triple mutant to bind fibronectin can be explained only by a defunct surface patch.

The observed results may also suggest a non-specific adhesion of AAF/I to acidic proteins. However, the presence of bovine serum albumin (pI 4.7) in excessive concentration did not affect the affinity of AggA to fibronectin (paper II, Figure S11).

In close proximity to the fibronectin-binding surface, we noticed some surface-exposed aromatic residues – Trp59, Trp57, Phe91, and partially exposed hydrophobic Ile85 (Figure 11). Interestingly, Trp59 is conserved within the major subunits from AAF and Afa/Dr families. The mutations did not affect the binding of AggA to fibronectin. However, they might be responsible for binding another, yet unknown receptor.

This study confirms the polyadhesive mode of AAF/I adhesion originating from multiple interactions of a fimbrial polymer with fibronectin. Fibronectin binding may play a key role in EAEC pathogenesis by anchoring the growing biofilm and activating signaling pathways in the host epithelium (Westerlund *et al.*, 1993; Henderson *et al.*, 2011). Surprisingly, AAF/I-mediated fibronectin binding is primarily based on electrostatic interactions, and even though the observed affinity is relatively low, the multiple contacts of fimbrial subunits with fibronectin ensure high-avidity binding. Note that the AAF/I-fibronectin interactions have been studied using DSC monomers, where the basic surface patch for the receptor was somewhat incomplete. Hence, the affinity to the receptor would likely be higher if the binding of the functional unit of AAF/I fiber (i.e. AggA-dimer) to fibronectin was analyzed.

Despite the relatively low sequence identity between different variants of AAF, AAF/II utilizes the same mechanism of fibronectin binding (paper II). Thus, receptor recognition mediated by electrostatic interactions can represent a characteristic feature of all AAF. This mode of fibronectin binding is strikingly different from the mechanisms employed by other bacterial adhesins (Schwarz-Linek *et al.*, 2003). For example, MSCRAMMs (microbial surface components recognizing adhesive matrix molecules) of Gram-positive bacteria utilize multiple repeats in the C-terminal region of the protein to bind several F1 fibronectin-binding modules and to ensure extremely high affinity in the nanomolar range (Joh *et al.*, 1994; Schwarz-Linek *et al.*, 2004). Each F1-module consists of a double-stranded (strands A and B) and a triple-stranded (strands C, D, E) antiparallel  $\beta$ -sheet. Upon binding, the bacterial peptide forms an additional antiparallel  $\beta$ -strand to the triple-stranded  $\beta$ -sheet of the module. Interactions of the fibronectin-binding protein with serial F1-modules constitute an extensive tandem  $\beta$ -zipper (Schwarz-Linek *et al.*, 2003). Hence, MSCRAMM-mediated adhesion is primarily based on hydrophobic interactions, although electrostatic interactions are also likely to be important in the binding (Schwarz-Linek *et al.*, 2003). In contrast to MSCRAMMs, a more generalized, purely electrostatic mode of AAF/I and AAF/II adhesion hints at their ability to recognize several host cell receptors with an appropriate surface distribution of acidic residues, such as negatively charged glycosylation sugars and sites of phosphorylation. For example, the major subunit Aaf of AAF/II was shown to bind laminin, type IV collagen, and cytokeratin 8 (Farfan *et al.*, 2008; Izquierdo *et al.*, 2014).

Interestingly, bacterial adhesion mediated by ionic interactions was previously demonstrated for several bacterial species. For example, ionic interactions are involved in collagen binding by YadA adhesin from *Y. enterocolitica* and *Y. pseudotuberculosis* (Nummelin *et al.*, 2004). The CfaE adhesive subunit from the CFA/I pili of the enterotoxigenic *E. coli* (ETEC) utilizes a cluster of positively charged residues to attach to erythrocytes (Li *et al.*, 2007). The binding of SdrF adhesin from *Staphylococcus epidermidis* to prosthetic material is also mediated by ionic interactions (Toba *et al.*, 2013). Basic residues might also play a key role in the

recognition of the sulfatide receptor by FasG adhesin from the 987P fimbriae of ETEC (Choi *et al.*, 1999) as well as laminin and fibronectin by the RrgA adhesin from *Streptococcus pneumoniae* (Izoré *et al.*, 2010).

The high positive charge of AAF/I and AAF/II distinguishes them from the majority of bacterial adhesins. To date, only few studies have reported the involvement of basic fimbriae in pathogenesis. For example, positively charged SMF-1 (*Stenotrophomonas maltophilia* fimbriae 1) was shown to mediate biofilm formation (Jucker *et al.*, 1996) and adhere to abiotic surfaces and cultured epithelial cells (de Oliveira-Garcia *et al.*, 2003). Thus, it would be interesting to study other positively charged adhesins to understand their role in pathogenesis.

#### **4.2.2 Myf binds to terminal $\beta$ -1-3- or $\beta$ -1-4-linked galactose of glycosphingolipids (paper III)**

It has been previously shown that Psa fimbriae bind phosphatidylcholine and glycosphingolipids (Payne *et al.*, 1998, Galván *et al.*, 2007). Considering the high sequence and structure similarity between the fimbrial subunits of Myf and Psa fimbriae, we hypothesized that MyfA can also recognize these receptors. Surprisingly, isolated Myf fimbriae did not interact with phosphatidylcholine but had a strong affinity towards lactosylceramide (paper III, Figure S2). Further analysis of the carbohydrate-binding specificity of MyfA showed that the protein binds to various glycosphingolipids with terminal  $\beta$ -1-3- or  $\beta$ -1-4-linked galactose (paper III, Table 1). To understand the molecular mechanism of galactose recognition, the crystal structure of MyfA<sub>dsc-D</sub>-galactose was determined. MyfA binds the galactose molecule using a compact shallow pocket located on the surface of the FC1D''D'  $\beta$ -sheet (Figure 12). The indole side chain of Trp94 serves as an anchor for the pyranose ring of the galactose, whereas the aromatic side chain of Tyr128 interacts with the hydrophobic C4-C5-C6 end of the molecule. Additionally, MyfA forms a dense network of hydrogen bonds with four hydroxyl groups in the galactose. Hydroxyl groups at the C2 and C6 atoms are bound to Asp89 and K56, respectively, whereas the C3-hydroxyl group can form a hydrogen bond with either His92 or Asn59. The latter also interacts with the hydroxyl group at the C4 position via the structured water molecule.

Since the isolated Myf fimbriae bound to lactosylceramide with a high affinity, we decided to investigate whether the MyfA subunit can also recognize a lactosyl moiety. The modeling of the lactose into the galactose-binding pocket revealed that MyfA interacts with both the galactose and glucose residues of the disaccharide. Thus, the glucose C3-hydroxyl group is hydrogen-bonded to Asp89 (paper III, Figure S7). This additional interaction might significantly increase binding affinity. To address this hypothesis, we analyzed the intrinsic fluorescence of MyfA in the presence of galactose and lactose at various concentrations. Indeed, the tryptophan-fluorescence



quenching assay showed nearly 5-fold tighter interactions of MyfA with lactose compared to galactose (paper III, Figure 5).

The size-shape complementarity of the binding pocket to galactose and the extensive interactions of the ligand with the protein suggest high specificity of the site. To analyze the ability of the galactose cavity to recognize other carbohydrate moieties, we modeled the docking of several head groups of glycosphingolipids into the binding pocket. The bulky carbohydrate moieties of glycosphingolipids, such as N-acetylgalactosamine, do not fit into the galactose-binding niche and clash with the pocket-forming residues (paper III, Figure S5). Similarly, MyfA is unable to recognize the terminal  $\alpha$ -1-3-linked galactose due to steric hindrance.

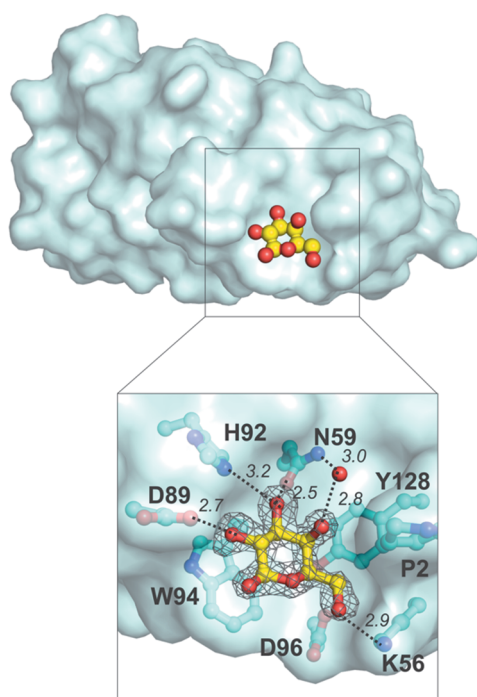


**Figure 12.** Structural basis for glycolipid recognition by Myf: surface representation of MyfA with bound galactose (yellow) and a close-up of the galactose-binding pocket. Interacting residues are shown as ball-and-sticks and labeled. Hydrogen bonds are depicted as dashed lines and their lengths are indicated. The conserved water molecule is shown as a red sphere. Electron density  $2F_o-F_c$  map contoured at  $1.0 \sigma$  is displayed around the ligand.

The Psa fimbriae were shown to have similar carbohydrate-binding specificity to Myf, as it recognizes glycosphingolipids with  $\beta$ -1-linked galactose (Payne *et al.*, 1998). The recently determined crystal structures of PsaA-galactose and PsaA-lactose complexes (Bao *et al.*, 2013) enabled the comparison of carbohydrate-binding pockets in two adhesins. As expected, in Myf and Psa the binding site is located in the same segment. The galactose molecules have a similar orientation, and they are hydrogen-bonded to the proteins via the same four hydroxyl groups (paper III, Figure 4E). However, the proteins use different residues to form the binding pocket. In PsaA, the bottom of the binding cavity is formed by the smaller phenyl group of Tyr95 instead of the indole

group of Trp94, as in MyfA. Additionally, residues establishing the hydrogen bonds with the ligand are different. Despite these differences, PsaA binds to galactose with a similar affinity ( $\approx 40$  mM) (Galván *et al.*, 2007). However, the affinity of PsaA to lactose was significantly lower than that of MyfA. The superposition of the PsaA-lactose structure with lactose-modeled MyfA revealed that, unlike MyfA, PsaA does not form a hydrogen bond with the glucose moiety (paper III, Figure S7). It explains the striking difference in the affinities of the two polyadhesins to lactose. Therefore, despite the similar carbohydrate-binding specificity, MyfA establishes more interactions with lactosyl-containing receptors in comparison with PsaA.

Cell surface carbohydrates are common binding determinants for various adhesive fimbriae (De Greve *et al.*, 2007). Galactose-specific adhesins have been found in a number of intestinal pathogens, such as EAEC (Grover *et al.*, 2007) and ETEC (Coddens *et al.*, 2009). Thus, FaeG subunit of K88 (F4) fimbriae (FGS CU systems) possesses a galactose-binding site, similar to that of MyfA and PsaA (Moonens *et al.*, 2015). The binding pocket of FaeG is composed of an aromatic platform (Phe150 instead of Trp94 in MyfA) and several residues hydrogen-bonded to the ligand (paper III, Figure S11). The identically located Asn59 of MyfA and Glu170 of F4 have the same dual function in carbohydrate binding, as they form a hydrogen bond with the hydroxyl group at the C3-position of galactose and stabilize the conserved water molecule bound to the hydroxyl group of the C4-atom of galactose. Thus, both adhesins developed a similar scaffold to ensure the precise recognition of galactose and lactose moieties. It is noteworthy that the ability of bacterial fimbriae to attach to specific cell surface carbohydrates makes their adhesion to host tissues extremely selective. For example, F17 fimbriae recognize glycolipids containing N-glycolylneuraminic acid present only on the enterocytes of newborn piglets (Buts *et al.*, 2003). Similarly, K99 (F5) fimbriae specifically bind to N-glycolyl-GM3 and N-glycolylsialoparagloboside, which is exclusively found in the small intestine of neonatal piglets, calves and lambs but is absent in both adult animals and humans (Kyogashima *et al.*, 1989).

#### 4.2.3 PsaA binds phosphatidylcholine using a tyrosine-rich surface (paper III)

To understand the structural basis for Psa-mediated phosphatidylcholine recognition, the crystal structure of PsaA-choline complex was determined. After a few cycles of refinement, the Fourier map revealed several blobs of prominent electronic density subsequently identified as choline molecules bound to the protein (Figure 13). Three unique binding pockets for choline on the same face of the PsaA subunit were found. The first choline-binding pocket located on the D-D' loop is formed by the side chains of two tyrosines (Tyr69 and Tyr77) facing each other. In the second binding site, choline is inserted into a deep pocket formed by two pairs of tyrosines (Tyr69 and Tyr81) and tryptophans (Trp87 and Trp94). This site was previously shown to bind

phosphocholine (Bao *et al.*, 2013). Interestingly, Tyr69 is involved in the formation of two choline-binding sites simultaneously. In the third binding site, choline interacts with a hydrophobic patch formed by Val88, Ile90, and Tyr95. Tyr95 also makes up the bottom of the galactose-binding pocket (Bao *et al.*, 2013).

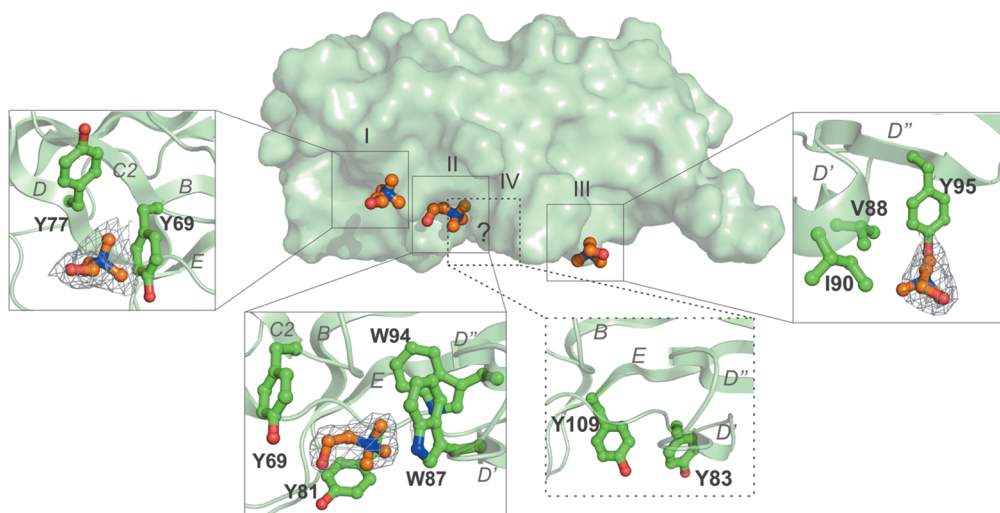


**Figure 13.** Structural basis for phosphatidylcholine recognition by Psa: surface representation of PsaA with bound choline molecules (orange) and a close-up of the choline-binding pockets I–IV. The  $\beta$ -strands are labeled; interacting residues are shown as ball-and-sticks and labeled. Electron density  $2F_o-F_c$  map contoured at  $1.0 \sigma$  is displayed around the ligands.

Intriguingly, PsaA has a surprisingly high number of tyrosine residues, forming a unique tyrosine-rich surface on the same face of the monomer. Four of the tyrosine residues were shown to be involved in choline recognition. Another pair of surface-exposed tyrosine residues (Tyr83 and Tyr109) might potentially form the fourth choline-binding site (Figure 13). In contrast, MyfA, lacking the tyrosine surface, was unable to interact with phosphatidylcholine. These results suggest that tyrosine-rich facade of PsaA governs its ability to recognize the phosphatidylcholine of host cells. To verify this hypothesis, we substituted tyrosines with alanine and analyzed the ability of purified Psa-fibers and Psa-mutant producing *E. coli* to bind immobilized phosphatidylcholine. Two single mutants (Tyr81Ala and Tyr95Ala) and two double mutants (Tyr69Ala+Tyr77Ala and Tyr83Ala+Tyr109Ala) were prepared. Isolated wild-type Psa fibers bound to the receptor at a concentration of 0.1–1  $\mu\text{g}/\text{ml}$  (paper III, Figure 7C), whereas all introduced mutations significantly decreased the binding affinity. The most pronounced effect was observed in the double Tyr69Ala+Tyr77Ala mutation, which practically abolished binding to phosphatidylcholine. The single Tyr81Ala mutation also drastically decreased the affinity of the adhesin to the receptor.

As previously mentioned, Tyr69 is involved in the formation of two choline-binding pockets. Thus, the Tyr69Ala+Tyr77Ala mutation fully abrogated the binding between Tyr69 and Tyr77. Moreover, it caused additional disruption to binding site II. Binding site II is likely to play a major role in phosphatidylcholine recognition, as can be concluded from the substantial decrease in the affinity of the Tyr81Ala mutant to the receptor. Interestingly, the impaired ability of the Y83A+Y109A mutant to bind choline indeed confirms the presence of the fourth site in PsaA. The mutation Y95A had the least dramatic effect on affinity to phosphatidylcholine. The decline, but not the full absence, of affinity to choline indicates that binding sites formed by Y95 and Y83+Y109 play a secondary role in receptor recognition.

Our results thereby clearly demonstrate that the tyrosine-rich surface of PsaA determines its ability to bind phosphatidylcholine. The identification of one dominant and three complementary choline-binding sites in a single PsaA subunit raised a logical question about the ability of the protein to simultaneously use them *in vivo*. To address this hypothesis, we modeled the interactions of PsaA with four membrane-localized molecules of phosphatidylcholine. Indeed, the specific positioning of the fimbrial subunit allows it to bind four phosphatidylcholine molecules on the outer surface of the plasma membrane (Figure 14).

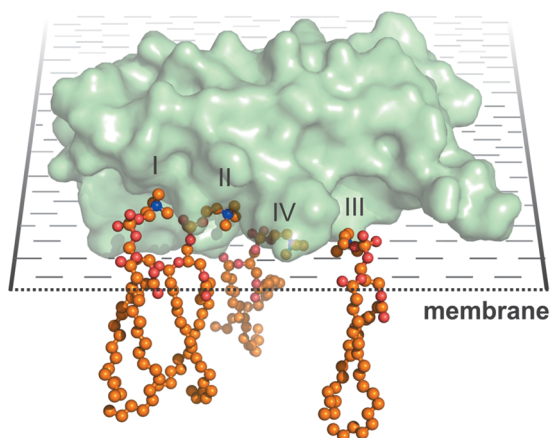


**Figure 14.** A model of the interactions of PsaA with four membrane-localized molecules of phosphatidylcholine (PDB code PCW). Three phosphatidylcholine structures were superimposed with cholines I–III of the Psa-choline complex. The fourth phosphatidylcholine structure was modeled in binding site IV.

The recognition of choline by PsaA represents a common mechanism utilized by various proteins (Dougherty & Stauffer, 1990; Sussman et al., 1991; Petersen et al., 2005; Hermoso *et al.*, 2005). The binding is primarily based on the hydrophobic interactions of the ligand with the aromatic and hydrophobic sidechains of the pockets' residues. In addition, the electrostatic attraction of choline toward the aromatic residues may partially compensate the positive charge of the ammonium group and thereby also contributes to the binding.

Here we demonstrate that tyrosines with surface-exposed side chains play a key role in phosphatidylcholine recognition by PsaA. The substitution of these residues with alanines showed a significant reduction or complete disruption of choline binding in PsaA mutants. The absence of the tyrosine-rich surface in the highly homologous MyfA showing no affinity to phosphatidylcholine provides an additional proof of the importance of tyrosines in phosphatidylcholine recognition.

Intriguingly, we discovered a fragment of the PEG molecule bound to MyfA in a shallow cavity corresponding to the major choline-binding site (II) in PsaA (paper III, Figure S12). Similarly to PsaA, two identically positioned tryptophan residues (Trp88 and Trp93) make the bottom of the cavity in MyfA. However, instead of tyrosines, MyfA contains histidine (His82) and glutamine (Gln70). This binding pocket cannot bind phosphatidylcholine, but it might instead be able to recognize another unknown receptor.

Our data demonstrate that both Myf and Psa fimbriae might mediate the attachment of bacteria to host cells and play an important role in the tissue tropism of pathogenic yersiniae. Despite the high degree of sequence and structure similarity of pilin subunits, the adhesins show significant differences in receptor binding specificity. Thus, Myf is capable of recognizing only glycosphingolipids, whilst Psa has additionally acquired the ability to bind phosphatidylcholine lipids. Despite the fact that the fimbriae display similar carbohydrate-binding specificity, Myf elaborates a larger binding site, enhancing the interactions of the protein with the receptor and enabling higher affinity towards the lactosyl moieties of glycosphingolipids. This observation suggests that, like many other fimbriae of intestinal pathogens, Myf has become a specialized carbohydrate-binding adhesin. The evolutionary development of Myf towards the exclusive recognition of glycosphingolipids is not surprising due to the fact that *Y. enterocolitica* expressing Myf is a strictly enteric pathogen. The dominating glycosphingolipids expressed by enterocytes of the human small intestine are galactosylceramide, blood group ABH, and Lewis glycolipids (Bjork *et al.*, 1987, Breimer *et al.*, 2012). Small amounts of lactotetraosylceramide and Le<sup>x</sup> and Le<sup>y</sup> terminated glycosphingolipids have also been identified (Bjork *et al.*, 1987). As MyfA recognizes  $\beta$ -1-3- or  $\beta$ -1-4-linked galactose, it may target galactosylceramide, lactotetraosylceramide Le<sup>a</sup> and Le<sup>x</sup> terminated glycosphingolipids specifically (paper III, Table 1). Thus, the ability of Myf fimbriae to adhere to intestinal epithelial cells may promote the colonization of the small intestine by *Y. enterocolitica* and facilitate the enteric route of infection.

The PsaA of *Y. pestis* and *Y. pseudotuberculosis* has acquired a prominent tyrosine-rich surface forming four distinct binding pockets for phosphatidylcholine on the same face of the protein. The ability of each PsaA subunit in the fiber to simultaneously attach to four phosphatidylcholine molecules ensures the high avidity of binding. The double receptor specificity acquired by Psa fimbriae might contribute to the versatile

tissue tropism of *Y. pestis* and *Y. pseudotuberculosis*. The carbohydrate-binding specificity of Psa could facilitate the colonization of the intestine by *Y. pseudotuberculosis*, whereas its ability to recognize phosphatidylcholine might promote the adhesion of both *Y. pseudotuberculosis* and *Y. pestis* to the pulmonary surfactant. The high avidity of Psa-mediated phosphatidylcholine binding might explain the fast progression of pneumonic plague and its high mortality rates throughout history.

### 4.3 The biological significance of polyvalent attachment (papers II–III)

Attachment to the host tissues is a critical step in the pathogenesis of many infections. In this study, we elucidated the structural basis for host cell receptor recognition by three important fimbrial adhesins: AAF/I, Myf, and Psa. Myf and Psa are homopolymers, whereas AAF/I is a polymer of major subunits AggA decorated by a single copy of a minor subunit AggB at the tip of the fiber. Similarly to previously studied CU adhesins, subunit polymerization in AAF/I, Myf and Psa fimbriae occurs via the DSC mechanism. Each subunit has a typical Ig-fold composed of 7 main antiparallel  $\beta$ -strands arranged in a two-layer  $\beta$ -sandwich. Intriguingly, in pathogenic bacteria this type of protein fold is employed exclusively to form virulence factors. In that context, the Ig-fold commonly found in eukaryotes can be considered a structural mimicry used by bacteria to deceive the host to enable the attachment of a pathogen to target cells (De Greve *et al.*, 2007). However, in spite of their similar structural organization, fimbriae recognize different receptors and use various mechanisms to ensure selective adhesion to host cells. Our study shows that the ability of fimbriae to recognize specific receptors is determined by the nature of surface-exposed residues (papers II, III). Thus, the AggA subunit of AAF/I interacts with fibronectin and potentially other negatively charged proteins via electrostatic interactions. The MyfA subunit of Myf exhibits a highly specialized binding pocket that selectively recognizes the terminal galactosyl and lactosyl moieties of glycosphingolipids. Each PsaA subunit of Psa fimbriae carries one galactose-binding pocket and four independent binding sites for phosphatidylcholine lipids due to the presence of the tyrosine surface. Despite the differences in receptor-binding specificity, all studied fimbriae are capable of multi-subunit adhesion to host cells (Figure 15). What would be the advantages of such polyvalent attachment for bacterial pathogens? Our results showed that a single fimbrial subunit binds the receptor with a relatively low affinity. Thus, multipoint interactions with host receptors will ensure sufficient avidity of binding to a target cell. For example, each PsaA subunit can simultaneously utilize four binding sites to phosphatidylcholine. Assuming that the architecture of the Psa fiber is similar to other members of FGL CU adhesins, every third subunit could potentially interact with a host cell. The ability of each Psa fiber to bind hundreds of phosphatidylcholine molecules will ensure tight fastening of the pathogen to the target tissue. The positioning of the bacteria close to a host cell might promote massive aggregation of

the receptors that will have an impact on cell signaling, triggering the deactivation of the host's immune defense (Zav'yalov *et al.*, 2010). For instance, in *Y. pestis*, a tight contact between the bacteria and the host initiates the Ca-dependent type III secretion system, destroying the cells of the immune system (Cornelis & Wolf-Watz, 1997; Viboud & Bliska, 2005). Thus, polyvalent adhesion could be crucial for bacterial virulence.

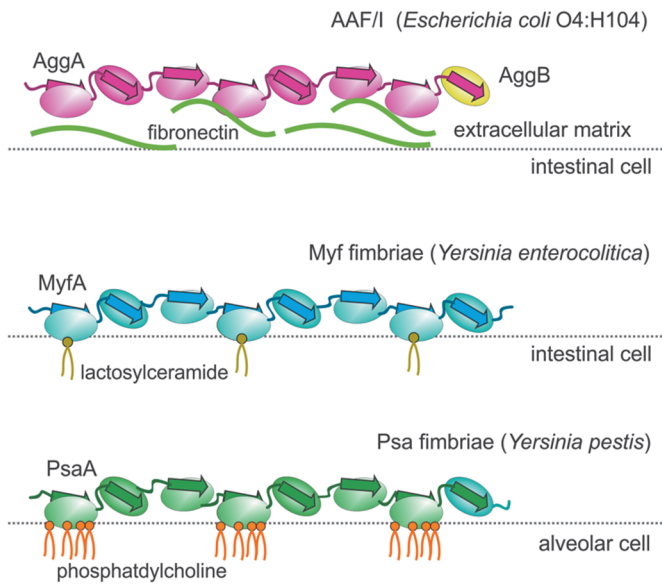


**Figure 15.** The scheme of bacterial attachment mediated by AAF/I, Myf and Psa fimbriae. Pilin subunits are shown as ovals, Gd strands are depicted as arrows.

Multi-subunit adhesion might play an important regulatory role by establishing firm interactions exclusively with cell-attached receptors (Moonens *et al.*, 2015). As affinity of a single subunit to its receptor is relatively low, only simultaneous interactions of several subunits with receptors will lead to a firm binding of the bacteria to the host cell. To achieve such firm contact, the fimbrial shaft of polyadhesins must be oriented parallel to the host cell surface. Furthermore, the high avidity of the binding is possible only when multiple cell-attached receptors are recognized.

The potential ability of polyadhesins to modulate their binding strength to host tissues would also be beneficial under various shear conditions inside the host. On the one hand, the bacteria must attach themselves strongly to the colonization surface to resist high shear stress. On the other hand, a permanently strong binding even under low shear force would limit the possibility of a pathogen to spread along the host tissue (Thomas *et al.*, 2002). Thus, the ability of polyadhesive fimbriae to potentially “switch” between the strong and the weak binding mode depending on the shear conditions would provide a serious advantage for the pathogen. The strong attachment



established when most binding sites are saturated could prevent the detachment of bacteria from the target surface, whereas the weaker binding would further facilitate the colonization of the host tissues.

Polyvalent adhesion represents a significant challenge for the development of drugs targeting the surface organelles of bacteria. The ability of fimbriae to establish multiple binding sites with one or more host cell receptors would substantially decrease the efficacy of conventional inhibitors. Thus, novel multivalent inhibitors have to be developed in order to suppress polyadhesin-mediated attachment and counter threatening bacterial infections.

## 4.4. Structural insights into archaic pili biogenesis (papers IV–VI)

### 4.4.1 DSC mechanism governs Csu pilus assembly (paper V)

Our knowledge of archaic pilus biogenesis is limited to a few biochemical studies (Zhu *et al.*, 2013; Wu *et al.*, 2014), whereas no structural information on either the architecture or the assembly of archaic fimbriae is currently available. To fill in the gap and unravel the precise molecular mechanism of archaic fimbriae assembly, we focused on the Csu-fimbriae of *Acinetobacter baumannii*. Csu fimbriae are involved in the formation of the dense biofilms of *A. baumannii* on both biotic and abiotic surfaces (Tomaras *et al.*, 2003), and as such they contribute directly to the exceptional antibiotic resistance of the pathogen. The *csu* operon encodes all components of the Csu-assembling machinery: CsuC (chaperone), CsuD (usher), and pilin subunits (CsuA/B, CsuA, CsuB; CsuE). The size of the CsuE subunit suggests that it has a two-domain structure. Its position within the *csu* gene cluster and the level of expression (Tomaras *et al.*, 2003; 2008) indicate that CsuE might cap the tip of the pili and carry a binding site for a host cell receptor, similarly to the two-domain tip-adhesive subunits of classical fimbriae (Choudhury *et al.*, 1999; Dodson *et al.*, 2001). The relatively high level of expression of the CsuA/B subunit (Tomaras *et al.*, 2003; 2008) indicates that it might form the shaft of the pili by self-polymerization. To verify this hypothesis, we produced a recombinant CsuC-CsuA/B preassembly complex and analyzed the ability of CsuA/B to spontaneously form a polymer. The incubation of the purified protein complex at room temperature followed by SDS-PAGE revealed a characteristic ladder of bands of various sizes (paper V, Figure 1B). In contrast, the incubation of the CsuC-CsuE preassembly complex produced only a single band for CsuE. Thus, our results suggest that CsuA/B constitute the pili shaft, whereas the two-domain CsuE is located on the tip of the fimbriae (Figure 16). The other pilin subunits CsuA and CsuB had significantly lower levels of expression (Tomaras *et al.*, 2008), and we thus reasoned that they might serve as adaptors in the formation of the Csu fimbriae.



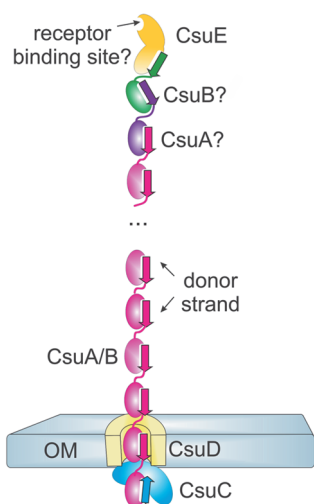


**Figure 16.** A schematic representation of the Csu pili based on the available data. The position of the CsuA and CsuB subunits are not yet known (OM – outer membrane).

Earlier studies demonstrated (Zhu *et al.*, 2013; Wu *et al.*, 2014) that the assembly of archaic fimbriae might be governed by the general mechanisms of DSC and donor strand exchange (DSE). Indeed, we found a sequence of a putative donor strand composed of alternating hydrophobic and hydrophilic residues at the N-terminus of CsuA/B, CsuA, and CsuB subunits. To confirm the role of this sequence in the assembly of CsuA/B, we substituted three potential donor residues (Val8, Leu10, and Ile12) with alanine and analyzed the effect of the mutations on the formation of the polymer using SDS PAGE. Single mutants Ile12Ala and Leu10Ala were not polymerizing as efficiently as the wild-type CsuA/B, whereas a triple mutant (Val8Ala, Leu10Ala, and Ile12Ala) fully lost its ability to polymerize (paper V, Figure 1C). These data demonstrated that the N-terminal sequence of the CsuA/B subunit indeed forms a donor strand governing the subunit assembly in the pili shaft.

To elucidate the precise molecular interactions between the main components of Csu pili, we performed high-resolution structural studies on the CsuC-CsuA/B chaperone-major subunit preassembly complex and the DSC-major subunit CsuA/B. To avoid the polymerization of the major subunits in the CsuC-CsuA/B complex, the N-terminal extension of CsuA/B was substituted with a His6-tag sequence.

#### 4.4.2 The CsuC chaperone displays several unique features

The structure of the CsuC-CsuA/B chaperone-major subunit preassembly complex has been determined to a resolution of 2.4 Å using the Se-SAD phasing method (Figure 17). The entire structure of the CsuC chaperone was automatically traced. Similarly to the chaperones from the classical and alternative families, CsuC has a canonical Ig-like

topology arranged as two domains nearly perpendicularly oriented in regard to each other. The structural superposition of CsuC with the classical Caf1M chaperone (F1-antigen, *Yersinia pestis*) (Zavialov *et al.*, 2003) and the alternative chaperone CfaA (CFA/I pili, ETEC) (Bao *et al.*, 2014) revealed that the N-terminal domains of the proteins are significantly more conserved than their C-terminal domains (paper V, Table S2). Furthermore, CfaA and CsuC share more equivalent  $\text{Ca}$  atoms than Caf1M with any of the non-classical chaperones.

CsuC has a typical tandem Ig-fold. However, it displays several unique features in both its domains as well as the linker sequence (paper V, Figure 3A). The N-terminal domain of CsuC exhibits an additional strand D1 and a long C1-D1 hairpin shielding the inter-domain cleft (Figure 17). The protruding C1-D1 hairpin has also been observed in the alternative chaperones: CfaA and EcpB. Interestingly, the C1-D1 sequence is highly conserved in both archaic and alternative chaperones (paper V, Figure S1). Even though the C1-D1 hairpin of CsuC does not form any interactions with the bound CsuaA/B, the obstruction of the inter-domain cleft might be crucial for other steps of pilus assembly in non-classical fimbriae.

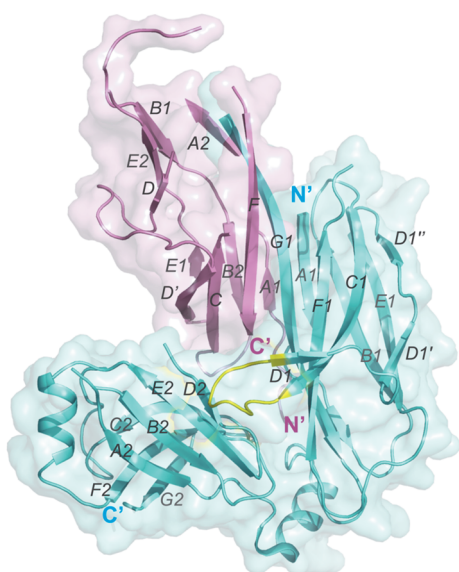


**Figure 17.** The high-resolution structure of the CsuC-CsuaA/B preassembly complex, cartoon and surface representations. CsuC and CsuaA/B are colored in cyan and pink, respectively. The  $\beta$ -strands as well as N- and C-termini are labeled. The C1-D1 hairpin of CsuC is colored in yellow.

The structure of the inter-domain linker also varies in the classical Caf1M and archaic CsuC chaperones. Thus, in CsuC an  $\alpha$ -helix of the linker is located closer to the N-terminal domain, whereas in Caf1M it belongs exclusively to the C-terminal domain. The position of the  $\alpha$ -helix might determine the degree of movements of the chaperone domains relative to each other (paper V, Figure 3A).

Additional remarkable features of the archaic CsuC chaperone are found in the topology of its C-terminal domain. Thus, CsuC displays an additional  $\alpha$ -helix absent in both Caf1M and CfaA. Moreover, CsuC exhibits a unique, nearly orthogonal packing of  $\beta$ -sheets in the C-terminal domain, whereas in Caf1M and CfaA the  $\beta$ -sheets are rotated towards each other only by 35–50° (paper V, Figure 7B). In the alternative EcpB chaperone, the  $\beta$ -sheets of the C-terminal domain have a practically parallel orientation (paper V, Figure 7B).

The CU pilus assembly strongly depends on the interactions of the chaperone with the usher assembly platform (Nishiyama *et al.*, 2008). In classical systems, binding to the usher is mediated by a hydrophobic patch of the C1D1F1G1  $\beta$ -sheet of the chaperone (Phan *et al.*, 2011). To verify the existence of the same usher binding surface in non-classical systems, we superposed the structures of CsuC and EcpB with Caf1M (paper V, Figure S10). Both CsuC and EcpB exhibit a set of hydrophobic residues in the putative usher-binding site. Thus, non-classical systems might utilize a similar mechanism of usher recognition.

#### 4.4.3 The CsuA/B subunit complexed with its chaperone is only partially folded

Despite the good values of the refinement statistics for the CsuC-CsuA/B complex (paper V, Table S1), nearly half of the CsuA/B sequence was not visible in the electron density map (Figure 17). Only strands positioned close to CsuC were automatically built. The quality of the electron density map for the regions located on the opposite side of the chaperone cleft drastically decreased, while their B-factors gradually increased (up to 113 Å<sup>2</sup> for C $\alpha$  atoms) (paper V, Figure 4A). The NMR spectrum obtained by our collaborators (paper V, Figure 4B) indicates that CsuA/B is largely disordered in solution. These structural data suggest that the CsuC chaperone captures and retains CsuA/B in a partially ordered state, similar to a pre-molten globule (Jeng & Englander, 1991). The pre-molten globule represents the state between the unfolded protein and the molten globule. Along with the secondary structure elements, this folding intermediate features a substantial part of disordered regions (Uversky & Ptitzyn, 1994; 1996).

The partially built model of CsuA/B revealed an incomplete Ig-fold comprised of six  $\beta$ -strands. As predicted from the sequence alignment, CsuA/B displays only marginal structural similarity to the classical chaperone-bound Caf1 subunit (paper V, Figure 4D). Caf1 does not have any disordered regions, whereas in CsuA/B, strands A, B, C and E are interrupted by the unstructured sequences. The associated loops between the strands of CsuA/B are also disordered, except for the B'-C loop stabilized by the disulphide bond between Cys16 and Cys62, which is highly conserved in archaic pilin subunits. Other important differences in Caf1 and CsuA/B are related to the topology of donor strand D and associated loops.

Finding that a large portion of the sequence is unstructured in the chaperone-bound CsuA/B is highly surprising, as such a phenomenon has never been reported for classical CU systems (paper V, Table S3). Classical subunits associated with the chaperone are fully folded, but maintained in an assembly-competent conformation (Zavialov *et al.*, 2003). In contrast, the disordered regions in CsuA/B constitute nearly 50 % of the protein sequence.

Intriguingly, our collaborators observed a similar phenomenon for the EcpA subunit complexed with the EcpB chaperone from alternative systems (paper V). While the NMR spectra of free donor strand complemented EcpAsc and EcpB proteins suggest a fully folded conformation, the  $^1\text{H}$ - $^{15}\text{N}$  TROSY NMR spectrum of the EcpB-EcpA complex clearly demonstrates the presence of disordered regions (paper V, Figure 9). Using free EcpA as a model, our colleagues were able to assign only 54 % of the chaperone-bound subunit sequence. Thus, the partially folded conformation of the chaperone-bound pilin subunit is likely to represent a common feature for both archaic and alternative systems.

The presence of natively unstructured proteins in bacteria is significantly less common than in eukaryotes. Thus, only 4 % of bacterial proteins are estimated to contain natively unfolded regions *in vivo* (Fink, 2005). The partially disordered state of the chaperone-bound subunit in the biogenesis of archaic and alternative pili raises a question of the biological significance of this phenomenon. To find an explanation, we focused on the interactions of CsuA/B with the CsuC chaperone.

#### 4.4.4 Both domains of CsuC are involved in the anchoring of CsuA/B

Our primary goal was to analyze the mechanism of subunit anchoring in the archaic systems. The C-terminus of CsuA/B is located precisely in the middle of the inter-domain cleft of CsuC (Figure 18). Interestingly, the C-carboxylate of the terminal Phe152 is oriented towards both domains of the chaperone. The particular positioning of the subunit C-terminal carboxylate and the makeup of the inter-domain cleft of CsuC allow CsuA/B to interact with both N- and C-terminal domains of the chaperone. Thus, one oxygen atom of the Phe152 carboxylate establishes an ionic bond with Arg89 (N-terminal domain), whereas the other oxygen atom is hydrogen-bonded to Tyr196 of the C-terminal domain. Arg174 interacting with Tyr196 additionally stabilizes the complex. Interestingly, all three residues are highly conserved within the archaic chaperones (paper V, Figure S1).

To investigate the role of each residue in subunit anchoring, we produced three single amino acid mutants of CsuC and analyzed the ability of the mutated chaperone to bind CsuA/B (paper V, Figure 6C). A sufficient CsuC level of expression similar to the wild-type confirmed that the introduced mutations did not affect the protein folding or

stability. However, they significantly reduced CsuC-CsuA/B complex formation. The Arg174Ala point mutation had the least dramatic effect on subunit recovery. This fact confirms the secondary role of this residue in C-terminal carboxylate binding. The substitution of either Arg89 or Tyr196 with alanine drastically reduced the level of CsuA/B in the periplasm. Furthermore, the CsuC chaperone combining both mutations was practically incapable of recovering the subunit. Based on these results, one can conclude that C-terminus anchoring is governed by both hydrogen and ionic interactions.

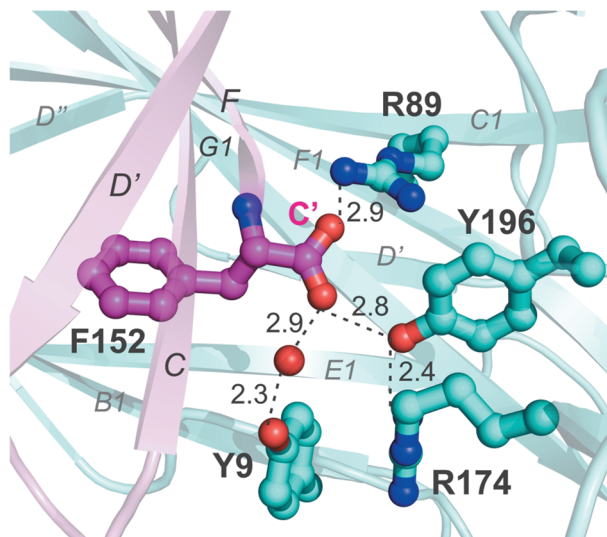


**Figure 18.** The mechanism of CsuA/B (pink) anchoring to the CsuC (cyan) chaperone, cartoon representation. The  $\beta$ -strands are labeled. Interacting residues are shown as ball-and-sticks and labeled. Hydrogen bonds are depicted as dashed lines and their lengths are indicated. The structured water molecule is shown as a red sphere.

Tyr9 from the N-terminal domain of CsuC might also play a supplementary role in carboxylate anchoring, as it interacts with the oxygen atom of Phe152 via a water molecule (Figure 18). However, Tyr9 is not conserved within the archaic systems, and its involvement in subunit fastening might be limited to just a few members of the archaic fimbriae.

Interestingly, residues corresponding to Arg89, Tyr196, and Arg174 in CsuC are highly conserved, not only among the members of the archaic CU pathway, but also within the alternative systems (paper V, Figure S1). This fact indicates that all non-classical chaperones might utilize the same mechanism for subunit anchoring. Indeed, the structural superposition of CsuC with the alternative chaperone EcpB shows that the conserved Arg, Tyr and Arg residues have identical positions in both proteins (paper V, Figure 8B). Our collaborators reproduced the same site-directed mutagenesis experiment on EcpB and subsequently analyzed the recovery of the EcpA subunit in the periplasm (paper V, Figures 8D). The obtained results confirmed that the conserved Arg89 and Tyr169 of EcpB play a key role in subunit binding in alternative systems.

The anchoring of the subunit's C-terminal carboxylate plays a critical role in the biogenesis of CU pili (Kuehn *et al.*, 1993). Thus, this mechanism has to be highly conserved among the related CU pathways. We demonstrated that archaic and alternative chaperones utilize the same residues to bind their nascent subunits in the periplasm. This mechanism strongly distinguishes archaic and alternative CU systems from the phylogenically distant classical CU machinery. In the classical fimbriae, only the N-terminal domain of the chaperone is involved in subunit capturing, and the interacting residues have no analogues in non-classical systems. In archaic and alternative fimbriae, both domains of the chaperone participate in subunit anchoring. The additional involvement of the C-terminal domain in the binding might be necessary for the stabilization of the partially disordered subunit.

#### 4.4.5 The donor-strand register is shifted in the CsuC-CsuA/B complex

Similarly to the classical CU pathway, the archaic CsuC chaperone stabilizes the subunit by inserting its four hydrophobic donor strand residues (Val110, Phe112, Met114, and Tyr116) into the hydrophobic cleft of CsuA/B, thus providing the “substitution” for the missing G strand and completing the Ig-fold. The subunit's strand F and the C-terminal part of strand A form hydrogen bonds with the G1 strand of the chaperone (paper V, Figure S2). The N-terminal part of the A strand of CsuA/B interacts with the A1 strand of CsuC.

The superposition of the CsuC-CsuA/B and Caf1M-Caf1 preassembly complexes revealed an intriguing feature of the archaic complex. CsuA/B is slightly shifted towards the C-terminal domain of CsuC and inserted deeper into its inter-domain cleft, compared to Caf1. To elucidate the molecular grounds for such a positioning of CsuA/B, we compared the donor strands of CsuC and Caf1M.

The donor strand of CsuC is shorter than that of Caf1M. Caf1M inserts five donor residues, whereas CsuC donates only four (paper V, Figure 5B). However, this is not a pathway-specific feature, as the length of the donor strand may vary within the same group of CU fimbriae. The most striking difference between the donor strands of classical and archaic chaperones is the relative position of their donor residues (Figure 19). In comparison with the classical chaperones, the donor strand register in CsuC is shifted along the G1 strand towards the C-terminus. In the classical systems the donor strand begins from position 1 (I134 in Caf1M), whereas in CsuC this position is occupied by the second donor residue (M114), and the first donor residue Tyr116 is placed in position 0 (Figure 19, paper V, Figure 5B). Thus, the shift of the donor strand motif towards the C-terminal end of the G1 strand determines the position of CsuA/B, which is inserted deeper into the inter-domain cleft of the chaperone.

The shift of the donor strand register has also been observed in alternative chaperones

CfaA (Bao *et al.*, 2014) and EcpB (paper V, Figure 8A). Interestingly, in all non-classical chaperones, position 0 is exclusively occupied by bulky residues such as tyrosine, methionine, leucine, and isoleucine (paper V, Figure S1).

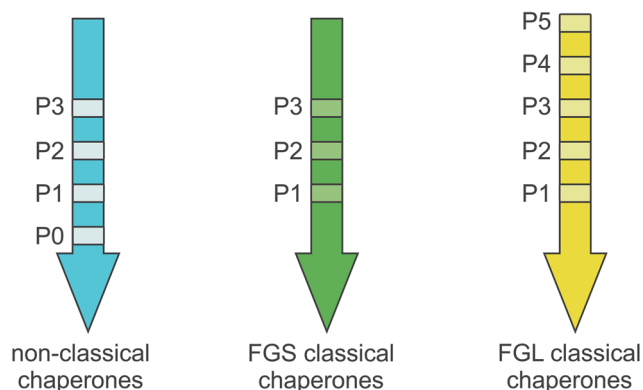


**Figure 19.** The scheme of the donor strands in classical (FGL and FGS subfamilies) and non-classical chaperones.

The shift of the donor strand residues towards the C-terminus of the chaperone in archaic and alternative systems might significantly alter the mechanism of subunit assembly. In classical systems, the DSE occurs via a “zip-in-zip-out” mechanism where the donor residues of the adjacent subunit gradually replace the chaperone G1 strand, starting from position P5 (Remaut *et al.*, 2006; Zavialov *et al.*, 2003). Is the DSE in non-classical systems governed by the same principle? To investigate this hypothesis, we determined the crystal structure of the fiber inserted conformation of CsuA/B subunit.

#### 4.4.6 The fiber-inserted conformation of the CsuA/B subunit has a unique structure of $\beta$ -sheet ABE

The crystal structure of CsuA/Bdsc has been solved to a resolution of 1.5 Å using the Se-SAD phasing method (paper IV, Table S1).

Unlike the chaperone-bound subunit, CsuA/Bdsc has a fully folded conformation, and the B-factors of C $\alpha$  atoms do not exceed 50 Å<sup>2</sup>. CsuA/Bdsc adopts a canonical Ig-fold composed of seven  $\beta$ -strands (Figure 20). The comparison of CsuA/Bdsc with available structures of polymerizing pilin subunits from alternative and classical systems revealed that the ABE  $\beta$ -sheet of CsuA/Bdsc has a unique structure (paper VI, Figure 2).  $\beta$ -sheet ABE features two prominent hairpins protruding from the  $\beta$ -barrel with a nearly 90°-kink (Figure 20). The sequence alignment of the single-domain archaic subunits revealed that A'-A'' and B'-B'' hairpins are present in  $\delta 2$  and  $\delta 2/3$

families of archaic fimbriae (paper VI, Figure S1). Indeed, the representatives of both families have corresponding glycine-rich sequences. Conserved glycine residues (Gly20, Gly25, Gly31, Gly57) form turns in the polypeptide chain and are responsible for the disruption of  $\beta$ -strands and the formation of hairpins.

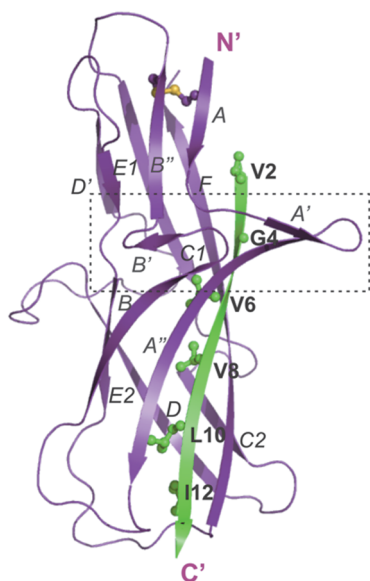


**Figure 20.** The high-resolution structure of Csua/Bdsc, cartoon representation. The  $\beta$ -strands as well as N- and C-termini are labeled. The Gd strand residues are shown as ball-and-sticks and labeled. The A'-A'' and B-B' hairpins are framed in rectangle.

The hairpins might play an important structural and functional role in the Csua/B-subfamily of archaic fimbriae. For example, they might be involved in the inter-subunit interactions within the fimbrial shaft or contribute to the development of bacterial communication and the formation of biofilms.

#### 4.4.7 Archaic CsuaC chaperone provides incomplete structural information for the folding of CsuaA/B

To understand why the chaperone-bound CsuaA/B is largely disordered, we compared the chaperone-bound and the fiber-inserted conformations of CsuaA/B (paper VI, Figure 3). The comparison revealed that the G1 strand sequence of CsuaC is only two thirds the length of the Gd strand of the attacking subunit. Four donor residues of CsuaC occupy acceptor pockets P0-P3, whereas pockets P4 and P5 remain unstructured. In contrast, the long Gd strand of the attacking subunit occupies all acceptor pockets in the hydrophobic cleft of CsuaA/B. These results suggest that the archaic CsuaC chaperone provides only partial information for subunit folding, thereby maintaining it largely disordered. The replacement of the short G1 strand of the chaperone with the long Gd strand of the subunit triggers the folding of disordered regions and leads to the



formation of a compact fiber module.

It was previously shown that the assembly of classical systems involves a large conformational change of the hydrophobic core of pilin subunits (Zavialov *et al.*, 2003; 2005). The G1 strand of the classical chaperone intercalates between the  $\beta$ -sheets of the subunit and maintains it in a high-energy conformation, whereas a less bulky Gd strand of the attacking subunit allows the collapse of the subunit. To check if a similar conformational change occurs during the assembly of archaic systems, we superimposed the self-complemented and the chaperone-bound CsuA/B subunit (paper VI, Figure S4). The superposition revealed that, in contrast to classical systems, the polymerization of archaic pilin subunits does not lead to a rearrangement of the  $\beta$ -sheets. Thus, the main outcome of DSE in archaic systems is the folding of the disordered segments of the subunit.

We also observed that strand B of the chaperone-bound CsuA/B subunit does not form a hairpin. The molecular basis of this structural variation became clear after the comparison of self-complemented and chaperone-bound CsuA/B (Figure 21). In the preassembly complex, the bulky Phe114 of the chaperone G1 strand would collide with the side chain of Val50 in the B-B'-hairpin of CsuA/Bdsc. Similarly, the bulky G1 strand of CsuC also prevents the folding of strand A in the chaperone-bound subunit due to the steric clashes of Met114 of CsuC with Phe30 of the A'-A'' hairpin.

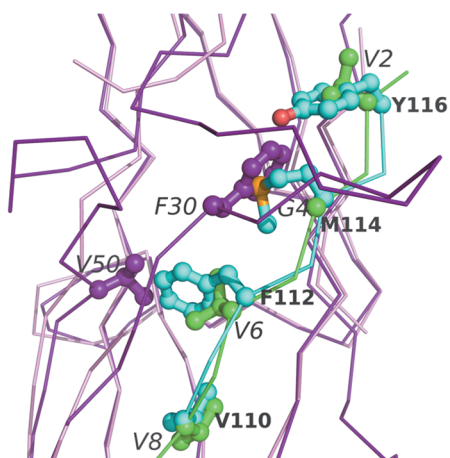


**Figure 21.** Superposition of chaperone-bound (pink) and self-complemented (purple) CsuA/B, ribbon representation. The G1 strand of CsuC and the Gd strand of CsuA/B are colored in blue and green, respectively. Phe30 and Val50 of CsuA/Bdsc and donor residues are shown as ball-and-sticks and labeled.

Thus, the short donor-strand of the archaic chaperone provides only partial information for subunit folding. Additionally, the bulky donor residues of CsuC preclude the formation of the hairpins in the chaperone-bound subunit.

#### 4.4.8 Assembly of the archaic fimbriae is driven by subunit folding energy

The unique anchoring mechanism and the substantially unfolded conformation of the chaperone-bound subunit might result in dramatically different thermodynamic and kinetic properties of the preassembly complex in comparison with the classical systems. To verify this assumption, we analyzed the association-dissociation kinetics of CsuC-CsuA/B using SPR. CsuC-CsuA/B-His6-tag was applied to a Ni-agarose coated sensor chip. Due to the presence of the His6-tag, CsuA/B attached to the chip, whereas CsuC could be gradually washed away. After the washing step, we added subunit-free CsuC and recorded the resonance signals of the association and dissociation phases (paper VI, Figure 5B). The experiment was repeated for the several concentrations of CsuC. Assuming that the CsuC chaperone binds the CsuA/B subunit in a 1:1 ratio, *k-on* and *k-off* rate constants were determined. Our results demonstrate that archaic CsuC binds to CsuA/B with an affinity similar to classical chaperones. However, the formation of the archaic CsuC-CsuA/B complex was 2–2.5 times slower than in classical systems (Yu *et al.*, 2012a). The lower rate of the preassembly complex formation in archaic systems might be explained by its particular anchoring mechanism, which requires specific positioning of the flexible chaperone domains for subunit binding. As CsuC is significantly slower in capturing its subunit compared to its classical counterpart, the archaic CU systems might represent a less efficient and consequently more primitive assembly pathway. However, to prove this statement, it is necessary to evaluate the kinetic properties of other steps of the pilus assembly in archaic systems.

We hypothesized that the partially disordered conformation of the CsuC-bound CsuA/B might have a strong impact on the stability of the preassembly complex in archaic systems. Hence, we characterized the thermodynamics of the CsuC-CsuA/B complex by using differential scanning calorimetry. Intriguingly, our results showed that the spectra of thermal denaturation for the archaic preassembly complex were similar to those of the classical Caf1M-Caf1 complex. Thus, thermal denaturation of CsuC-CsuA/B gave two heat absorption peaks with maxima at 48 °C and 62 °C, corresponding to the unfolding of CsuA/B and CsuC, respectively (paper VI, Figure 5A). Melting of the classical Caf1M-Caf1 complex occurs at 45 °C, whereas the free Caf1M melts at 62 °C (Zavialov *et al.*, 2005). How is it possible that, despite the different folding states of the chaperone-bound subunits, the classical and archaic preassembly complexes have nearly identical thermal denaturation curves? In the archaic CsuC-CsuA/B complex, the low stability of the subunit might be explained by its partially folded conformation (41 % of the sequence). In classical systems, the chaperone-associated subunit is fully folded, but the bulky donor residues of the G1 strand of the Caf1M chaperone prevent the collapse of the subunit hydrophobic core and set its  $\beta$ -sheets apart (Zavialov *et al.*, 2005). Thus, in both CU systems the chaperone-bound subunits are maintained in energetically unfavorable conformation,

but at the different stages of folding. Thus, in classical systems the subunit is retained at the last folding step, whereas in archaic systems, the folding is blocked at a significantly earlier stage (Figure 22).

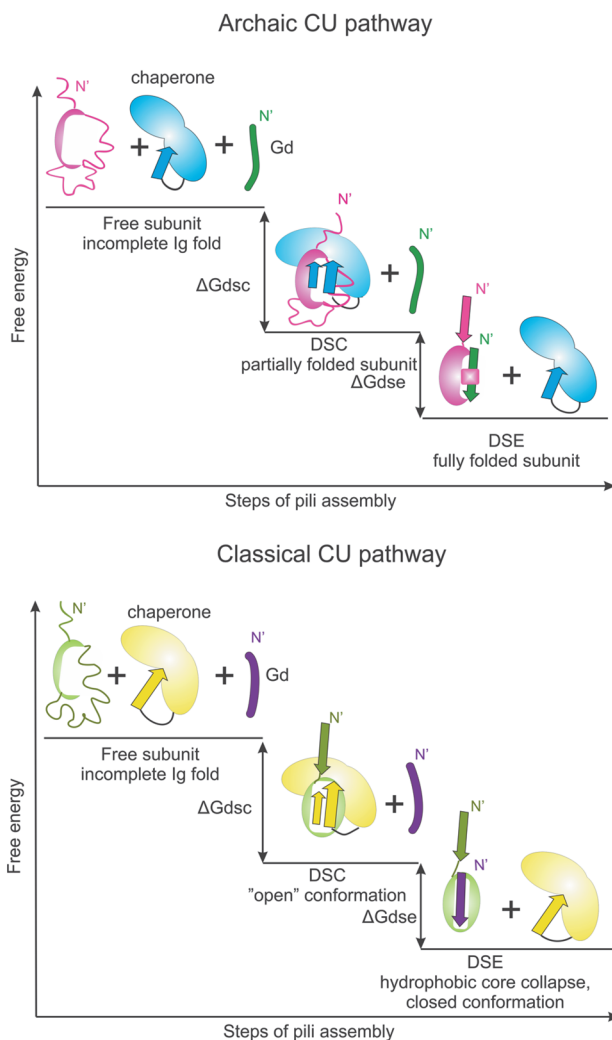


**Figure 22.** Changes in the free energy of pilin subunits during the assembly process of classical and archaic pili. Donor strands are depicted as arrows, N-termini are indicated. The free energy of classical pilin subunit is redrawn based on Zavialov *et al.*, 2003.

Our structural data showed that, upon DSE, the archaic *CsuA/Bdsc* adopts a fully folded low-energy conformation, suggesting its high stability. To verify this assumption, we compared the thermodynamic parameters of the chaperone-bound *CsuA/B* and *CsuA/Bdsc* by using differential scanning calorimetry. As expected, the melting temperature of the chaperone-free DSC subunit was significantly higher (90

°C) than in complex with CsuC (paper VI, Figure 5A). A free energy potential resulting from the differences in the conformations of the chaperone-bound and DSC subunits triggers their polymerization in the archaic pili (Figure 22).

The transition temperature of CsuA/Bdsc is similar to that of Caf1dsc, which has been determined previously (Zavialov *et al.*, 2005). Thus, in both classical and archaic systems, DSC subunits have exceptional stability, thereby representing the most stable protein-protein interaction known to date (Makhatadze & Privalov, 1995; Puorger *et al.*, 2008).

#### 4.4.9 Non-classical CU systems might display a more flexible mode of DSE

The high-resolution structures of the CsuC-CsuA/B preassembly complex and the CsuA/Bdsc subunit suggest a possible mechanism for DSE in archaic systems. CsuA/Bdsc forms a tightly packed structure while the CsuC chaperone maintains CsuA/B in a partially ordered state, leaving open the hydrophobic core of the molecule. Since the donor motif of the chaperone is shifted towards the C-terminus of the G1 strand by two residues, the donor strand occupies only P0–P3 acceptor pockets, whereas the P4 and P5 are not formed. Thus, CsuC-CsuA/B preassembly complex is lacking a DSE initiation site common for classical systems (Figure 23). The donor-strand of the attacking subunit might easily enter the loosely packed hydrophobic core of CsuA/B.

The replacement of the G1 strand of the chaperone most likely occurs via the classical zip-in-zip-out mechanism (Zavialov *et al.*, 2003; Remaut *et al.*, 2006). However, the presence of large unstructured regions should allow higher flexibility for DSE. Thus, in archaic and alternative systems, DSE might be governed by the combination of zip-in-zip-out and lateral displacement mechanisms. For example, the G1 strand of the alternative chaperone EcpB is formed by small hydrophobic residues (Ala111, Ala113, and Ala115) in positions P1–P3 and bulky isoleucine in position P0 (paper V, Figure S6B). The Gd strand of the EcpA pilin subunit features a bulky tryptophan residue (Trp11) in the middle. Thus, Gd donates alanine residues for acceptor pockets P0, P1, P3, and P4 as well as tryptophan for the acceptor pocket P2. Considering that the chaperone-bound EcpA subunit is only partially ordered, it seems plausible that the Gd of the attacking subunit can penetrate much deeper into a loosely packed structure. According to that scenario, the initiation of the DSE may also occur at other acceptor pockets, rather than strictly at the P5 pocket as in the classical systems. Thus, for Ecp-pili, the initiation site might be located in the P2 acceptor pocket, where the attacking EcpB inserts the bulky Trp11 (paper V, Figure S8). DSE might also occur simultaneously in several acceptor pockets, enabling the lateral displacement the G1 strand. However, additional experiments are required to verify the exact mechanism of DSE in non-classical fimbriae.

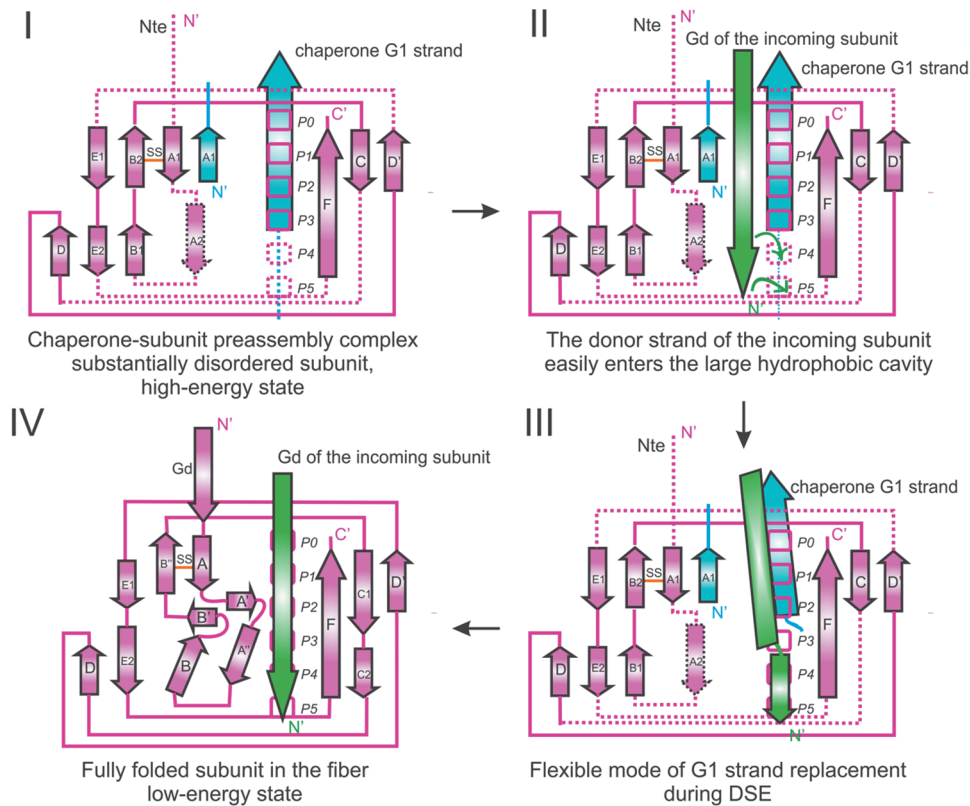


**Figure 23.** The proposed mechanism of donor strand exchange in the archaic Csu pili, topology diagram.

The relative movement of chaperone domains may play an important role during subunit assembly in archaic and alternative systems. Our results showed that, in the subunit-bound conformation, the angles between the N- and C-terminal domains of archaic CsuC and classical Caf1M are nearly identical (paper V, Figure 7B). The orientation of domains in free Caf1M is also similar. In contrast, in the subunit-free alternative chaperones CfaA and EcpB, the inter-domain angle varies significantly, indicating a high degree of domain movement in the absence of subunits in non-classical systems. As both the C- and N-terminal domains of the chaperone participate in subunit anchoring, they are set in a fixed conformation upon subunit attachment. Hence, the relative movements of domains apart from each other would promote the release of the subunit during DSE. This conformational change could be facilitated by the usher.

#### **4.4.10 Archaic and alternative systems – a distinct assembly pathway of CU organelles**

The biogenesis of archaic and alternative pili is governed by the common principles of CU organelle assembly. However, our structural and biochemical data demonstrated significant deviations from the mechanisms of DSC and DSE as described for classical fimbriae. The observed differences indicate that archaic and alternative systems utilize a distinct pathway of pilus assembly. The most intriguing feature of non-classical systems is a significantly disordered state of the chaperone-bound subunit. Non-classical chaperones use short register-shifted donor strand motives that provide incomplete structural information for subunit folding.

The unfolded conformation of the subunit and the shift of the donor strand register allow for a different, possibly more flexible mode of DSE. The transition from a partially folded to a more energetically favorable fully folded conformation releases the energy driving the pilus assembly.

Non-classical systems also utilize a strikingly different mechanism for subunit anchoring, which involves both domains of the chaperone. This finding is of great fundamental and practical significance. The anchoring of the subunit's C-terminus is likely to be the first step in chaperone-subunit complex formation, and thus the C-terminal carboxylate binding site represents a potential inhibition target. However, our results clearly demonstrate that different inhibitors have to be used to suppress pili formation in classical and non-classical CU machineries. Interestingly,  $\beta$ -fimbriae currently categorized as classical systems (Nuccio & Baumber, 2007) are likely to bind the subunit in a “non-classical” manner. Thus, instead of basic residues interacting with the subunit in classical pili,  $\beta$ -fimbriae possess analogous residues anchoring the subunit to those in alternative and archaic systems.

Despite the differences in the assembly process, all CU systems presumably employ a similar mechanism for the binding of the chaperone-subunit preassembly complexes to the usher platform. Thus, an inhibitor targeting the usher-binding site of the chaperone may be able to prevent pilus assembly in different CU systems.

## 5. CONCLUDING REMARKS AND FUTURE PROSPECTS

The importance of bacterial adhesion in pathogenesis is undeniable, and its role goes beyond simple attachment to target tissues. The adhesion mediates the activation and delivery of toxins and affects host cell signaling, enabling a pathogen to evade the immune defense and prosper in the host environment. The sticking of bacteria to each other creates a biofilm – an important tool of antibiotic resistance. The key role of adhesion in establishing and spreading an infection underlines the need to thoroughly characterize bacterial adhesins and unravel their assembly process. In this thesis I aimed to elucidate the structural basis for polyadhesin-mediated attachment and the biogenesis of fimbriae via the recently discovered archaic chaperone-usher (CU) pathway.

Our findings demonstrate that polyvalent adhesins form a distinct class of bacterial surface organelles. Their common feature is the ability to establish multipoint contacts with a target cell, as each pilin subunit binds one or several host cell receptors. Although all studied pilin monomers have a similar structural organization, their mechanism of binding, the make-up of the binding pocket, as well as the nature of the target receptor significantly varies between the adhesins. The binding interface might be designed to interact with a specific ligand (e.g.  $\beta$ -1-3 or  $\beta$ -1-4 terminal galactose in the case of MyfA and PsaA) or with a group of receptors with similar properties (e.g. negatively charged proteins in the case of AggA). Polyvalent adhesion gives the pathogen a number of benefits in the host cell environment. Firstly, multipoint attachment places the bacteria closer to its host cell and, as a consequence, might accelerate the release and the delivery of toxins. Secondly, polyvalent attachment ensures adhesion only to cell-attached receptors. Thirdly, it allows the bacteria to modulate the avidity of binding whenever necessary.

The ability of pathogens to employ a polyvalent binding mode represents a serious problem for the development of antibacterial therapy, as it clearly challenges the utility of monovalent anti-adhesion inhibitors. Furthermore, the phenomenon of multipoint attachment underlines the necessity to target fimbriae biogenesis rather than the receptor-binding site in already assembled organelles. Thus, future studies on polyvalent adhesins should focus on finding the most appropriate inhibition target at the different steps of fimbrial assembly. For example, the effect of pilicides on the formation of various polyadhesins should be carefully analyzed.

This thesis also explored the biogenesis of adhesive organelles via the recently discovered archaic CU pathway. The archaic Csu fimbriae from *Acinetobacter baumannii* are used as a model. High-resolution structural data supported by biochemical studies reveal several unique features of pilus assembly via the archaic

CU pathway. We demonstrate that the CsuC chaperone traps the CsuA/B subunit in a substantially disordered state, which is likely to affect the mode of donor strand exchange (DSE) during subunit polymerization. Interestingly, similar results have been obtained for the alternative fimbriae Ecp and CFA/I. Thus, the archaic and alternative pili form a distinct group within the CU machinery.

This thesis is the first work focused on the molecular basis for non-classical fimbrial assembly. Thus, many questions remain to be addressed. Firstly, our assumption regarding the flexible mode of DSE needs to be verified and supported by additional biochemical and structural data. In particular, it is important to elucidate whether there is a specific initiation site for DSE. Can it be located in any other acceptor pockets besides P5 in different non-classical fimbriae?

Another critical step in pili biogenesis involves the binding of the chaperone-subunit preassembly complex to the usher assembly platform. Structural analysis of these interactions will provide several important insights into the non-classical fimbrial assembly and might further facilitate the development of inhibitors targeting archaic and alternative pili.

Regarding the clinically important archaic Csu pili of *A. baumannii* and the homologous CupE pili of *Pseudomonas aeruginosa*, it is crucial to unravel the structural basis for fimbriae-mediated biofilm formation and host cell receptor recognition. These data will provide a range of new tools to counter the multi-resistant pathogens. The suppression of *A. baumannii* and *P. aeruginosa* biofilm-mediating fimbriae will significantly reduce bacterial virulence and the severity of the infections while increasing the susceptibility of the pathogens to traditional antibiotics.



## 6. ACKNOWLEDGEMENTS

The research for this thesis was performed at the Department of Biochemistry, University of Turku during 2012-2016. I thank Professor Jyrki Heino and PhD Jarmo Niemi for providing the opportunity to use excellent facilities and enjoy the inspirational research spirit of the Department of Biochemistry.

I would like to express my gratitude to the Doctoral Program of Molecular Life Sciences, Erasmus Mundus Triple I program and Finnish cultural foundation for providing funding to work on my PhD thesis and allowing me fully concentrate on my research. I also thank Minna Lintala, Satu Jasu, Kaisa Ketomäki and Maritta Löytömäki for the excellent help and guidance during my PhD project.

During my studies, I have attended various interesting courses and symposia. I am greatly thankful to the Doctoral Program of Molecular Life Sciences, Turku University Foundation and Academy of Finland for making these trips possible.

I want to thank Dr. Julie Bouckaert for acting as the opponent in the public defence of my dissertation. I am grateful to the reviewers of my thesis, Professor Adrian Goldman and Professor Stefan Knight for their valuable comments and constructive criticism.

I deeply thank my primary supervisor Dr. Anton Zavialov for the guidance, support and engaging discussions all the way during my PhD project. You made me discover an amazing world of structural biology and X-ray crystallography, and I am genuinely grateful for that. I am also thankful to my co-supervisor Professor Urpo Lämminmäki for the excellent advice and support during my PhD studies.

I am grateful to all present and former members of the Joint Biotechnology laboratory: Minna Tuittila, Sari Paavilainen, Vladimir Zav'yalov, Timo Korpela, Elvira Khalikova, Maksim Skaldin, Olena Parilova, Jyoti Gurung, Henri Malmi, Mubin Rahman and Saumendra Roy. It has been a pleasure and great experience to work with all of you. A big thank you belongs to our collaborators – Professor Steve Matthews and his group from the Imperial College of London and Professor Susann Teneberg and her team from the University of Gothenburg. Our joint work together gave incredible results.

During my PhD studies, I have made numerous trips to the European Synchrotron Radiation facility (ESRF, Grenoble, France) to collect diffraction data. I wish to thank all beamline scientists I worked with for their help and sincere interest in every research project. In addition, I am grateful to the administrative staff of ESRF for organization of travel formalities and cooperation regarding the transportation of our samples.

I would like to thank all personnel of the Department of Biochemistry and especially my “brothers in arms” - PhD students Erika Nordbo, Tuuli Ahlstrand, Matti Turtola, Benjamin Nji Wandji, Johannes Merilahti, Maria Salmela, Anna-Brita Puranen and no longer PhD students, but honored PhD Kalle Sipilä, Heidi Luoto and Vilja Siitonen. It has been very nice to participate in the Journal Club and discuss our research projects with fun and creativity. A special thanks goes to Vilja Siitonen who was my “lodestar” on my way to the pre-examination and defence. I would also like to thank Amruta Prasanna Deshpande and Liz Gutiérrez for the friendship and for making a great company during lunch and coffee breaks.

I deeply thank Professor Timo Korpela, Dr. Yury Sukhanov and Professor Irina Larina for literally changing my life and bringing me to Finland. Thank you, Timo and Elvira for your invaluable help since my first day in Turku, I will never forget that!

I am thankful to Reetta Liukkonen and all members of Pilkahdus singing group who generously shared with me the joy of music and immersed me in the Finnish culture and the language.

I thank my wonderful friends (and the list will be long) from all over the world who bring so much joy to my life – Anna Firsova, Natalia Elina, Olga Firsova, Alena Bogdanova, Karolina Losenkova, Luca Marangone, Kevin Minet, Marina Karlova, Justina Brazinskaite, OGKnight Lee, Oxana Tarasyuk, Yana Kruglikova, Eugene Goncharko, Joseph Aduayi-Akue, Tina Spoljar, Jussi Vessanto, Ana Spoljar, Anders Wittrup, Susanne Ylikoski-Rogmann, Johannes Ylikoski, Kalen Lin, Juha-Pekka Ansio, Maria Vesti, Elena Zvereva, Olga Bogomolova, Ekaterina Denisova, Oxana Trifonova, Olga Obratsova, Ludmila Pastushkova, Olga Lagutina and Julia Golubchikova. Special thank you goes to my friends, who are always supporting me despite living far away.

I thank my whole family – Mom, Dad, my dear Sister and The Cat for the warmth and encouragement all the way though. Finally, I thank my new family Rudy (Komochek) and A-a-a-drian! Your love and support were the greatest motivation for me. Rudy, you are amazing - despite being far from biochemistry, you patiently listened about my project all those years without feeling bored (or, at least, without looking bored?) and even came up with questions and ideas! This is fascinating!  
But seriously... thank you, Komochek, for making Finland my home.

I chose this great quote of Lao Tzu as an epigraph for my thesis – *A journey of a thousand miles begins with a single step*. I am glad that today I made one more step. And I also thank myself for that.

Turku, September, 2016

Natalia

## REFERENCES

- Adams, P.D., Grosse-Kunstleve, R.W., Hung, L.W., Ioerger, T.R., McCoy, A.J., Moriarty, N.W., Read, R.J., Sacchettini, J.C., Sauter, N.K., and Terwilliger, T.C. (2002). PHENIX: building new software for automated crystallographic structure determination. *Acta crystallographica. Section D, Biological crystallography* 58, 1948-1954.
- Anderson, G.W., Worsham, P. L., Bolt, C. R., Andrews, G. P., Welkos, S. L., Friedlander, A. M. and Burans, J. P., (1997) Protection of mice from fatal bubonic and pneumonic plague by passive immunization with monoclonal antibodies against the F1 protein of *Yersinia pestis*. *American Journal of Tropical Medicine and Hygiene* 56, 471-473.
- Anderson, K.L., Billington, J., Pettigrew, D., Cota, E., Simpson, P., Roversi, P., Chen, H.A., Urvil, P., du Merle, L., Barlow, P.N., *et al.* (2004). An atomic resolution model for assembly, architecture, and function of the Dr adhesins. *Molecular Cell* 15, 647-657.
- Anisimov, A.P., Lindler, L.E., and Pier, G.B. (2004). Intraspecific diversity of *Yersinia pestis*. *Clinical Microbiology Reviews* 17, 434-464.
- Austin Alchon, S. (2003). *A pest in the land: new world epidemics in a global perspective*. University of New Mexico Press, Albuquerque, U.S.A.
- Balcázar, J.L., Subirats, J., and Borrego, C.M. (2015). The role of biofilms as environmental reservoirs of antibiotic resistance. *Frontiers in Microbiology* 6, 1216-1225.
- Bao, R., Fordyce, A., Chen, Y.X., McVeigh, A., Savarino, S.J., and Xia, D. (2014). Structure of CfaA suggests a new family of chaperones essential for assembly of class 5 fimbriae. *Plos Pathogens* 10, e1004316.
- Bao, R., Nair, M.K., Tang, W.K., Esser, L., Sadhukhan, A., Holland, R.L., Xia, D., and Schifferli, D.M. (2013). Structural basis for the specific recognition of dual receptors by the homopolymeric pH 6 antigen (Psa) fimbriae of *Yersinia pestis*. *Proceedings of the National Academy of Sciences of the United States of America* 110, 1065-1070.
- Battye, T.G., Kontogiannis, L., Johnson, O., Powell, H.R., and Leslie, A.G. (2011). iMOSFLM: a new graphical interface for diffraction-image processing with MOSFLM. *Acta crystallographica. Section D, Biological crystallography* 67, 271-281.
- Bergogne-Bérézin, E., and Towner, K.J. (1996). *Acinetobacter spp.*, as nosocomial pathogens: Microbiological, clinical, and epidemiological features. *Clinical Microbiology Reviews* 9, 148-165.
- Björk, S., Breimer, M.E., Hansson, G.C., Karlsson, K.A., and Leffler, H. (1987). Structures of blood-group glycosphingolipids of human small-Intestine. A relation between the expression of fucolipids of epithelial cells and the ABO-, Le- and Se-phenotype of the donor. *Journal of Biological Chemistry* 262, 6758-6765.
- Black, J.G. (1999). *Microbiology. Principles and explorations*. Prentice Hall, Upper Saddle River, New Jersey, U.S.A.
- Boisen, N., Melton-Celsa, A.R., Scheutz, F., O'Brien, A.D., and Nataro, J.P. (2015). Shiga toxin 2a and Enterotoxigenic *Escherichia coli* - a deadly combination. *Gut Microbes* 6, 272-278.
- Boisen, N., Struve, C., Scheutz, F., Krogfelt, K.A., and Nataro, J.P. (2008). New adhesin of enterotoxigenic *Escherichia coli* related to the Afa/Dr/AAF family. *Infection and Immunity* 76, 3281-3292.
- Bouckaert, J., Berglund, J., Schembri, M., De Genst, E., Cools, L., Wuhrer, M., Hung, C.S., Pinkner, J., Slättegård, R., Zavialov, A., *et al.* (2005). Receptor binding studies disclose a novel class of high-affinity inhibitors of the *Escherichia coli* FimH adhesin. *Molecular Microbiology* 55, 441-455.
- Breimer, M.E., Hansson, G.C., Karlsson, K.A., Larson, G., and Leffler, H. (2012). Glycosphingolipid composition of epithelial cells isolated along the villus axis of small intestine of a single human individual. *Glycobiology* 22, 1721-1730.
- Buts, L., Bouckaert, J., De Genst, E., Loris, R., Oscarson, S., Lahmann, M., Messens, J., Brosens, E., Wyns, L., and De Greve, H. (2003). The

- fimbrial adhesin F17-G of enterotoxigenic *Escherichia coli* has an immunoglobulin-like lectin domain that binds N-acetylglucosamine. *Molecular Microbiology* 49, 705-715.
- Capitani, G., Eidam, O., and Grütter, M.G. (2006). Evidence for a novel domain of bacterial outer membrane ushers. *Proteins* 65, 816-823.
- Cegelski, L., Marshall, G.R., Eldridge, G.R., and Hultgren, S.J. (2008). The biology and future prospects of antivirulence therapies. *Nature Reviews Microbiology* 6, 17-27.
- Chessa, D., Dorsey, C.W., Winter, M., and Baumler, A.J. (2008). Binding specificity of *Salmonella* plasmid-encoded fimbriae assessed by glycomics. *The Journal of Biological Chemistry* 283, 8118-8124.
- Choi, B.K., and Schifferli, D.M. (1999). Lysine residue 117 of the FasG adhesin of enterotoxigenic *Escherichia coli* is essential for binding of 987P fimbriae to sulfatide. *Infection and Immunity* 67, 5755-5761.
- Chorell, E., Pinkner, J.S., Phan, G., Edvinsson, S., Buelens, F., Remaut, H., Waksman, G., Hultgren, S.J., and Almqvist, F. (2010). Design and synthesis of C-2 substituted thiazolo and dihydrothiazolo ring-fused 2-pyridones: pilicides with increased antivirulence activity. *Journal of Medicinal Chemistry* 53, 5690-5695.
- Choudhury, D., Thompson, A., Stojanoff, V., Langermann, S., Pinkner, J., Hultgren, S.J., and Knight, S.D. (1999). X-ray structure of the FimC-FimH chaperone-adhesin complex from uropathogenic *Escherichia coli*. *Science* 285, 1061-1066.
- Coddens, A., Diswall, M., Angstrom, J., Breimer, M.E., Goddeeris, B., Cox, E., and Teneberg, S. (2009). Recognition of blood group ABH type 1 determinants by the FedF adhesin of F18-fimbriated *Escherichia coli*. *The Journal of Biological Chemistry* 284, 9713-9726.
- Collaborative Computational Project, N. (1994). The CCP4 suite: programs for protein crystallography. *Acta crystallographica. Section D, Biological crystallography* 50, 760-763.
- Coque, T.M., Baquero, F., Canton R. Increasing prevalence of ESBL-producing *Enterobacteriaceae* in Europe. (2008). *Eurosurveillance* 13. pii:19044.
- Cornelis, G.R., and Wolf-Watz, H. (1997). The *Yersinia* Yop virulon: a bacterial system for subverting eukaryotic cells. *Molecular Microbiology* 23, 861-867.
- Costa, T.R., Felisberto-Rodrigues, C., Meir, A., Prevost, M.S., Redzej, A., Trokter, M., and Waksman, G. (2015). Secretion systems in Gram-negative bacteria: structural and mechanistic insights. *Nature Reviews Microbiology* 13, 343-359.
- Cusumano, C.K., and Hultgren, S.J. (2009). Bacterial adhesion - a source of alternate antibiotic targets. *Idrugs - the Investigational Drugs journal* 12, 699-705.
- Cusumano, C.K., Pinkner, J.S., Han, Z., Greene, S.E., Ford, B.A., Crowley, J.R., Henderson, J.P., Janetka, J.W., and Hultgren, S.J. (2011). Treatment and prevention of urinary tract infection with orally active FimH inhibitors. *Science Translational Medicine* 3, 109-115.
- Czczulin, J.R., Balepur, S., Hicks, S., Phillips, A., Hall, R., Kothary, M.H., Navarro-Garcia, F., and Nataro, J.P. (1997). Aggregative adherence fimbria II, a second fimbrial antigen mediating aggregative adherence in enteroaggregative *Escherichia coli*. *Infection and Immunity* 65, 4135-4145.
- De Greve, H., Wyns, L., and Bouckaert, J. (2007). Combining sites of bacterial fimbriae. *Current Opinion in Structural Biology* 17, 506-512.
- de Oliveira-Garcia, D., Dall'Agnol, M., Rosales, M., Azzuz, A.C., Alcantara, N., Martinez, M.B., and Girón, J.A. (2003). Fimbriae and adherence of *Stenotrophomonas maltophilia* to epithelial cells and to abiotic surfaces. *Cellular Microbiology* 5, 625-636.
- Dodson, K.W., Jacob-Dubuisson, F., Striker, R.T., and Hultgren, S.J. (1993). Outer-membrane PapC molecular usher discriminately recognizes periplasmic chaperone-pilus subunit complexes. *Proceedings of the National Academy of Sciences of the United States of America* 90, 3670-3674.
- Dodson, K.W., Pinkner, J.S., Rose, T., Magnusson, G., Hultgren, S.J., and Waksman, G. (2001). Structural basis of the interaction of the pyelonephritic *E. coli* adhesin to its human kidney receptor. *Cell* 105, 733-743.
- Doublé, S. (2007). Production of selenomethionyl proteins in prokaryotic and eukaryotic expression systems. *Methods in Molecular Biology* 363, 91-108.
- Dougherty, D.A., and Stauffer, D.A. (1990). Acetylcholine binding by a synthetic receptor: implications for biological recognition. *Science* 250, 1558-1560.

- Dubnovitsky, A.P., Duck, Z., Kersley, J.E., Härd, T., MacIntyre, S., and Knight, S.D. (2010). Conserved hydrophobic clusters on the surface of the Caf1A usher C-terminal domain are important for F1 antigen assembly. *Journal of Molecular Biology* 403, 243-259.
- ECDC/EMEA joint technical report (2009). The bacterial challenge: time to react
- [http://ecdc.europa.eu/en/publications/Publications/0909\\_TER\\_The\\_Bacterial\\_Challenge\\_Time\\_to\\_React.pdf](http://ecdc.europa.eu/en/publications/Publications/0909_TER_The_Bacterial_Challenge_Time_to_React.pdf) (retrieved 2016-05-03).
- Emsley, P., Lohkamp, B., Scott, W.G., and Cowtan, K. (2010). Features and development of Coot. *Acta crystallographica. Section D, Biological crystallography* 66, 486-501.
- Eslava, C., Navarro-Garcia, F., Czczulin, J.R., Henderson, I.R., Cravioto, A., and Nataro, J.P. (1998). Pet, an autotransporter enterotoxin from enteroaggregative *Escherichia coli*. *Infection and Immunity* 66, 3155-3163.
- Farfan, M.J., Inman, K.G., and Nataro, J.P. (2008). The major pilin subunit of the AAF/II fimbriae from enteroaggregative *Escherichia coli* mediates binding to extracellular matrix proteins. *Infection and Immunity* 76, 4378-4384.
- Felek, S., Tsang, T.M., and Krukons, E.S. (2010). Three *Yersinia pestis* adhesins facilitate Yop delivery to eukaryotic cells and contribute to plague virulence. *Infection and Immunity* 78, 4134-4150.
- Fink, A.L. (2005). Natively unfolded proteins. *Current Opinion in Structural Biology* 15, 35-41.
- Frank, C., Werber, D., Cramer, J. P., Askar, M., Faber, M., an der Heiden, M., Bernard, H., Fruth, A., Prager, R., Spode, A., *et al.* (2011) Epidemic profile of Shiga-toxin-producing *Escherichia coli* O104:H4 outbreak in Germany. *The New England Journal of Medicine* 365, 1771-1780.
- Fredrickson, J.K., Zachara, J.M., Balkwill, D.L., Kennedy, D., Li, S.M., Kostandarithes, H.M., Daly, M.J., Romine, M.F., and Brockman, F.J. (2004). Geomicrobiology of high-level nuclear waste-contaminated vadose sediments at the hanford site, washington state. *Applied and Environmental Microbiology* 70, 4230-4241.
- Gaastra, W., and Svennerholm, A.M. (1996). Colonization factors of human enterotoxigenic *Escherichia coli* (ETEC). *Trends in Microbiology* 4, 444-452.
- Galindo, C.L., Rosenzweig, J.A., Kirtley, M.L., and Chopra, A.K. (2011). Pathogenesis of *Y. enterocolitica* and *Y. pseudotuberculosis* in human yersiniosis. *Journal of Pathogens*, 2011:182051.
- Galván, E.M., Chen, H., and Schifferli, D.M. (2007). The Psa fimbriae of *Yersinia pestis* interact with phosphatidylcholine on alveolar epithelial cells and pulmonary surfactant. *Infection and Immunity* 75, 1272-1279.
- Geibel, S., and Waksman, G. (2014). The molecular dissection of the chaperone-usher pathway. *Biochimica et Biophysica Acta* 1843, 1559-1567.
- Giraud, C., Bernard, C.S., Calderon, V., Yang, L.A., Filloux, A., Molin, S., Fichant, G., Bordi, C., and de Bentzmann, S. (2011). The PprA-PprB two-component system activates CupE, the first non-archetypal *Pseudomonas aeruginosa* chaperone-usher pathway system assembling fimbriae. *Environmental Microbiology* 13, 666-683.
- Giraud, C., and de Bentzmann, S. (2012). Inside the complex regulation of *Pseudomonas aeruginosa* chaperone usher systems. *Environmental Microbiology* 14, 1805-1816.
- Gomes, M.Z., Oliveira, R.V., Machado, C.R., Conceição, S., Souza, C.V., Lourenço, M.C., and Asensi, M.D. (2012). Factors associated with epidemic multiresistant *Pseudomonas aeruginosa* infections in a hospital with AIDS-predominant admissions. *The Brazilian Journal of Infectious Diseases* 16, 219-225.
- Greene, S.E., Pinkner, J.S., Chorell, E., Dodson, K.W., Shaffer, C.L., Conover, M.S., Livny, J., Hadjifrangiskou, M., Almqvist, F., and Hultgren, S.J. (2014). Pilicide ec240 disrupts virulence circuits in uropathogenic *Escherichia coli*. *mBio* 5, e02038.
- Grover, V., Ghosh, S., Chakraborti, A., Majumdar, S., and Ganguly, N.K. (2007). Galactose-specific fimbrial adhesin of enteroaggregative *Escherichia coli*: a possible aggregative factor. *Current Microbiology* 54, 175-179.
- Guex, N., Peitsch, M.C. (1997). SWISS-MODEL and the Swiss-PdbViewer: an environment for comparative protein modeling. *Electrophoresis* 18, 2714-2723.
- Guo-Xin, M., Dan-Yang, S., Xi-Zhou, G., Jun-Chang, C., Rui, W., Zhi-Gang, C., and Liang-An, C. (2014). Laboratory to clinical investigation of carbapenem resistant *Acinetobacter baumannii* outbreak in a general hospital. *Jundishapur Journal of Microbiology* 7, e13120.
- Harrington, S.M., Dudley, E.G., and Nataro, J.P. (2006). Pathogenesis of enteroaggregative

- Escherichia coli* infection. FEMS Microbiology Letters 254, 12-18.
- Harrington, S.M., Strauman, M.C., Abe, C.M., and Nataro, J.P. (2005). Aggregative adherence fimbriae contribute to the inflammatory response of epithelial cells infected with enteroaggregative *Escherichia coli*. Cellular Microbiology 7, 1565-1578.
- Henderson, B., Nair, S., Pallas, J., and Williams, M.A. (2011). Fibronectin: a multidomain host adhesin targeted by bacterial fibronectin-binding proteins. FEMS Microbiology Reviews 35, 147-200.
- Hermoso, J.A., Lagartera, L., González, A., Stelter, M., Garcia, P., Martínez-Ripoll, M., García, J.L., and Menéndez, M. (2005). Insights into pneumococcal pathogenesis from the crystal structure of the modular teichoic acid phosphorylcholine esterase Pce. Nature Structural & Molecular Biology 12, 533-538.
- Hill, J., Eyles, J.E., Elvin, S.J., Healey, G.D., Lukaszewski, R.A., and Titball, R.W. (2006). Administration of antibody to the lung protects mice against pneumonic plague. Infection and Immunity 74, 3068-3070.
- Holmgren, A., and Bränden, C.I. (1989). Crystal structure of chaperone protein Papd reveals an immunoglobulin fold. Nature 342, 248-251.
- Huang, X.Z., and Lindler, L.E. (2004). The pH 6 antigen is an antiphagocytic factor produced by *Yersinia pestis* independent of *Yersinia* outer proteins and capsule antigen. Infection and Immunity 72, 7212-7219.
- Hung, C.S., Bouckaert, J., Hung, D., Pinkner, J., Widberg, C., DeFusco, A., Auguste, C.G., Strouse, R., Langermann, S., Waksman, G., et al. (2002). Structural basis of tropism of *Escherichia coli* to the bladder during urinary tract infection. Molecular Microbiology 44, 903-915.
- Hung, D.L., and Hultgren, S.J. (1998). Pilus biogenesis via the chaperone/usher pathway: an integration of structure and function. Journal of Structural Biology 124, 201-220.
- Hung, D.L., Knight, S.D., Woods, R.M., Pinkner, J.S., and Hultgren, S.J. (1996). Molecular basis of two subfamilies of immunoglobulin-like chaperones. The EMBO Journal 15, 3792-3805.
- Iriarte, M., and Cornelis, G.R. (1995). Myf, an element of the network regulating the synthesis of fibrillae in *Yersinia enterocolitica*. Journal of Bacteriology 177, 738-744.
- Iriarte, M., Vanooteghem, J.C., Delor, I., Díaz, R., Knutton, S., and Cornelis, G.R. (1993). The Myf fibrillae of *Yersinia enterocolitica*. Molecular Microbiology 9, 507-520.
- Izoré, T., Contreras-Martel, C., El Mortaji, L., Manzano, C., Terrasse, R., Vernet, T., Di Guilmi, A.M., and Dessen, A. (2010). Structural basis of host cell recognition by the pilus adhesin from *Streptococcus pneumoniae*. Structure 18, 106-115.
- Izquierdo, M., Navarro-García, F., Nava-Acosta, R., Nataro, J.P., Ruiz-Perez, F., and Farfan, M.J. (2014). Identification of cell surface-exposed proteins involved in the fimbria-mediated adherence of enteroaggregative *Escherichia coli* to intestinal cells. Infection and Immunity 82, 1719-1724.
- Jacob-Dubuisson, F., Striker, R., and Hultgren, S.J. (1994). Chaperone-assisted self-assembly of pili independent of cellular energy. The Journal of Biological Chemistry 269, 12447-12455.
- Jeng, M.F., and Englander, S.W. (1991). Stable submolecular folding units in a non-compact form of cytochrome c. Journal of Molecular Biology 221, 1045-1061.
- Jiang, X.H., Abgottspon, D., Kleeb, S., Rabbani, S., Scharenberg, M., Wittwer, M., Haug, M., Schwardt, O., and Ernst, B. (2012). Antiadhesion therapy for urinary tract infections - a balanced PK/PD profile proved to be key for success. Journal of Medicinal Chemistry 55, 4700-4713.
- Joh, H.J., House-Pompeo, K., Patti, J.M., Gurusiddappa, S., and Höök, M. (1994). Fibronectin receptors from gram-positive bacteria: comparison of active sites. Biochemistry 33, 6086-6092.
- Jones, C.H., Dexter, P., Evans, A.K., Liu, C., Hultgren, S.J., and Hruby, D.E. (2002). *Escherichia coli* DegP protease cleaves between paired hydrophobic residues in a natural substrate: the PapA pilin. Journal of Bacteriology 184, 5762-5771.
- Jucker, B.A., Harms, H., and Zehnder, A.J. (1996). Adhesion of the positively charged bacterium *Stenotrophomonas (Xanthomonas) maltophilia* 70401 to glass and Teflon. Journal of Bacteriology 178, 5472-5479.
- Kabsch, W. (2010). XDS. Acta crystallographica. Section D, Biological crystallography 66, 125-132.
- Kato, C., Li, L., Nogi, Y., Nakamura, Y., Tamaoka, J., and Horikoshi, K. (1998). Extremely barophilic

- bacteria isolated from the Mariana Trench, Challenger Deep, at a depth of 11,000 meters. *Applied and Environmental Microbiology* *64*, 1510-1513.
- Kyogashima, M., Ginsburg, V., and Krivan, H.C. (1989). *Escherichia coli* K99 binds to N-glycolylsialoparagloboside and N-glycolyl-Gm3 found in piglet small intestine. *Archives of Biochemistry and Biophysics* *270*, 391-397.
- Knight, S.D., Choudhury, D., Hultgren, S., Pinkner, J., Stoyanoff, V., and Thompson, A. (2002). Structure of the S pilus periplasmic chaperone SfaE at 2.2 Å resolution. *Acta crystallographica. Section D, Biological crystallography* *58*, 1016-1022.
- Kuehn, M.J., Heuser, J., Normark, S., and Hultgren, S.J. (1992). P pili in uropathogenic *E. coli* are composite fibres with distinct fibrillar adhesive tips. *Nature* *356*, 252-255.
- Kuehn, M.J., Ogg, D.J., Kihlberg, J., Slonim, L.N., Flemmer, K., Bergfors, T., and Hultgren, S.J. (1993). Structural basis of pilus subunit recognition by the PapD chaperone. *Science* *262*, 1234-1241.
- Leng, X.Y., Zhu, W., Jin, J., and Mao, X.H. (2011). Evidence that a chaperone-usher-like pathway of *Myxococcus xanthus* functions in spore coat formation. *Microbiology* *157*, 1886-1896.
- Li, H.L., Qian, L.P., Chen, Z.Q., Thibault, D., Liu, G., Liu, T.B., and Thanassi, D.G. (2004). The outer membrane usher forms a twin-pore secretion complex. *Journal of Molecular Biology* *344*, 1397-1407.
- Li, Y.F., Poole, S., Rasulova, F., McVeigh, A.L., Savarino, S.J. and Xia D. (2007). A receptor-binding site as revealed by the crystal structure of CfaE, the colonization factor antigen I fimbrial adhesin of enterotoxigenic *Escherichia coli*. *Journal of Biological Chemistry* *282*, 23970-23980.
- Li, Y.F., Poole, S., Nishio, K., Jang, K., Rasulova, F., McVeigh, A.L., Savarino, S.J., Xia D., and Bullitt, E. (2009). Structures of CFA/I fimbriae from enterotoxigenic *Escherichia coli*. *Proceedings of the National Academy of Sciences of the United States of America* *106*, 10793-10798.
- Lindler, L.E., Klempner, M.S., and Straley, S.C. (1990). *Yersinia pestis* pH 6 antigen: genetic, biochemical, and virulence characterization of a protein involved in the pathogenesis of bubonic plague. *Infection and Immunity* *58*, 2569-2577.
- Lindler, L.E. and Tall, B.D. (1993). *Yersinia pestis* pH 6 antigen forms fimbriae and is induced by intracellular association with macrophages. *Molecular Microbiology* *8*, 311-324.
- Liu, F., Chen, H., Galván, E.M., Lasaro, M.A., and Schifferli, D.M. (2006). Effects of Psa and F1 on the adhesive and invasive interactions of *Yersinia pestis* with human respiratory tract epithelial cells. *Infection and Immunity* *74*, 5636-5644.
- Lo, A.W., Moonens, K., and Remaut, H. (2013). Chemical attenuation of pilus function and assembly in Gram-negative bacteria. *Current Opinion in Microbiology* *16*, 85-92.
- Makhatadze, G.I., and Privalov, P.L. (1995). Energetics of protein structure. *Advances in Protein Chemistry* *47*, 307-425.
- Maragakis, L.L. and Perl, T.M. (2008). *Acinetobacter baumannii*: epidemiology, antimicrobial resistance, and treatment options. *Clinical Infectious Diseases*, *46*, 1254-1263.
- McGrath, E.J., and Asmar, B.I. (2011a). Nosocomial infections and multidrug-resistant bacterial organisms in the pediatric intensive care unit. *Indian Journal of Pediatrics* *78*, 176-184.
- McGrath, E.J., Chopra, T., Abdel-Haq, N., Preney, K., Koo, W., Asmar, B.I., and Kaye, K.S. (2011b). An outbreak of carbapenem-resistant *Acinetobacter baumannii* infection in a neonatal intensive care unit: investigation and control. *Infection Control and Hospital Epidemiology* *32*, 34-41.
- Mikula, K.M., Kolodziejczyk, R., and Goldman, A. (2012). *Yersinia* infection tools-characterization of structure and function of adhesins. *Frontiers in Cellular and Infection microbiology* *2*, 169.
- Monaco, S., Gordon, E., Bowler, M.W., Delagenière, S., Guijarro, M., Spruce, D., Svensson, O., McSweeney, S.M., McCarthy, A.A., Leonard, G., et al. (2013). Automatic processing of macromolecular crystallography X-ray diffraction data at the ESRF. *Journal of Applied Crystallography* *46*, 804-810.
- Moonens, K., Van den Broeck, I., De Kerpel, M., Deboeck, F., Raymaekers, H., Remaut, H., and De Greve, H. (2015). Structural and functional insight into the carbohydrate receptor binding of F4 fimbriae-producing enterotoxigenic *Escherichia coli*. *Journal of Biological Chemistry* *290*, 8409-8419.
- Nataro, J.P. (2011). Outbreak of hemolytic-uremic syndrome linked to Shiga toxin-producing

- enteroaggregative *Escherichia coli* O104:H4. *Pediatric Research* 70, 221.
- Nataro, J.P., Kaper, J.B., Robinsbrowne, R., Prado, V., Vial, P., and Levine, M.M. (1987). Patterns of adherence of diarrheagenic *Escherichia coli* to HEp-2 Cells. *The Pediatric Infectious Diseases Journal* 6, 829-831.
- Nataro, J.P., Seriwatana, J., Fasano, A., Maneval, D.R., Guers, L.D., Noriega, F., Dubovsky, F., Levine, M.M., and Morris, J.G., Jr. (1995). Identification and cloning of a novel plasmid-encoded enterotoxin of enteroinvasive *Escherichia coli* and *Shigella* strains. *Infection and Immunity* 63, 4721-4728.
- Nataro, J.P., Yikang, D., Giron, J.A., Savarino, S.J., Kothary, M.H., and Hall, R. (1993). Aggregative adherence fimbria I expression in enteroaggregative *Escherichia coli* requires two unlinked plasmid regions. *Infection and Immunity* 61, 1126-1131.
- Navarro-Garcia, F. (2014). *Escherichia coli* O104:H4 pathogenesis: an enteroaggregative *E. coli*/Shiga Toxin-Producing *E. coli* explosive cocktail of high virulence. *Microbiology Spectrum* 2.
- Navarro-Garcia, F., and Elias, W.P. (2011). Autotransporters and virulence of enteroaggregative *E. coli*. *Gut Microbes* 2, 13-24.
- Navarro-Garcia, F., Eslava, C., Villaseca, J.M., López-Revilla, R., Czczulin, J.R., Srinivas, S., Nataro, J.P., and Cravioto, A. (1998). In vitro effects of a high-molecular-weight heat-labile enterotoxin from enteroaggregative *Escherichia coli*. *Infection and Immunity* 66, 3149-3154.
- Ng, T.W., Akman, L., Osisami, M., and Thanassi, D.G. (2004). The usher N terminus is the initial targeting site for chaperone-subunit complexes and participates in subsequent pilus biogenesis events. *Journal of Bacteriology* 186, 5321-5331.
- Nishiyama, M., Horst, R., Eidam, O., Herrmann, T., Ignatov, O., Vetsch, M., Bettendorff, P., Jelasarov, I., Grutter, M.G., Wuthrich, K., et al. (2005). Structural basis of chaperone-subunit complex recognition by the type I pilus assembly platform FimD. *The EMBO Journal* 24, 2075-2086.
- Nishiyama, M., Ishikawa, T., Rechsteiner, H., and Glockshuber, R. (2008). Reconstitution of pilus assembly reveals a bacterial outer membrane catalyst. *Science* 320, 376-379.
- Nummelin, H., Merckel, M.C., Leo, J.C., Lankinen, H., Skurnik, M., and Goldman, A. (2004). The *Yersinia* adhesin YadA collagen-binding domain structure is a novel left-handed parallel beta-roll. *The EMBO Journal* 23, 701-711.
- Nuccio, S.P., and Baumler, A.J. (2007). Evolution of the chaperone/usher assembly pathway: Fimbrial classification goes Greek. *Microbiology and Molecular Biology Reviews* 71, 551-575.
- Ouwehand, A., and Vesterlund, S. (2003). Health aspects of probiotics. *I drugs - the Investigational Drugs journal* 6, 573-580.
- Paczosa, M.K., Fisher, M.L., Maldonado-Arocho, F.J., and Mecsas, J. (2014). *Yersinia pseudotuberculosis* uses Ail and YadA to circumvent neutrophils by directing Yop translocation during lung infection. *Cellular Microbiology* 16, 247-268.
- Payne, D., Tatham, D., Williamson, E.D., and Titball, R.W. (1998). The pH 6 antigen of *Yersinia pestis* binds to beta1-linked galactosyl residues in glycosphingolipids. *Infection and Immunity* 66, 4545-4548.
- Perry, R.D., and Fetherston, J.D. (1997). *Yersinia pestis* - etiologic agent of plague. *Clinical Microbiology Reviews* 10, 35-66.
- Petersen, F.N., Jensen, M.Ø., and Nielsen, C.H. (2005). Interfacial tryptophan residues: a role for the cation- $\pi$  effect? *Biophysical Journal* 89, 3985-3996.
- Phan, G., Remaut, H., Wang, T., Allen, W.J., Pirker, K.F., Lebedev, A., Henderson, N.S., Geibel, S., Volkan, E., Yan, J., et al. (2011). Crystal structure of the FimD usher bound to its cognate FimC-FimH substrate. *Nature* 474, 49-53.
- Piatek, R., Zalewska-Piatek, B., Dzierzbicka, K., Makowiec, S., Pilipczuk, J., Szemiako, K., Cyranka-Czaja, A., and Wojciechowski, M. (2013). Pilicides inhibit the FGL chaperone/usher assisted biogenesis of the Dr fimbrial polyadhesin from uropathogenic *Escherichia coli*. *BMC Microbiology* 13, 131.
- Pinkner, J.S., Remaut, H., Buelens, F., Miller, E., Aberg, V., Pemberton, N., Hedenström, M., Larsson, A., Seed, P., Waksman, G., et al. (2006). Rationally designed small compounds inhibit pilus biogenesis in uropathogenic bacteria. *Proceedings of the National Academy of Sciences of the United States of America* 103, 17897-17902.
- Poole, S.T., McVeigh, A.L., Anantha, R.P., Lee, L.H., Akay, Y.M., Pontzer, E.A., Scott, D.A., Bullitt, E., and Savarino, S.J. (2007). Donor strand complementation governs intersubunit



- interaction of fimbriae of the alternate chaperone pathway. *Molecular Microbiology* 63, 1372-1384.
- Powell, B.S., Andrews, G. P., Enama, J. T., Jendrek, S., Bolt, C., Worsham, P., Pullen, J. K., Ribot, W., Hines, H., Smith, L., *et al.* (2005). Design and testing for a nontagged F1-V fusion protein as vaccine antigen against bubonic and pneumonic plague. *Biotechnology Progress* 21, 1490-1510.
- Proft, T., and Baker, E.N. (2009). Pili in Gram-negative and Gram-positive bacteria - structure, assembly and their role in disease. *Cellular and Molecular Life Sciences* 66, 613-635.
- Pugsley, A.P. (1993). The complete general secretory pathway in gram-negative bacteria. *Microbiological Reviews* 57, 50-108.
- Puorger, C., Eidam, O., Capitani, G., Erilov, D., Grütter, M.G., and Glockshuber, R. (2008). Infinite kinetic stability against dissociation of supramolecular protein complexes through donor strand complementation. *Structure* 16, 631-642.
- Remaut, H., Rose, R.J., Hannan, T.J., Hultgren, S.J., Radford, S.E., Ashcroft, A.E., and Waksman, G. (2006). Donor-strand exchange in chaperone-assisted pilus assembly proceeds through a concerted beta strand displacement mechanism. *Molecular Cell* 22, 831-842.
- Remaut, H., Tang, C., Henderson, N.S., Pinkner, J.S., Wang, T., Hultgren, S.J., Thanassi, D.G., Waksman, G., and Li, H. (2008). Fiber formation across the bacterial outer membrane by the chaperone/usher pathway. *Cell* 133, 640-652.
- Roberts, J.A., Marklund, B. I., Ilver, D., Haslam, D., Kaack, M. B., Baskin, G., Louis, M., Mollby, R., Winberg, J. and Normark, S. (1994) The Gal(alpha 1-4)Gal-specific tip adhesin of *Escherichia coli* P-fimbriae is needed for pyelonephritis to occur in the normal urinary tract. *Proceedings of the National Academy of Sciences of the United States of America* 91, 11889-11893.
- Rose, R.J., Welsh, T.S., Waksman, G., Ashcroft, A.E., Radford, S.E., and Paci, E. (2008). Donor-strand exchange in chaperone-assisted pilus assembly revealed in atomic detail by molecular dynamics. *Journal of Molecular Biology* 375, 908-919.
- Roy, S.P., Rahman, M.M., Yu, D.X., Tuutila, M., Knight, S.D., and Zavialov, A.V. (2012). Crystal structure of enterotoxigenic *Escherichia coli* colonization factor CS6 reveals a novel type of functional assembly. *Molecular Microbiology* 86, 1100-1115.
- Sakellaris, H. and Scott, J.R. (1998). New tools in an old trade: CS1 pilus morphogenesis. *Molecular Microbiology* 30, 681-687.
- Sakellaris, H., Balding, D.P., and Scott, J.R. (1996). Assembly proteins of CS1 pili of enterotoxigenic *Escherichia coli*. *Molecular Microbiology* 21, 529-541.
- Sauer, F.G., Remaut, H., Hultgren, S.J., and Waksman G (2004). Fiber assembly by the chaperone-usher pathway. *Biochimica et Biophysica Acta* 1694, 259-267.
- Sauer, F.G., Pinkner, J.S., Waksman, G., and Hultgren, S.J. (2002). Chaperone priming of pilus subunits facilitates a topological transition that drives fiber formation. *Cell* 111, 543-551.
- Sauer, F.G., Barnhart, M., Choudhury, D., Knight, S. D., Waksman, G. and Hultgren, S. J. (2000) Chaperone-assisted pilus assembly and bacterial attachment. *Current Opinion in Structural Biology* 10, 548-556.
- Sauer, F.G., Futterer, K., Pinkner, J.S., Dodson, K.W., Hultgren, S.J., and Waksman, G. (1999). Structural basis of chaperone function and pilus biogenesis. *Science* 285, 1058-1061.
- Saulino, E.T., Bullitt, E., and Hultgren, S.J. (2000). Snapshots of usher-mediated protein secretion and ordered pilus assembly. *Proceedings of the National Academy of Sciences of the United States of America* 97, 9240-9245.
- Saulino, E.T., Thanassi, D.G., Pinkner, J.S., and Hultgren, S.J. (1998). Ramifications of kinetic partitioning on usher-mediated pilus biogenesis. *The EMBO Journal* 17, 2177-2185.
- Savarino, S.J., Fasano, A., Watson, J., Martin, B.M., Levine, M.M., Guandalini, S., and Guerry P. (1993). Enterotoxigenic *Escherichia coli* heat-stable enterotoxin 1 represents another subfamily of *E. coli* heat-stable toxin. *Proceedings of the National Academy of Sciences of the United States of America* 90, 3093-3097.
- Schiffer, M., Chang, C.H., and Stevens, F.J. (1992). The functions of tryptophan residues in membrane proteins. *Protein Engineering* 5, 213-214.
- Schwarz-Linek, U., Pilka, E.S., Pickford, A.R., Kim, J.H., Höök, M., Campbell, I.D., and Potts, J.R. (2004). High affinity streptococcal binding to human fibronectin requires specific recognition of sequential F1 modules. *Journal of Biological Chemistry* 279, 39017-39025.

- Schwarz-Linek, U., Werner, J.M., Pickford, A.R., Gurusiddappa, S., Kim, J.H., Pilka, E.S., Briggs, J.A.G., Gough, T.S., Hook, M., Campbell, I.D., *et al.* (2003). Pathogenic bacteria attach to human fibronectin through a tandem beta-zipper. *Nature* *423*, 177-181.
- Sears, C.L. (2005). A dynamic partnership: Celebrating our gut flora. *Anaerobe* *11*, 247-251.
- Sheikh, J., Hicks, S., Dall'Agnol, M., Phillips, A.D., and Nataro, J.P. (2001). Roles for Fis and YafK in biofilm formation by enteroaggregative *Escherichia coli*. *Molecular Microbiology* *41*, 983-997.
- Soto, G.E., and Hultgren, S.J. (1999). Bacterial adhesins: common themes and variations in architecture and assembly. *Journal of Bacteriology* *181*, 1059-1071.
- Stones, D.H., and Krachler, A.M. (2015). Fatal attraction: how bacterial adhesins affect host signaling and what we can learn from them. *International Journal of Molecular Sciences* *16*, 2626-2640.
- Svensson, A., Larsson, A., Emtenäs, H., Hedenström, M., Fex, T., Hultgren, S.J., Pinkner, J.S., Almqvist, F., and Kihlberg, J. (2001). Design and evaluation of pilicides: potential novel antibacterial agents directed against uropathogenic *Escherichia coli*. *ChemBioChem* *2*, 915-918.
- Sussman, J.L., Harel, M., Frolow, F., Oefner, C., Goldman, A., Toker, L., and Silman, I. (1991). Atomic structure of acetylcholinesterase from *Torpedo californica* - a prototypic acetylcholine-binding protein. *Science* *253*, 872-879.
- Thanassi, D.G., Stathopoulos, C., Dodson, K., Geiger, D., and Hultgren, S.J. (2002). Bacterial outer membrane ushers contain distinct targeting and assembly domains for pilus biogenesis. *Journal of Bacteriology* *184*, 6260-6269.
- Thomas, W.E., Trintchina, E., Forero, M., Vogel, V., and Sokurenko, E.V. (2002). Bacterial adhesion to target cells enhanced by shear force. *Cell* *109*, 913-923.
- Toba, F.A., Visai, L., Trivedi, S., and Lowy, F.D. (2013). The role of ionic interactions in the adherence of the *Staphylococcus epidermidis* adhesin SdrF to prosthetic material. *FEMS Microbiology Letters* *338*, 24-30.
- Todar, K. (2012). The Impact of Microbes on the Environment and Human Activities. Online Textbook of Bacteriology, University of Wisconsin-Madison, U.S.A. [http://textbookofbacteriology.net/Impact\\_3.html](http://textbookofbacteriology.net/Impact_3.html) (Retrieved 2016-05-18).
- Tomaras, A.P., Dorsey, C.W., Edelman, R.E., and Actis, L.A. (2003). Attachment to and biofilm formation on abiotic surfaces by *Acinetobacter baumannii*: involvement of a novel chaperone-usher pili assembly system. *Microbiology* *149*, 3473-3484.
- Tomaras, A.P., Flagler, M.J., Dorsey, C.W., Gaddy, J.A., and Actis, L.A. (2008). Characterization of a two-component regulatory system from *Acinetobacter baumannii* that controls biofilm formation and cellular morphology. *Microbiology* *154*, 3398-3409.
- Tommasi, R., Brown, D.G., Walkup, G.K., Manchester, J.I., and Miller, A.A. (2015). ESKAPEing the labyrinth of antibacterial discovery. *Nature Reviews Drug Discovery* *14*, 529-542.
- Unal, S., and Garcia-Rodriguez, J.A. (2005). Activity of meropenem and comparators against *Pseudomonas aeruginosa* and *Acinetobacter spp.* isolated in the MYSTIC Program, 2002-2004. *Diagnostic Microbiology and Infectious disease* *53*, 265-271.
- Uversky, V.N., and Ptitsyn, O.B. (1994). "Partly folded" state, a new equilibrium state of protein molecules: four-state guanidinium chloride-induced unfolding of beta-lactamase at low temperature. *Biochemistry* *33*, 2782-2791.
- Uversky, V.N., and Ptitsyn, O.B. (1996). Further evidence on the equilibrium "pre-molten globule state": four-state guanidinium chloride-induced unfolding of carbonic anhydrase B at low temperature. *Journal of Molecular Biology* *255*, 215-228.
- Van den Broeck, W., Cox, E., Oudega, B., and Goddeeris, B.M. (2000). The F4 fimbrial antigen of *Escherichia coli* and its receptors. *Veterinary Microbiology* *71*, 223-244.
- Vial, P.A., Robins-Browne, R., Lior, H., Prado, V., Kaper, J.B., Nataro, J.P., Maneval, D., Elsayed, A., and Levine, M.M. (1988). Characterization of enteroadherent-aggregative *Escherichia coli*, a putative agent of diarrheal disease. *The Journal of Infectious Diseases* *158*, 70-79.
- Viboud, G.I., and Bliska, J.B. (2005). *Yersinia* outer proteins: role in modulation of host cell signaling responses and pathogenesis. *Annual Review of Microbiology* *59*, 69-89.
- Viboud, G.I., McConnell, M.M., Helander, A., and Svennerholm, A.M. (1996). Binding of

- enterotoxigenic *Escherichia coli* expressing different colonization factors to tissue-cultured Caco-2 cells and to isolated human enterocytes. *Microbial Pathogenesis* *21*, 139-147.
- Villanueva-Millán, M.J., Pérez-Matute, P., and Oteo, J.A. (2015). Gut microbiota: a key player in health and disease. A review focused on obesity. *Journal of Physiology and Biochemistry* *71*, 509-525.
- Vitagliano, L., Ruggiero, A., Pedone, C., and Berisio, R. (2008). Conformational states and association mechanism of *Yersinia pestis* CafI subunits. *Biochemical and Biophysical Research Communications* *372*, 804-810.
- Voegele, K., Sakellaris, H., and Scott, J.R. (1997). CooB plays a chaperone-like role for the proteins involved in formation of CS1 pili of enterotoxigenic *Escherichia coli*. *Proceedings of the National Academy of Sciences of the United States of America* *94*, 13257-13261.
- Wagner, J.E. and Manning, P.J. (1976) *The Biology of the guinea pig*. Academic Press, New York, U.S.A.
- Westerlund, B., and Korhonen, T.K. (1993). Bacterial proteins binding to the mammalian extracellular-matrix. *Molecular Microbiology* *9*, 687-694.
- Wilks M., Wilson, A., Warwick, S., Price, E., Kennedy, D., Ely, A., Millar, M. R. (2006). Control of an outbreak of multidrug-resistant *Acinetobacter baumannii-calcoaceticus* colonization and infection in an intensive care unit (ICU) without closing the ICU or placing patients in isolation. *Infection Control and Hospital Epidemiology* *27*, 654-658.
- Williamson, E.D., Flick-Smith, H.C., LeButt, C., Rowland, C.A., Jones, S.M., Waters, E.L., Gwyther, R.J., Miller, J., Packer, P.J., and Irving, M. (2005). Human immune response to a plague vaccine comprising recombinant F1 and V antigens. *Infection and Immunity* *73*, 3598-3608.
- World Health Organization (2014). WHO's first global report on antibiotic resistance reveals serious, worldwide threat to public health. <http://www.who.int/mediacentre/news/releases/2014/amr-report/en/> (Retrieved 2015-10-08).
- Worsham, P.L., Mou, S., Cote, C.K., and Fritz, D. (2012). Virulence of *Yersinia pseudotuberculosis* in aerosol models. *Advances in Experimental Medicine and Biology* *954*, 217-222.
- Wright, K.J., Seed, P.C., and Hultgren, S.J. (2007). Development of intracellular bacterial communities of uropathogenic *Escherichia coli* depends on type 1 pili. *Cellular Microbiology* *9*, 2230-2241.
- Wu, M.M., Xu, S.H., Zhu, W., and Mao, X.H. (2014). The archaic chaperone-usher pathways may depend on donor strand exchange for intersubunit interactions. *Microbiology* *160*, 2200-2207.
- Yang, Y.X., Merriam, J.J., Mueller, J.P., and Isberg, R.R. (1996). The *psa* locus is responsible for thermoinducible binding of *Yersinia pseudotuberculosis* to cultured cells. *Infection and Immunity* *64*, 2483-2489.
- Yu, X.D., Visweswaran, G.R., Duck, Z., Marupakula, S., MacIntyre, S., Knight, S.D., and Zavialov, A.V. (2009). CafIA usher possesses a CafI subunit-like domain that is crucial for CafI fibre secretion. *Biochemical Journal* *418*, 541-551.
- Yu, X.D., Fooks, L.J., Moslehi-Mohebi, E., Tischenko, V.M., Askarieh, G., Knight, S.D., MacIntyre, S., and Zavialov, A.V. (2012a). Large is fast, small is tight: determinants of speed and affinity in subunit capture by a periplasmic chaperone. *Journal of Molecular Biology* *417*, 294-308.
- Yu, X.D., Dubnovitsky, A., Pudney, A.F., Macintyre, S., Knight, S.D., and Zavialov, A.V. (2012b). Allosteric mechanism controls traffic in the chaperone/usher pathway. *Structure* *20*, 1861-1871.
- Zav'yalov, V., Zavialov, A., Zav'yalova, G., and Korpela, T. (2010). Adhesive organelles of Gram-negative pathogens assembled with the classical chaperone/usher machinery: structure and function from a clinical standpoint. *FEMS Microbiology Reviews* *34*, 317-378.
- Zav'yalov, V.P., Zav'yalova, G.A., Denesyuk, A.I., and Korpela, T. (1995). Modelling of steric structure of a periplasmic molecular chaperone CafIM of *Yersinia pestis*, a prototype member of a subfamily with characteristic structural and functional features. *FEMS Immunology and Medical Microbiology* *11*, 19-24.
- Zavialov, A., Zav'yalova, G., Korpela, T., and Zav'yalov, V. (2007). FGL chaperone-assembled fimbrial polyadhesins: anti-immune armament of Gram-negative bacterial pathogens. *FEMS Microbiology Reviews* *31*, 478-514.
- Zavialov, A.V., Berglund, J., Pudney, A.F., Fooks, L.J., Ibrahim, T.M., MacIntyre, S., and Knight, S.D. (2003). Structure and biogenesis of the capsular F1 antigen from *Yersinia pestis*:

- Preserved folding energy drives fiber formation. *Cell* *113*, 587-596.
- Zavialov, A.V., Kersley, J., Korpela, T., Zav'yalov, V.P., MacIntyre, S., and Knight, S.D. (2002). Donor strand complementation mechanism in the biogenesis of non-pilus systems. *Molecular Microbiology* *45*, 983-995.
- Zavialov, A.V., Tischenko, V.M., Fooks, L.J., Brandsdal, B.O., Aqvist, J., Zav'yalov, V.P., Macintyre, S., and Knight, S.D. (2005). Resolving the energy paradox of chaperone/usher-mediated fibre assembly. *Biochemical Journal* *389*, 685-694.
- Zhu, W., Wu, M., Cao, S., Peng, Y., and Mao, X. (2013). Characterization of McuB, a periplasmic chaperone-like protein involved in the assembly of *Myxococcus* spore coat. *Journal of Bacteriology* *195*, 3105-3114.